Bioactive Materials 42 (2024) 478–518

Contents lists available at ScienceDirect

Bioactive Materials

journal homepage: www.keaipublishing.com/en/journals/bioactive-materials

Review article

Electrospun nanofibrous membranes meet antibacterial nanomaterials: From preparation strategies to biomedical applications

Shengqiu Chen [a], Yi Xie [b], Kui Ma [c,d,e], Zhiwei Wei [b], Xingwu Ran [a,f,****], Xiaobing Fu [c,d,e,***], Cuiping Zhang [c,d,e,**], Changsheng Zhao [b,*]

[a] Innovation Research Center for Diabetic Foot, West China Hospital, Sichuan University, Chengdu, 610041, China
[b] College of Polymer Science and Engineering, State Key Laboratory of Polymer Materials and Engineering, Sichuan University, Chengdu, 610065, China
[c] Research Center for Tissue Repair and Regeneration Affiliated to the Medical Innovation Research Department, PLA General Hospital and PLA Medical College, Beijing, 100853, China
[d] PLA Key Laboratory of Tissue Repair and Regenerative Medicine and Beijing Key Research Laboratory of Skin Injury, Repair and Regeneration, Beijing, 100048, China
[e] Research Unit of Trauma Care, Tissue Repair and Regeneration, Chinese Academy of Medical Sciences, 2019RU051, Beijing, 100048, China
[f] Department of Endocrinology and Metabolism, Diabetic Foot Care Center, West China Hospital, Sichuan University, Chengdu, 610041, China

ARTICLE INFO

Keywords:
Bacterial infection
Antibacterial nanomaterials
Electrospinning
Antimicrobial therapies
Biomedical applications

ABSTRACT

Electrospun nanofibrous membranes (eNFMs) have been extensively developed for bio-applications due to their structural and compositional similarity to the natural extracellular matrix. However, the emergence of antibiotic resistance in bacterial infections significantly impedes the further development and applications of eNFMs. The development of antibacterial nanomaterials substantially nourishes the engineering design of antibacterial eNFMs for combating bacterial infections without relying on antibiotics. Herein, a comprehensive review of diverse fabrication techniques for incorporating antibacterial nanomaterials into eNFMs is presented, encompassing an exhaustive introduction to various nanomaterials and their bactericidal mechanisms. Furthermore, the latest achievements and breakthroughs in the application of these antibacterial eNFMs in tissue regenerative therapy, mainly focusing on skin, bone, periodontal and tendon tissues regeneration and repair, are systematically summarized and discussed. In particular, for the treatment of skin infection wounds, we highlight the antibiotic-free antibacterial therapy strategies of antibacterial eNFMs, including (i) single model therapies such as metal ion therapy, chemodynamic therapy, photothermal therapy, and photodynamic therapy; and (ii) multi-model therapies involving arbitrary combinations of these single models. Additionally, the limitations, challenges and future opportunities of antibacterial eNFMs in biomedical applications are also discussed. We anticipate that this comprehensive review will provide novel insights for the design and utilization of antibacterial eNFMs in future research.

1. Introduction

Electrospinning is a straightforward and continuous micro/nanofiber processing technology [1], which serves as a robust tool for producing ultrafine one-dimensional (1D) nanofibers and two-dimensional (2D) membranes with desirable wettability, adjustable pore structures, high porosity, and excellent pore connectivity. These characteristics are crucial for effectively integrating the immense potential of nanomaterials into practical macroscale components, such as advanced sensing, smart manufacturing, efficient catalysis, *etc*. [1–5]. After nearly two decades of development, electrospinning has emerged as a popular technology that has garnered extensive and significant attentions in the

Peer review under responsibility of KeAi Communications Co., Ltd.
* Corresponding author.
** Corresponding author. Research Center for Tissue Repair and Regeneration Affiliated to the Medical Innovation Research Department, PLA General Hospital and PLA Medical College, Beijing, 100853, China.
*** Corresponding author. Research Center for Tissue Repair and Regeneration Affiliated to the Medical Innovation Research Department, PLA General Hospital and PLA Medical College, Beijing, 100853, China.
**** Corresponding author. Innovation Research Center for Diabetic Foot, West China Hospital, Sichuan University, Chengdu, 610041, China.
E-mail addresses: ranxingwu@163.com (X. Ran), fuxiaobing@vip.sina.com (X. Fu), zcp666666@sohu.com (C. Zhang), zhaochsh70@163.com (C. Zhao).

https://doi.org/10.1016/j.bioactmat.2024.09.003
Received 22 May 2024; Received in revised form 14 August 2024; Accepted 1 September 2024

field of tissue regenerative therapy [1,6–10]. As an ideal material for cell adhesion and proliferation, electrospinning nanofibrous membranes (eNFMs) possess highly porous three-dimensional (3D) networks with excellent pore interconnections due to the entanglement of these micro/nanofibers. These eNFMs can mimic the texture and composition of natural extracellular matrix (ECM), depending on the choice of materials employed, making them highly promising candidates in tissue regenerative therapies [11–13]. Consequently, electrospun fibrous scaffolds exhibit an inherent capability to attract fibroblasts to dermis and facilitate the secretion of growth factors, collagen and other ECM components, thereby accelerating tissue regeneration and repair processes [14–16].

However, the emergence of the antimicrobial resistance has hindered the further development and application of eNFMs in clinic settings. Over the last decade, the threat posed by antimicrobial resistance has reached such a critical level that it has been recognized by the Word Health Organization (WHO) as a "global health and development threat" and "one of the top 10 global public health threats facing humanity" [17]. The clinical management of pathogenic infections poses an escalating challenge in the realm of global public health [18]. In contrast to the rapid emergence of antibiotic-resistant bacteria, the discovery of novel antibiotics proceeds at a sluggish pace and entails substantial costs. Therefore, it is imperative to develop alternative bactericidal agents to combat bacterial infections for comprehensive health governance. In the field of emerging biomaterials, it is unsurprising that investigations related to antibacterial properties are rapidly advancing. Recently, multifunctional eNFMs with distinctive structure and unique physiochemical properties have emerged as a potent tool for targeting bacteria and overcoming deadly bacterial invasion. Given the continuous evolution of drug-resistant bacteria, there has been an increasing focus on antibiotic-free modification to confer bactericidal property onto eNFMs in order to prevent bacterial attachment, inhibit bacteria proliferation and eradicate bacteria. Owing to the remarkable advancement in nanomaterials, a wide range of antibacterial nanomaterials, including metal nanoparticles (NPs), metal oxide/sulfide NPs, carbon-based nanomaterials, and some emerging 2D nanomaterials, have been incorporated into eNFMs with antimicrobial properties. The properties of material itself plays a critical role in the antibacterial effect, with metals (Ag, Au, *etc.*), metal oxides (ZnO, CuO, TiO_2, *etc.*) and others nanomaterials being reported [19,20]. Meanwhile, various antibacterial strategies such as metal ion release, free radical generation, hyperthermia, and edge cutting have been developed. In addition, the synergistic coordination of multiple antibacterial mechanisms has gained increasing attention.

Therefore, the incorporation of antimicrobial nanomaterials into eNFMs is a timely and significant topic in the field of electrospinning [21], showcasing promising biomedical applications in tissue regenerative therapies [22]. Given that unique properties of electrospinning have been extensively reviewed in numerous publications, this review aims to primarily focus on providing a comprehensive overview of recent advances and breakthroughs in antibacterial eNFMs. Additionally, it will highlight the most relevant and up-to-date advancements concerning eNFMs integrated with diverse nanomaterials for effective bacterial ablation within the realm of tissue regeneration and repair. Furthermore, a comprehensive analysis of the current limitations of electrospinning technology will be conducted, along with an exploration of future trends and challenges in the development of antibacterial eNFMs for biomedical applications. It is anticipated that this review will offer novel insights into the development of bactericidal nanomaterials to combat bacterial infections and provide valuable inspiration for the future design of electrospun tissue engineering scaffolds for practical clinical implementations.

2. Antibacterial strategy and mechanism of eNFMs

Electrospinning is a highly versatile technique that employs high electrostatic power to process polymers or related materials into nonwoven fabrics or final eNFMs [4,23]. By optimizing the spinning equipment configuration and adjusting various parameters such as preparation process, materials design, and structure design, the electrospinning technique enables successful integration of diverse materials with bactericidal activities including nanomaterials, natural macromolecules, and synthetic polymers into electrospun fibers.

With the development of materials science, a wide range of antibacterial nanomaterials have been developed as potential alternatives to antibiotics for the functionalization of eNFMs. The design and fabrication of antibacterial eNFMs need to consider three key properties: antibacterial activity (killing bacteria), *anti*-biofilm efficacy (biofilm inhibition/prevention) and anti-biofouling performance (biofouling inhibition/prevention). Specially, bacterial biofilm formation is a primary contributor to the escalation of bacterial resistance. The multifaceted bactericidal mechanisms exhibited by the nanomaterials enable the rational design of antibacterial eNFMs that hold promise for replacing or partially substituting antibiotics [24].

In the subsequent sections, we will elucidate the diverse antibacterial mechanisms exhibited by nanomaterial-loaded eNFMs, including (i) direct infliction of physical harm to bacterial cell walls and/or membranes, (ii) suppression of bacterial metabolism, and (iii) induction of chemical impairment to bacterial cell membranes.

2.1. Physical damage to bacterial cell membrane

Bacterial membranes serve as crucial and efficacious targets for diverse antimicrobial nanomedicines [25,26]. The physical/mechanical disruption of bacterial cell membrane proves particularly effective in compromising the local integrity of the membrane [27]. Functional 2D nanomaterials, such as graphene and its derivatives, black phosphorous (BP) nanosheets (NSs), MoS_2 NSs, MXenes, or structurally similar electrospun nanofibers can achieve damage to cell membrane integrity through their sharp cutting edges. As an illustrative example, one of the antibacterial mechanisms exhibited by graphene oxide (GO) involves its utilization as a "nano-knife" to destroy the bacterial cell membrane through sharp edge cutting effects, resulting in the release of intracellular contents and ultimately leading to bacteria eradication. Notably, graphene and its derivatives have been found extensive application as antimicrobial additives for enhancing the functionality of eNFMs in combating bacterial infections within the biomedical domain [28]. Wang et al. employed electrospinning technology to prepare blended nanofibers comprising silker fiber (SF) and GO [29]. Through systematic antibacterial experiments, the authors found that SF/GO nanofibers exhibited higher bactericidal activity compared to the pristine SF-decorated nanofibers due to the incorporation of GO, which effectively disrupted bacterial cell membranes. Additionally, Phan et al. anchored $Cu(OH)_2$ and CuO nanowires (NWs) onto polyacrylonitrile (PAN)-based eNFMs [30]. The antibacterial efficacy of $Cu(OH)_2$ or CuO-decorated eNFMs was attributed to the physical morphology and surface area of the incorporated nanomaterials.

In general, physical/mechanical damage to bacterial cell membranes is induced by direct interaction between functional nanomaterial-based eNFMs and bacterial pathogens. Physical/mechanical damage exhibits efficacy against a wide range of bacteria, as the potential for bacteria to develop resistance to bacterial envelope disruption is limited, thus rendering physical damage strategies promising for long-term utilization with minimal risk of bacterial resistance.

Additionally, the presence of phosphate groups on the bacterial membrane imparts negative charges to bacterial cell surfaces, thereby facilitating electrostatic interactions between eNFMs with highly positive surfaces and bacteria. This ultimately leads to membrane destruction and cell lysis. Similar to the antimicrobial peptides (AMPs) that accumulate on the bacterial membrane and form pores disrupting membrane stability, the antimicrobial activity of these polymers is regulated by adjusting their structural factors, such as positive charge

and hydrophobic groups. For example, Guo et al. fabricated a series of eNFMs with bactericidal, antioxidant and electroactive properties by electrospinning polymer solutions of poly(ε-caprolactone) (PCL) and quaternized chitosan-graft-polyaniline (QCSP) [15]. The QCSP contains amino and quaternary ammonium groups that possess positive charges capable of effectively elimination bacteria through direct electrostatic adherence. Notably, the presence of polyaniline down-regulates the expression of crucial genes responsible for bacterial survival in gram-negative bacteria, thereby influencing cell wall formation and energy metabolism, ultimately leading to the demise of bacterial pathogens.

2.2. Suppression of bacterial metabolism

In addition to direct destruction of bacterial cell membranes, another antimicrobial strategy employed by eNFMs involves inducing metabolic suppression. This includes the breakdown of essential nutrients for bacterial growth, modulation of gene expression, and inhibition or interference with the synthesis of crucial cellular biochemical substances in bacterial cell walls. The inhibition of gene replication and protein activity is a common bactericidal method with antibacterial eNFMs. For instance, Liu and co-workers demonstrated that silver nanoparticles (Ag NPs) possess potent antibacterial properties by inhibiting DNA synthesis during bacterial replication [31]. Wang et al., on the other hand, achieved surface incorporation of citrate-capped Ag NPs onto poly (vinyl alcohol-*co*-ethylene) (PVA-*co*-PE) nanofibers through charge adsorption grafting tricyanogen chloride-polyethyleneimine (TC-PEI) [32]. The PVA-co-PE nanofibers loaded with Ag NPs presented good sterilization performance against *Escherichia coli* (*E. coli)* and *Staphylococcus aureus* (*S. aureus*), with antibacterial rates of 99.99 %. Additionally, blocking nutrient uptake is also an effective antibacterial strategy for eNFMs. Cui et al. demonstrated that La_2O_3 NPs-doped PAN eNFMs (LPNFs) had a high phosphate removal efficiency in aqueous solution based on the strong affinity between phosphate and lanthanum, which could create a phosphorous deficient environment and inhibit bacterial growth [33]. Although the accumulated phosphate is essential for bacterial growth, LPNFs wound not be conductive to bacteria survival in the presence of unsaturated $LaPO_4$.

2.3. Chemical damage to bacterial cell membrane

In addition to physical/mechanical damage to bacterial cell membrane or inhibition of bacterial metabolism, eNFMs can also eliminate bacterial pathogens through biocatalytic generation of reactive oxygen species (ROSs), such as superoxide anion radical ($O_2^{\bullet-}$), hydrogen peroxide (H_2O_2), hydroxyl radical (•OH), ozone (O_3), *etc*. [34]. The chemical damage caused by ROSs to the bacterial cells membrane involves a variety of antibacterial mechanisms that target the physical structure, metabolic pathway, DNA synthesis, and other processes leading to cell death [35]. To date, a wide range of biocatalytic nanomaterials with catalytic ROS generation activities have been developed and demonstrated to effectively eliminate bacteria or eradicate bacterial biofilms. These biocatalytic nanomaterials include 0D metal oxide nanoparticles (such as CuO, ZnO, TiO_2) [36–38], 2D nanosheets (such as graphene, metal carbides, and carbon nitrides) [39–42], metal-organic frameworks (MOFs) [43,44], and peroxidase-mimicking nanozymes [45–47]. For instance, Sekar et al. incorporated Fe-doped ZnO NPs into eNFMs, which exhibited remarkable antibacterial properties through ROS generation. The generated ROS could induce damage to the bacterial cell wall or membrane, interfere with protein synthesis and processing, inhibit DNA replication, and intracellular content leakage [48].

3. Processing methods of nanomaterial-loaded eNFMs

Nanomaterials encompass a diverse range of organic, inorganic and hybrid nanocomposites with unique physicochemical characteristics such as size, shape, and surface properties that differ from their bulk counterparts. Recently, the antibacterial nanomaterials have been widely incorporated into eNFMs to inhibit the growth of pathogenic microorganisms and disrupt bacterial cellular structure [49,50]. In the following sections, we will primarily discuss different routes for the fabrication of antibacterial eNFMs by incorporating antibacterial nanomaterials, and the corresponding bactericidal performance of different types of antibacterial nanomaterial-incorporated eNFMs.

3.1. Different routes for fabricating antibacterial eNFMs

Incorporating antibacterial nanomaterials has been recognized as a feasible method for fabricating antibacterial eNFMs for combat bacterial infection. Generally, there are two main routes for incorporating antibacterial nanomaterials into eNFMs: (i) one-step modification, where the matrix polymer solutions are directly electrospun together with the antibacterial nanomaterials using techniques such as blending, core-shell encapsulation, or colloid-electrospinning; and (ii) post-modification, which involves a two-step process: pre-electrospinning to obtain a pristine fiber substrate followed by deposition/growth of antibacterial nanomaterials onto the surfaces of the fibers.

3.1.1. One-step method for construction antibacterial eNFMs

As depicted in Fig. 1A, one of the most commonly employed strategies for fabricating antibacterial eNFMs involves blending nanomaterials with matrix polymers to prepare spinning solutions, which are subsequently subjected to direct electrospinning. Specifically, prior to electrospinning, the antibacterial nanomaterials are fully dissolved or dispersed within the spinning solution, ensuring their homogeneous distribution throughout the entire spinning process. Simultaneously, fiber formation and encapsulation of nanomaterials occur during this process. Researchers have successfully assembled antibacterial nanomaterials with multiple dimensions ranging from 0D to 3D on polymeric eNFMs for antibacterial applications. For example, MOFs, as novel organic-inorganic hybrid porous nanomaterials in the form of 0D structures, show great potential in the fields of antibacterial research due to their intrinsic bactericidal activity and/or ability to load antibacterial nanomaterials. Li et al. initially prepared zeolitic imidazolate frameworks (ZIF-8) nanocrystals and then dispersed them into a thermoplastic polyurethane (TPU)/DMF solution for electrospinning, resulting in scalable fabrication ZIF-8-contained eNFMs. Upon exposure to sunlight irradiation, ZIF-8 can induce the generation of ROS ($\bullet O_2^-$), which effectively renders bacteria to inactive [51].

Another facile method for the direct fabrication of antibacterial eNFMs involves the utilization of co-axial electrospinning technique. Co-axial electrospinning enables the fabrication of core-shell nanofibers with multiple components by employing two injectors, each containing separate solutions of polymer and antibacterial nanomaterials, to produce core-shell structures. For instance, Shalumon et al. developed multifunctional antibacterial core-sheath eNFMs with hyaluronic acid (HA)/ibuprofen as inner core and the Ag NPs-loaded poly(ethylene glycol) (PEG)/PCL as outside sheath [52]. The incorporation of Ag NPs into the outside sheath ensures the sustained release of Ag^+ ions, thereby providing sufficient bactericidal properties during the initial post-tenson surgery period. In another study, Xing et al. developed a coaxial scaffold mimicking the extracellular matrix (ECM) as a spatial delivery system to synergistically enhance bone regeneration. Briefly, the co-axial scaffold was fabricated by incorporating ZnO and lysophosphatidic acid (LPA) NPs into the sheath layer of poly-lactic-co-glycolic acid/PCL (PLGA/PCL, PP), which encapsulated deferoxamine (DFO) NPs in the core layer [53]. After loading these three active NPs, the obtained PP-LPA-ZnO/DFO coaxial scaffolds are porous nanofiber structure. Particularly, through the spatially sustained release of these three NPs, the antibacterial properties, biocompatibility, osteogenesis, and angiogenesis of the coaxial scaffold were synergistically enhanced, which

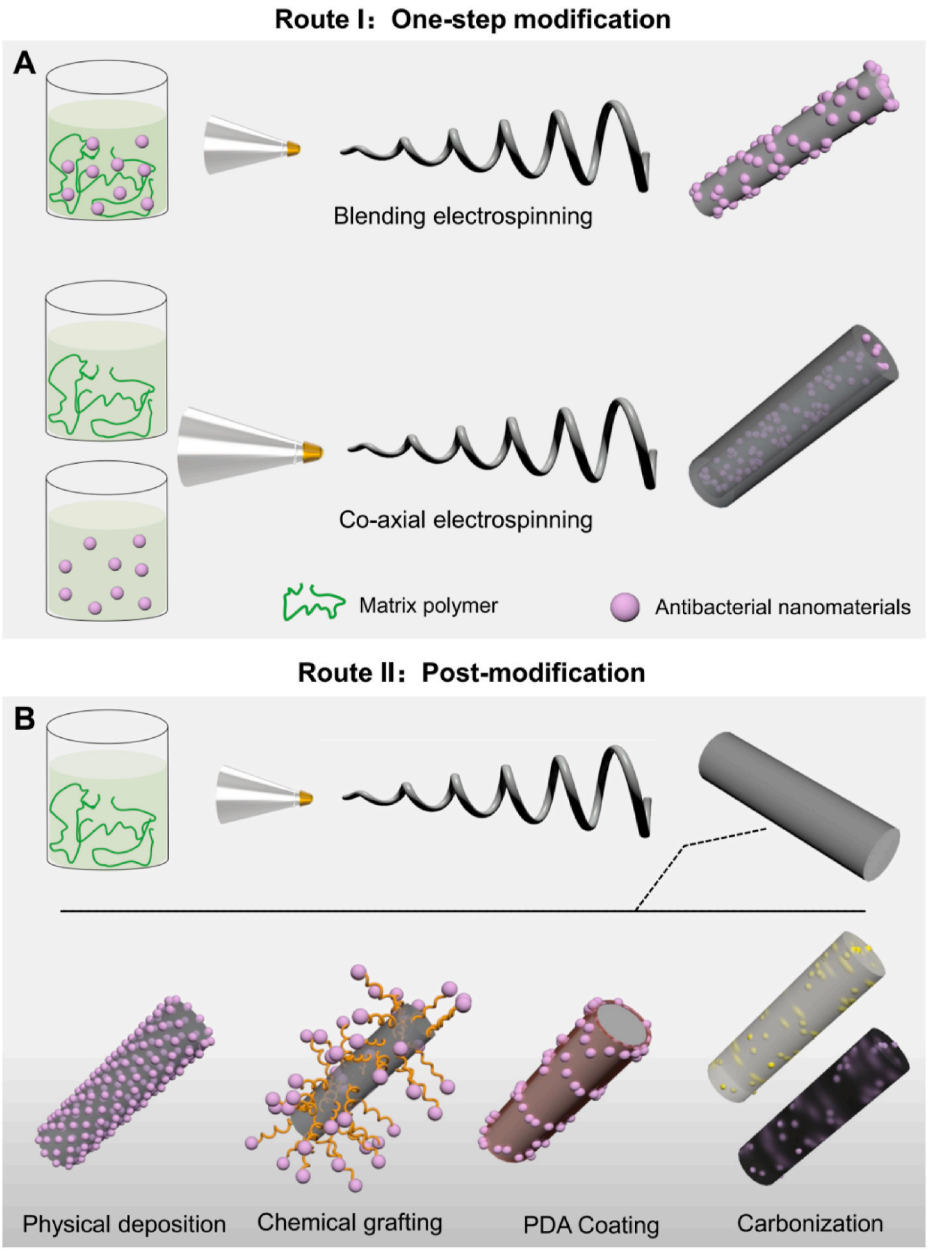

Fig. 1. The two main routes for preparing antibacterial eNFMs through the incorporation of bactericidal nanomaterials. (A) One-step modification methods primarily involving blending electrospinning and co-axial electrospinning techniques. (B) Post-modification methods mainly encompassing physical deposition, chemical grafting, PDA coating and carbonization treatment to incorporate antibacterial nanomaterials onto the surface of electrospun nanofibers.

were ultimately beneficial for bone regeneration.

3.1.2. *Post modification for construction antibacterial eNFMs*

After electrospinning, nanofibers or eNFMs are widely modified by physical or chemical methods to endow them with antibacterial functionality for various antibacterial applications. Surface modification after electrospinning has emerged as the primary strategy for enhancing the functionalities of nanofibers in combating bacterial infection, encompassing techniques such as physical deposition, chemical grafting, mussel coating, carbonization and others, as depicted in Fig. 1B. In this section, we will provide a comprehensive summary of post-modification strategies employed to confer antibacterial properties on eNFMs.

3.1.2.1. Antibacterial surface design. Antibacterial surface modification of eNFMs can be achieved by directly depositing antibacterial compounds or nanomaterials, thereby forming thin antibacterial layers on the surfaces of the nanofibers. A variety of methods such as dip-coating, spray-coating, and brush-coating have been employed for this purpose [54]. It is worth mentioning that ensuring the stability of these coating on the nanofiber surfaces remain a significant challenge in practical applications [55], prompting researchers to explore different approaches to enhance the adhesion between antibacterial layers and nanofibers. For instance, Zhang and co-workers presented a study where graphdiyne (GDY) was self-assembled onto electrospun TiO_2 nanofibers using an electrostatic force to improve the photocatalytic bactericidal efficacy [56]. Under UV light illumination, TiO_2 is photo-catalytically activated and transfers free electrons (e^-) to the GDY surface, resulting in more ROSs production. This leads to irreversible dysfunction of crucial biomolecules in bacteria and ultimately causes bacterial death. Similarly, Chen et al. prepared Ag NPs-decorated polyethersulfone (PES) eNFMs by the combination of the electrostatic interaction between Ag^+ and polyacrylic acid (PAA) and the reduction property of sodium

borohydride [57]. Briefly, hydrophilic homopolymer PAA was semi-interpenetrated with PES chains through an *in-situ* crosslinking polymerization strategy. The resulting mixture was then subjected to electrospinning to form nanofibers. Subsequently, Ag NPs were formed on the surfaces of PAA/PES fibers via a reduction treatment. The Ag NPs-decorated PAA/PES fiber membrane presented bactericidal rates against *E. coli* and *S. aureus* of 93.4 % and 95.7 %, respectively.

To enhance the stability of nanomaterials-based coatings, a chemical covalent grafting method was employed for the design of antibacterial surface on eNFMs. In 2022, Mi and co-workers demonstrated an improved bactericidal property by modifying chitosan (CS) nanofibers with CuS NPs and fucoidan (Fu) [58]. Briefly, CS nanofibers were immersed in a mixed solution of Fu and CuS NPs over 1 h to facilitate their anchoring through electrostatic interaction. Subsequently, and genipin was added to crosslink CuS NPs and CS nanofibers. The resulting nanofibers presented durable Fenton-like catalytic activity (ROS generation), enabling them to effectively deactivate bacteria through photocatalytic and photothermal effects.

3.1.2.2. Mussel-inspired modification. In recent past decades, mussel-inspired dopamine (DA) and its analogues have been broadly employed as molecules for surface modification of materials, imparting desired functionalities such as unique adhesiveness and reductive properties [59–61]. Specifically, the catechol groups derived from DA or its analogues can chemically reduce of metal ions like Ag^{+} and Au^{+}, leading to the formation of metallic NPs with antibacterial properties [62]. Coating with DA is also a popular conformal strategy to confer antibacterial properties on eNFMs. For instance, Wang et al. prepared GO-catechol hybrid poly(lactic acid) (PLA) nanofibers to enhance the immobilization of GO onto eNFMs [63]. In this process, catechol groups were conjugated onto the GOs (GO-DMA), thereby enhancing the adhesive ability of GO on the PLA fibers. Subsequently, the as-prepared GO-DMA was dip-coated onto the PLA nanofibers to form PLA-GO-DMA. In comparison with the PLA-GO eNFMs, PLA-GO-DMA showed remarkable sterilization properties against both gram-positive and gram-negative bacteria due to the pivotal role of catechol in promoting the adhesion of GO onto the PLA nanofiber, along with its intrinsic antibacterial ability conferred by catechol groups. Additionally, mussel-inspired DA or its analogues can also serve as linkers for coupling specific biomedical molecules. Shi et al. developed an infection-responsive electrospinning membrane for antimicrobial guided tissue regeneration [64]. In brief, for the preparation of an infection-responsive membrane, polydopamine (PDA) was initially utilized to modify PCL fibers in order to introduce hydroxyl groups onto the surfaces of nanofibers. Subsequently, silane coupling agents were employed to cap the hydroxyl groups and anchor amino groups onto the nanofiber surfaces. Finally, antibiotic metronidazole was esterified and grafted onto the nanofiber surface by Michael addition reaction.

3.1.2.3. Combination and other strategies. In addition to the aforementioned strategies, the fabrication of antibacterial eNFMs has also been reported through the integration of various processes such as carbonization and oxidation treatment [65,66], solvothermal method [67], chemical deposition method [68], and electrospinning technology [69,70]. Thermo-oxidative stabilization and carbonization treatments are employed to treat the precursors of polymeric eNFMs and/or antibacterial components, offering a promising approach for constructing nanofibers with incorporated antibacterial nanomaterials [71,72]. PAN, known for its excellent stability and mechanical properties, is commonly utilized as a matrix polymer for preparing carbonized nanofibers [73], wherein antibacterial activity can be achieved by carbonizing and oxidizing. For example, Xia et al. constructed ZnO/nanocarbons (C-ZnO) modified antibacterial nanofibrous scaffolds. Briefly, the synthesized ZIF-8 NPs were carbonized at 800 °C for 2 h under argon followed by oxidization at 300 °C for 2 h in air. Subsequently, the obtained C-ZnO nanocomposites were embedded into a PCL spinning solution and electrospun into a fibrous scaffold. Antibacterial experiments demonstrated that the embedded C-ZnO endowed the scaffold with good bactericidal properties, whereas no significant antibacterial activity was observed on the pristine PCL [74]. Additionally, Wang et al. employed a combination of the solvothermal method, chemical deposition method and electrospinning technology to prepare PAN/Al-ZnO/Ag nanofibrous composites with antibacterial properties [75]. Briefly, a mixture of ZnO NPs and PAN was electrospun to fabricate PAN/ZnO seed fiber (termed as P). Then, a solvothermal method was conducted to prepare the PAN/Al-ZnO NF membrane (labeled as PZ). Subsequently, PZ fibers were immersed in a $AgNO_3$ solution for 20 h and reduced with polyvinylpyrrolidone (PVP)/ethanol solution to obtain the silver seeds. Following this step, Ag NPs were deposited onto the PZ fibers through electroless plating. Throughout this process, numerous active sites provided by ZnO NPs facilitated the subsequent solvothermal and electroless plating processes, ensuring their feasibility for further recombination. Finally, Ag NPs were uniformly distributed onto the fiber surface.

3.2. Various nanomaterials loaded eNFMs with bactericidal properties

Nanomaterials in the nanoscale realm are widely recognized for their distinctive physicochemical properties, encompassing size, shape, and surface characteristics [76]. These nanomaterials, comparable in size to biomolecules and bacterial intracellular structures, have been engineered as innovative therapeutic modalities and hold great promise in the fight against bacterial infections [26], by circumventing established mechanisms associated with acquired resistance [77]. In addition, owing to their unique dimensions and physicochemical attributes, nanomaterials exhibit targeted action against biofilms and offer a potential solution for tackling recalcitrant infections [78].

To prevent pathogenic microbial contamination and infection, a diverse range of nanomaterials are utilized to modify eNFMs in the biomedical field for enhancing bactericidal activities. Based on their chemical composition and structural characteristics, antibacterial nanomaterials can be categorized into different groups, including inorganic, organic, and inorganic-organic hybrid nanomaterials, as illustrated in Table 1. Inorganic nanomaterials usually have good stability and high thermal and chemical resistance, while organic nanomaterials may have better biocompatibility and processability. Inorganic-organic hybrid nanomaterials combine the advantages of both, providing more possibilities for specific biomedical applications. The inorganic nanomaterials are usually composed of inorganic compounds such as metals, metal oxides, sulfides, and ceramics, and the representative examples include nano Ag, nano Au, nano TiO_2, nano ZnO, nano CNT, and some emerging nanomaterials such as Mxene, BP, BN, *etc*. Organic nanomaterials were made from organic compounds or polymer materials, and the examples include natural organic polymer nanoparticles and synthesized polymer nanoparticles, nanocellulose, and some organic nanotubes, hydrogen-bonded organic frameworks (HOF) nanocrystalline [69]. Inorganic-organic hybrid nanomaterials, also known as composite nanomaterials, combined the properties of inorganic and organic materials, and this blending can improve the properties of the material, such as enhancing stability, improving mechanical properties, providing synergistic bactericidal activity or specific functions. The typical Inorganic-organic hybrid nanomaterials include inorganic nanoparticles surface modification of organic molecules (such as AIE-featured Au nanoclusters [79], APA modified Au nanoparticles [80], MBA-activated Au NPs [81]), indole derivative-capped Au NPs [82], organic-inorganic hybrid materials (such as some types of MOFs [83]), nanocomposites, *etc*. The following subsections mainly summarize different fabrication approaches for antibacterial eNFMs incorporating diverse nanomaterials, along with their corresponding antimicrobial mechanisms and antibacterial performance.

Table 1
A comprehensive overview of antibacterial eNFMs containing a diverse range of antibacterial nanomaterials including inorganic, organic, and inorganic-organic hybrid nanomaterials, for advanced biomedical applications.

Categories	Antibacterial nanomaterials	eNFMs	Target microorganism	Antimicrobial effect	Antimicrobial Mechanism	Refs.
Inorganic	Ag NPs	Patterned nano-Ag/PLLA hybrid fibrous matrices	*E. coli*	Precise and arbitrary manipulation of live/dead *E. coli* distribution and antibacterial area	Release of Ag or Ag^+ from the surrounding fibrous matrices	[187]
	CuO	PAN/CuO	*E. coli* and *B. subtilis*	Excellent antimicrobial feature	Release of Cu	[112]
	ZnO	PCL/n-HA/ZnO	*E. coli* and *S. aureus*	>95 % reduction in bacterial adhesion of *E. coli and S. aureus* with the incorporation of 15 wt % and 30 wt % ZnO	Controllable release of ZnO and producing ROS	[188]
	TiO_2	TiO_2/PAN	*S. aureus*	5.5 antibacterial activity	Generation of ROS including ·OH, H_2O_2 and HO_2• under UV light irradiation	[189]
	CeO_{2-x} nanozymes	PVA mats with CeO_{2-x} NRs	*E. coli*	69 % reduction of bacterial adhesion	Haloperoxidase-like activity that can efficiently trigger oxidative bronmination	[190]
	SWNTs	SWNTs-PAN/TPU/PANI composite nanofiber membrane	*E. coli*	Complete (5 log) inactivation of bacteria within 20 min at 3.0 v applied voltage	Electrochemical disinfection mainly involving (i) direct oxidation of pathogens in contact with the nanofiber membrane anode and (ii) indirect oxidation of pathogens that produced aqueous oxidants through the anode	[191]
	GO	PCL/Gel/GO nanofibrous web	*E. coli* and *S. aureus*	99 % antibacterial properties against *E. coli* and *S. aureus*	Sharp edges of graphene nanosheet, inducing physical damage on bacterial cell membrane, resulting in loss of bacterial membrane integrity	[192]
	BN	mBN-PVA/PAA composite nanofibers	*E. coli* and *S. aureus*	65 % and 75 % reduction for *E. coli* and *S. aureus*, respectively	Oxidative stress from the generation of ROSs, membrane damage from the insertion of BN nanomaterials into the bacterial cell membrane and the ability to perform endocytosis	[193]
	BP	Apt-modified PCL-BP hybrid fiber scaffold	*S. aureus*	Significant inhibition effect on bacterial growth	NIR-induced photothermal effect to eliminate bacteria and prevent infection	[194]
	g-C_3N_4	Cl/S-*g*-C_3N_4 composite membranes	*E. coli* and *S. aureus*	94.2 % and 90.4 % antibacterial rates against *E. coli* and *S. aureus*, respectively	Generation of active free radicals by Cl/S-*g*-C_3N_4 under visible light	[195]
	$Ti_3C_2T_z$	MXene/CS	*E. coli* and *S. aureus*	95 % reduction rate against *E. coli* and 62 % against *S. aureus*	Antibacterial nature of $Ti_3C_2T_z$ flakes	[196]
Organic	Car-NPs	G-Car-NPs-NF	*E. coli*, *S. aureus*, and *C. albicans*	Bacteriostatic zone on the medium coated with *E. coli*, *S. aureus* and *C. albicans*	Interaction between the antibacterial activity of Car itself and microbial cell membrane components	[197]
	CS-NPs	PA6/CS-NPs hybrid nanofibers	*E. coli* and *S. aureus*	99.9 % and 98.9 % antibacterial efficiencies against *E. coli* and *S. aureus*, respectively	Excellent antibacterial activity due to the CS-NPs adhered to the surface of the nanofibers	[198]
	LgNP	LgNP/PCL nanofiber scaffold	*S. aureus*	Bactericidal efficacy against the major orthopedic infectious staphylococcal species	Contact mechanism-based antibacterial action between the phenolic fragments of lignin and bacterial cell wall, leading to lysis effect	[199]
	HOF-101 nanocrystalline	HOF-101@PVDF-HFP nanofibers	*E. coli*	Almost 97 % of *E. coli* killed after illumination under simulated daylight for 5 min	Excellent $^1O_2$ productivity of HOF-101 under simulated daylight irradiation for 5 min	[69]
Inorganic-organic hybrid	AIE-featured Au NCs	Au NCs-functionalized fiber	*E. coli* and *S. aureus*	≥98.5 % and ≥99.94 % antibacterial activities against *S. aureus* and *E. coli* under visible-light irradiation, respectively	ROSs generation and Au NCs	[79]
	APA-modified Au NPs	APA_Au-modified PCL/gelatin	MDR *E. coli*	Superior activity on MDR *E. coli*-infected wound	Synthetic effects of antibacterial intermediates (APA) and Au NPs	[80]
	PDA adherent Cu-NPs	PLLA@PDA/Cu	*E. coli* and *S. aureus*	99 % and 94 % inhibitory rates against *E. coli* and *S. aureus*	Synergistic antibacterial effect with PTT	[200]
	CHS/AgNPs	PEO/CHS(AgNPs)	*E. coli* and *S. aureus*	Good antibacterial activity with ZOI against *E. coli* and *S. aureus* of 51.2 ± 3.2 and 47.2 ± 2.1, respectively	Synergistic effect between Ag NPs and CHS	[201]
	ZIF-8	PCL-LSMM-CMZIF-8	*E. coli* and *S. aureus*	Up to 22.6 mm and 24.0 mm inhibition zones against *E. coli and S. aureus*, respectively	Release of Zn^{2+}	[202]
	Ag_2[HBTC][im] compound	Ag-MOF/PLA	*E. coli*, *S. aureus*, *P. aeruginosa* and *M. smegmatis*	>95.0 % bacteria inhibition rate for broad-spectrum bacteria killing performance; 99.9 % wound healing rate towards *in vivo S. aureus*-infected wound therapy	Controllable Ag^+ release and ROS generation	[83]

Abbreviations: PLLA, poly(L-lactic acid); *E. coli*, *Escherichia coli*; PAN, polyacrylonitrile; *B. subtilis*, *Bacillus subtilis*; PCL, polycaprolactone; nHA, nano-hydroxyapatite; *S. aureus*, *Staphylococcus aureus*; PVA, polyvinyl alcohol; SWNTs, single-walled carbon nanotubes; TPU, polyurethane; PANI, polyaniline; Gel, gelatin; GO, graphene oxide; BN, boron nitride; PAA, polyacrylic acid; BP, black phosphorus; CS, chitosan; Car, carvacrol; G-Car-NPs-NF, gelatin nanofiber membranes containing carvacrol nanoparticles; *C. albicans*, *Candida albicans*; PA-6, polyamide-6; LgNP, lignin nanoparticles; HOF, hydrogen-bonded organic frameworks; CS-NPs, chitosan nanoparticles; PVDF, polyvinylidene fluoride; AIE, aggregation-induced emission; NCs, nanoclusters; APA, 6-aminopenicillanic acid; Apt, aptamer; MDR, multidrug-resistant; PDA, polydopamine; PEO, polyethylene oxide; CHS, chitosan; ZOI, Zone of inhibition; HBTC, 1,3,5-benzenetricarboxylate; im, imidazole; *P. aeruginosa*, *Pseudomonas aeruginosa*; *M. smegmatis*, *Mycobacterium smegmatis*.

3.2.1. Metal nanomaterials loaded eNFMs

In recent decades, metal NPs (*e.g.*, Au, Ag, and Cu) or their oxides and sulfides have demonstrated with potent antibacterial activity by inducing bacterial membrane damage or ROSs accumulation. Consequently, great efforts have been made to incorporate metal or metal oxide/sulfide nanomaterials into eNFMs due to their exceptional stability, distinct antimicrobial property, and targeted efficacy against bacteria instead of conventional antibiotic small molecules. The following subsections will mainly discuss diverse fabrication strategies for metal NPs-based eNFMs and metal oxide/sulfide-based eNFMs, elucidating their antibacterial mechanisms and bactericidal performance.

3.2.1.1. Metal NPs loaded eNFMs. Historically, Ag-based nanomaterials, such as Ag-polymers complex, Ag NPs, Ag NWs and so on, have been extensively exploited as potent bactericidal nanomaterials against a broad spectrum of pathogenic micro-organisms including viruses, microbes, bacteria, and other eukaryotic micro-organisms [84–86]. Among Ag-based nanomaterials, Ag NPs have garnered much attentions due to their unique properties, such as high electrical conductivity, chemical stability, catalytic activity and antibacterial property [87,88]. Owing to their unique physicochemical properties, diverse strategies for the synthesis of Ag NPs onto eNFMs have been proposed involving the reduction of Ag^{+} ions in $AgNO_3$ through (i) *in situ* formation Ag NPs onto eNFMs by reducing agents (including traditional chemical reductants and natural reductant agents) [57,89], (ii) mussel-inspired synthesis of Ag NPs onto eNFMs [90], (iii) electroless deposition of Ag NPs onto eNFMs [91], and (iv) magnetic sputtering of Ag NPs onto eNFMs [92].

Conventional chemical reductants, such as $NaBH_4$, $N_2H_4{\bullet}H_2O$, and NaOH, are commonly employed for the synthesis of Ag NPs from Ag NO_3. For instance, via the electrostatic interaction between carboxylate ions and Ag^{+} and followed by reducing with $NaBH_4$, a cross-linked poly (acrylic acid) (PAA) modified poly(ether sulfone) (PES) nanofibrous membrane (NFM) was prepared by Chen et al. [57], and then immersed into $AgNO_3$ solution and $NaBH_4$ solution, respectively. Consequently, the Ag NPs were *in situ* formed onto PAA/PES NFM from $AgNO_3$ using $NaBH_4$ as reducing agent, as illustrated in Fig. 2A. The Ag NPs-loaded NFM presented 93.4 % and 95.7 % bactericidal efficiency against *E. coli* and *S. aureus*, respectively.

In addition, in order to study the effects of different reducing agents on bactericidal properties, Muhammad et al. prepared nanofibers containing Ag NPs with different reducing agents such as NaOH, $NaBH_4$, sodium citrate, and ultraviolet (UV) [89]. The results of water contact angle measurements showed that the surface wettability of NaOH treatment was poor, while that of $NaBH_4$ and sodium citrate treatment was better. UV treatment resulted in a slight increase in surface wettability. Inhibition zone tests indicated that NaOH and UV treatments had significant inhibitory effects on *E. coli* and *Bacillus subtilis* (*B. subtilis*), while $NaBH_4$ and sodium citrate treatments had moderate inhibitory effects. Additionally, as shown in Fig. 2B, the Ag release profile showed a continuous release of Ag^{+} over time, with a higher release rate for the sodium citrate treatment.

To address the environmental and potential healthcare concerns associated with the traditional chemical reductants, naturally derived reducing agents, such as citric acid, ascorbic acid, glucose, histidine, heparin, polysaccharides, and dopamine (DA) have been employed in the synthesis of Ag NPs. For instance, El-Aassar et al. prepared Ag NPs-embedded polygalacturonic acid/HA/PVA) ((Ag-PGA/HA)-PVA) electrospun nanofibers by pre-encapsulating Ag NPs with an average size 8.6 nm within PGA [93]. In this system, PGA containing abundant carboxylic and hydroxylic groups served as an effective reducing and stabilizing agent for converting Ag^{+} into Ag NPs. Notably, the mussel-inspired green method is capable of synthesizing Ag NPs on eNFMs. Owing to the presence of abundant catechol groups, PDA, a biomimetic polymer derived from mussel adhesive protein, exhibits reductive capacity for the formation of Ag NPs [94]. This unique reducing property of PDA enables the preparation of Ag NPs-loaded eNFMs without the need for organic solvents or chemical reducing agents. Moreover, the strong interactions between PDA and Ag contribute to long-term bactericidal effects. To address issues related to uncontrolled size and aggregation of Ag NPs, GhavamiNejad and co-workers proposed a versatile method involving catechol redox chemistry for synthesizing novel catechol moieties that can be used in functionalized electrospun nanofibers with embedded Ag NPs [90]. The mussel-inspired copolymer solution of poly(dopamine methacrylamide-*co*-methyl methacrylate) (MADO) was spun and subsequently nanofibers were decorated with Ag NPs through the catecholic moiety of DA in polymeric backbone. This mussel-inspired approach facilitated the homogeneous dispersion of highly monodispersed Ag NPs with well-controlled particle sizes on the nanofiber surfaces (Fig. 2C). With containing 1 % Ag NPs, the resulting MADO-AgNPs composite nanofibers exhibited remarkable bactericidal activity and demonstrated enhanced efficacy for wound healing.

Through electroless deposition method, Ag NPs could be immobilized on the surface of $Ti_3C_2T_x$-modified electrospun thermoplastic polyurethane (TPU) fibrous membranes, resulting in AgNPs/$Ti_3C_2T_x$/TPU fibrous membranes [95], as shown in Fig. 2D. In addition, Ag NPs could be also incorporated on the surface of electrospun membranes by magnetic sputtering method [92], as shown in Fig. 2E. Furthermore, ultrasonication irradiation is also a valuable technique for the incorporation of Ag NPs onto/into eNFMs to confer antibacterial activity. With the aid of ultrasonication, Shi and co-workers fabricated a nanofiber composite consisting of polyurethane-*g*-polyethylene glycol (TPU-*g*-PEG) by immobilizing Ag NPs onto the surface of electrospun nanofibers [96]. Briefly, upon ultrasonication treatment, cavitation bubbles were initially generated in the liquid medium. As these bubbles approached the Ag NPs, they underwent asymmetric collapse, resulting in the production of high-speed jets and shock waves that propelled, the Ag NPs towards the surface of electrospun nanofibers at remarkable velocities. Consequently, an interfacial collision between Ag NPs and eNFMs was achieved. Meanwhile, these jets and shock waves can exert a tremendous force on the surface, causing the TPU electrospun nanofibers to soften or even partially melt at the impact sites. Through the combined effects mentioned above, Ag NPs can be securely anchored onto the surface of TPU nanofibers. In addition, due to its superior expansion ability, TPU-*g*-PEG exhibits a softer surface compared to TPU nanofibers, facilitating enhanced embedding Ag NPs on TPU-*g*-PEG nanofiber surface with ultrasonication assistance.

Herein, despite the unique advantages of Ag NPs-based eNFMs in combating bacterial infection and eliminating biofilm, their excessive and nonspecific toxicity pose a potential threat to healthy cells and tissues, thereby limiting their clinical applications. Moreover, the metal ion-release antibacterial mechanism hinders the long-term retention of bactericidal effects in practical applications.

Additionally, due to their low toxicity, facile functionalization, excellent biocompatibility, ease of characterization, and extensive surface chemistry knowledge base, Au NPs have garnered sustained interest in the field of biomedical applications [97,98]. Moreover, the incorporation of Au NPs into eNFMs has been reported for their bactericidal properties. Wang et al. integrated mercaptophenylboronic acid (MBA)-activated Au NPs (Au_MBA NPs) into electrospun PCL/Gel NFMs to combat Gram-positive MDR bacteria and facilitate infected wound healing [81]. TEM tests demonstrated that Au_MBA NPs adhered to the bacterial wall and located in the cytosol area of bacteria, leading to the disruption of bacterial cell walls and bacteriolysis. The prepared Au_MBA/PCL/Gel NFMs were effective in *S. aureus*- or MDR *S. aureus*-infected wound model on rats. In another study, Zhao and co-workers developed indole derivate-capped Au NPs (Au_IDs) to fight MDR bacteria [82]. Au_IDs can effectively eliminate majority of multidrug-resistant (MDR) bacteria even at high concentrations of

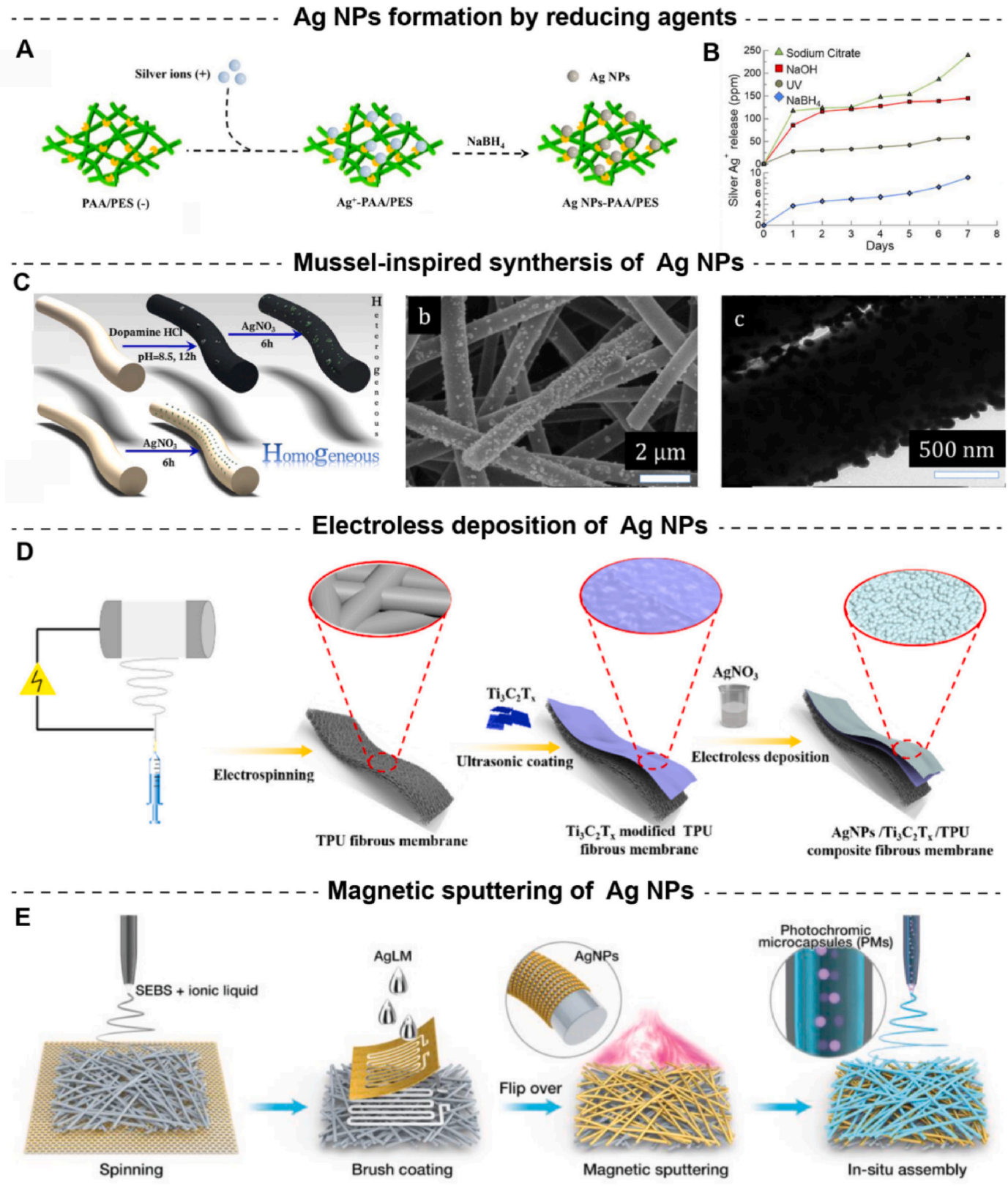

Fig. 2. Various strategies for incorporating Ag NPs into eNFMs. (A) The preparation of Ag NPs decorated PAA/PES NFM through $NaBH_4$ reduction. Reprinted with permission from Ref. [57]. Copyright 2018, Elsevier Inc. (B) The effect of different reducing agents (including NaOH, $NaBH_4$, sodium citrate, and under UV light) on Ag^+ release behaviors by Ag NPs doped MoO_3/PAN nanofiber membranes. Reprinted with permission from Ref. [89]. Copyright 2023, American Chemical Society. (C) The synthesis of size-controlled Ag NPs functionalized electrospun nanofibers through a mussel-inspired approach. Reprinted with permission from Ref. [90]. Copyright 2015, American Chemical Society. (D) The fabrication of AgNPs/$Ti_3C_2T_X$/TPU composite fibrous membrane via a chemical Ag plating process involving the electrostatic interaction between negatively-charged and reductive $Ti_3C_2T_X$ and selectively adsorbed Ag^+ onto TPU fibrous membrane. Reprinted with permission from Ref. [91]. Copyright 2023, American Chemical Society. (E) Magnetically sputtering to decorate non-woven textiles with Ag NPs. Reprinted with permission from Ref. [92]. Copyright 2023, Wiley-VCH.

bacteria, superior to the traditional antibiotics. Additionally, *in vivo* experiments demonstrated that the Au_IDs electrospun fibers possessed remarkable bactericidal activities against MDR bacterial infection when used as wound dressings.

3.2.1.2. Metal oxides/sulfides loaded eNFMs. As mentioned above, metal oxide/sulfide (such as ZnO, CuO, TiO_2, CuS, and MoS_2) nanomaterials have been widely employed as antibacterial additives [99–101] in the preparation of antibacterial eNFMs due to their potent antibacterial effect against a broad spectrum of bacteria.

Among metal oxides nanomaterials, ZnO NPs have gained much attention due to their recognized safety by the US FDA (21CFR 182.8991) [102], as well as their potent antimicrobial activity and pronounced inhibitory effect on various bacteria, even at low concentrations. Compared with other metal oxide nanoparticles, ZnO NPs not only have good antibacterial properties and can be used in food preservation and medical devices to reduce the risk of bacterial infection, but also exhibit lower toxicity, good biocompatibility, low production cost and versatility. Additionally, ZnO NPs can be produced by green synthesis methods that avoid the use of harmful and expensive precursors, thereby improving their safety and environmental protection. Moreover, ZnO NPs are generally recognized as safe based on their history of use and safety assessment in food, pharmaceutical and cosmetic products. However, it should be noted that the safety of ZnO NPs is also affected by factors such as their dose, size, shape and surface properties. Long-term or high dose use may result in dose-dependent toxicity. Therefore, although ZnO NPs are generally considered safe, their safety in specific applications needs to be carefully evaluated and good manufacturing practices followed.

These remarkable antimicrobial properties stem from their photocatalytic nature and ability to product ROS upon UV/Vis illumination, leading to bacterial membrane leakage and intracellular damage [103]. Moreover, different structures of ZnO nanomaterials, including spherical, branched, and rod-shaped forms, have been incorporated into eNFMs through embedding or post-solution growth techniques to enhance bactericidal activities. As an illustrative example, Liu and co-workers developed ethylcellulose/Gel nanofibers containing ZnO NPs for antimicrobial packaging [104]. Upon UV illumination, the bactericidal efficiency of the ZnO-containing nanofibers against *S. aureus* was 43.7 %, which further increased to 62.5 % due to a significant elevation in intracellular ROS levels. By integrating ZnO NPs, Grande et al. demonstrated that ZnO-modified PLA composite mats not only exhibited increased bactericidal effect but also improved mechanical properties [105]. To mitigate the aggregation of ZnO in the polymer matrix, Abdalkarim et al. prepared sheet-like cellulose nanocrystal (CNC)-ZnO nanohybrid composite poly(3-hydroxybutyrate-co-3-hydroxy valerate (PHBV) nanofibers by electrospinning [106]. In this particular system, the dispersibility of ZnO within the polymer matrix was significantly enhanced by exploiting electrostatic interactions between ZnO and CNC.

Besides directly blending electrospinning, coaxial electrospinning is also employed for the fabrication of ZnO-based antibacterial eNFMs. For instance, Hadisi et al. prepared a core-shell structured HA-based silk fibroin (SF)/ZnO electrospun dressing for burn wound management [107]. The core layer was loaded with ZnO NPs, enabling sustained drug release and preservation of its bioactivity. Transmission electron microscopy (TEM) confirmed the presence of a core-shell structure in the ZnO-loaded HA-SF fiber. With the increase of ZnO content, the bactericidal efficacy against *E. coli* and *S. aureus* were enhanced, which may be ascribed to the induced oxidative stress by ROS generation from ZnO NPs and direct or electrostatic interaction between bacterial cell surface and Zn^{2+} ions, leading to damage to bacterial cell membranes.

Particularly, Nasajpour et al. incorporated anisotropic branched-shaped ZnO NPs into a fibrous scaffold [108], which demonstrated the ability of ZnO to induce physical damage to bacterial cell membranes. During the electrospinning process, phase separation was suppressed, allowing the particles to be distributed throughout the fiber network and creating branching protrusions on the fiber surface that resemble rose spikes. As shown in Fig. 3A, the surface of the nanofibers embedded spherical particles appeared slightly rough between fiber interphase, while the surface of bare PCL fiber remained smooth. Compared to the pristine PCL, reduced adhesion and proliferation ability of prokaryotic microorganisms (*E. coli* and *P. aeruginosa*) on ZnO composite fiber scaffolds were observed, leading to a decrease in bacterial biofilms formation, thus confirming the antibacterial properties conferred by ZnO incorporation. This disparity may be attributed to the surface morphology of the fibrous substrates containing spherical and branched particles. In addition, exposure to ZnO nanospikes may also help to improve bactericidal performance while promoting eukaryotic cell growth.

Recently, zinc acetyl acetonate dihydrate ($Zn(Ac)_2•2H_2O$) has gained much attention as a precursor for the *in situ* formation of ZnO nanomaterials on electrospun nanofibers. As a typical example, Chen and co-workers prepared a pine-needle-like PVDF/(ZnO NRs@PAN) membrane containing ZnO NRs [109]. Briefly, as presented in Fig. 3B, the PAN-$Zn(Ac)_2$ precursor solution was electrospun onto the surface of electrospun PVDF membranes to fabricate a PVDF/(PAN-$Zn(Ac)_2$) composite membrane. Subsequently, $Zn(AC)_2$ was converted into ZnO by subjecting it to a thermal treatment at 130 °C for 10 h. During this hydrothermal process, *in-situ* formation of ZnO NRs occurred and their morphology was optimized by controlling the concentrations of Zn^{2+}. Interestingly, the resulting pine-needle-like structures of ZnO NRs facilitated to killing bacteria. The composite membrane effectively inactivated nearly all bacteria in the solution with a bactericidal rate exceeding 99.99 %, which could be attributed to the released Zn^{2+} from ZnO NRs.

Similarly, Qu and co-workers developed a *N*-halamine/ZnO-based platform for bacterial inactivation with multi-modal antibacterial mechanisms by the combination of electrospinning, hydrothermal reaction and chlorination [110]. Briefly, PAM was firstly prepared by copolymerizing 3-allyl-5, 5-dimethylhydantoin (ADMH) and methyl methacrylate (MMA). Then by mixing PAM with $Zn(Ac)_2$ and PAN in DMF, the spinning solution was further electrospun into PAM/$Zn(Ac)_2$ microfibers. Subsequently, PAM/ZnO microfibers were prepared by a hydrothermal reaction. Finally, PAM-Cl/ZnO microfibers were fabricated through chlorinating PAM/ZnO microfibers. *In vitro* antibacterial tests demonstrated that the obtained microfibers presented an enhanced synergistic effect against *E. coli* and *S. aureus*. The bactericidal effect was due to the contact killing of *N*-halamine on N-Cl bond and multiple-release bactericidal action such as ROSs under light irradiation, and Zn^{2+} and Cl^{+} ions.

Similarly, in the study conducted by Mascia and co-workers, ZnO NPs were *in situ* generated onto PEI-based nanofibers through successive sol-gel reaction steps [111]. In this system, $Zn(Ac)_2•2H_2O$ was selected as the precursor for the sol-gel reaction, leading to nucleation and growth of wurtzite crystals within PEI matrix. The resulting zein/PEI-ZnO nanofibers showed presented a significant inhibitory zone (0.80 ± 0.1 cm) against bacterial proliferation according to *in vitro* tests.

Pure copper and copper compounds such as CuO, CuS, and $Cu(OH)_2$ are also potential candidates for imparting bactericidal activity to eNFMs. These compounds can act as chemical nanoreactors that generate Cu^{2+} ions and ROSs through Fenton-like and Haber-Weiss reactions. For instance, in the study conducted by Hashmi and co-workers, incorporation of CuO NPs into electrospun PAN membranes demonstrated bactericidal activity [112]. The antimicrobial efficacy of released Cu from PAN nanofibers was confirmed by the presence of bacterial inhibition zones. With increasing CuO concentration, the inhibition zone exhibited a gradual increase. Due to the exceptional antimicrobial properties of CuO, nanofibers containing 1 % CuO concentration demonstrated excellent antibacterial efficacy. To study the effect of Cu^{2+} ions on antibacterial performance, Cordeiro and colleagues

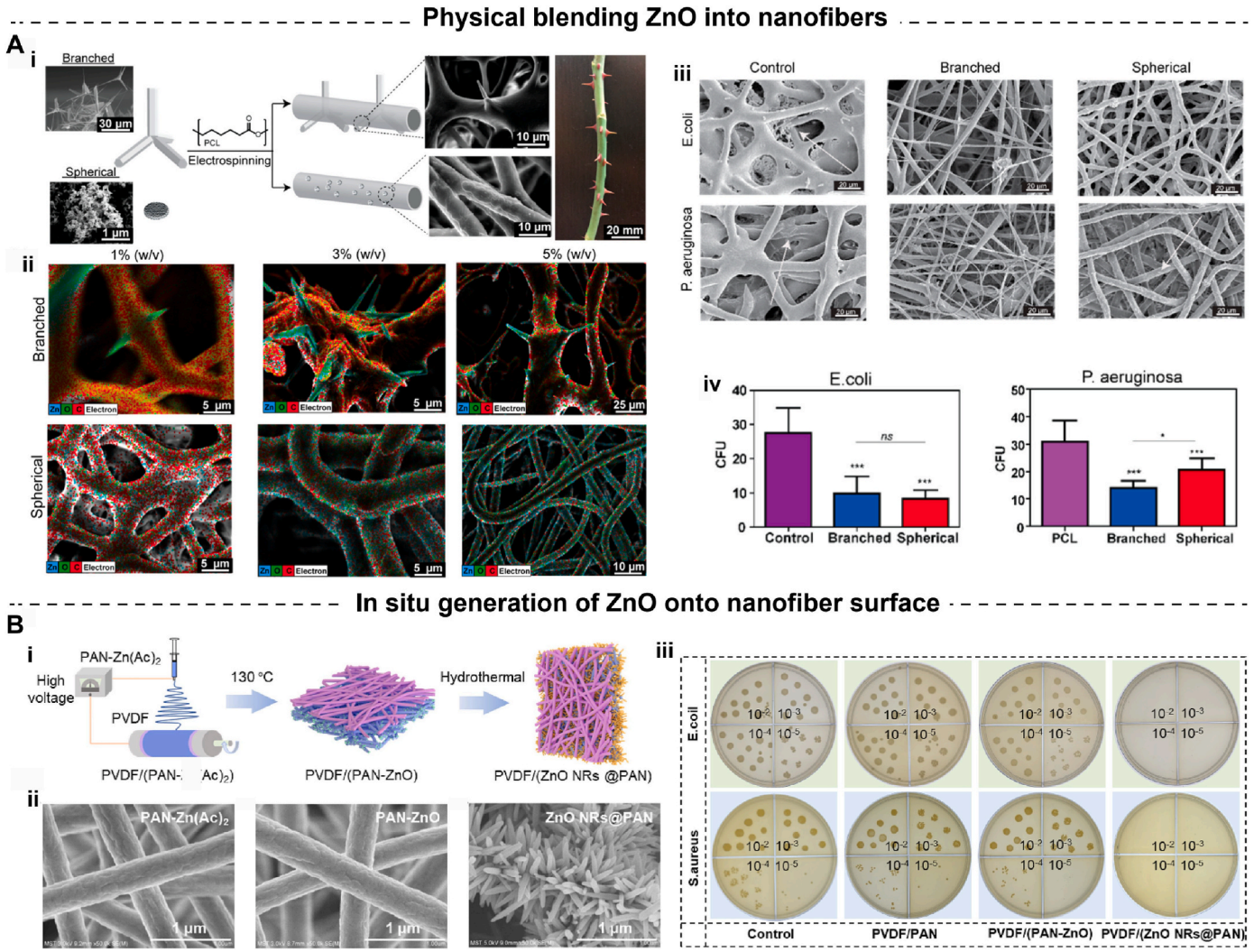

Fig. 3. Two representative strategies for incorporating ZnO with various structures (including spherical, branched, and rod-shaped) into eNFMs to enhance antibacterial activities. (A) (i) Schematic representation of a fibrous composite PCL membrane containing spherical and branched ZnO particles. (ii) EDAX mapping of branched and spherical ZnO particles at different concentrations and their distribution within the fibers. (iii) SEM images of the control sample (PCL), as well as the branched and spherical samples and (iv) corresponding quantification of CUFs after incubation with *E. coli* and *P. aeruginosa* for 24 h. Reprinted with permission from Ref. [108]. Copyright 2017, American Chemical Society. (B) (i) Schematic illustration of PVDF/(ZnO NRs@PAN) nanofibrous membrane fabrication processes. (ii) SEM images of PAN membranes at different stages during fabrication. (iii) Photographs showing colonies of *E. coli* and *S. aureus* on agar dishes from different experimental groups. Reprinted with permission from Ref. [109]. Copyright 2023, Elsevier B.V.

prepared electrospun membranes loaded with varying concentrations of CuO (ranging from 0.05% to 1%) using the electrospinning technique [113]. They observed sustained release of pH-sensitive Cu^{2+} ions from these membranes for up to 7 days and, and noted that the bactericidal effect was dependent on the concentration of copper.

Titanium dioxide (TiO_2), a typical photocatalytic agent, can generate ROS when exposed to UV irradiation [114]. It is commonly employed as a photocatalytic antibacterial additive for functionalizing eNFMs. Typically, three main approaches have been reported for preparing TiO_2-incorporated eNFMs with bactericidal activities: (i) direct electrospinning a homogeneous TiO_2 spinning solution, (ii) electrospinning a fibrous substrate followed by coating with TiO_2, and (iii) combining an electrospun TiO_2 fiber precursor with a high-temperature calcination process. To prepare TiO_2-loaded nanofibers by direct electrospinning, as a typical example, Karbowniczek et al. presented two types of electrospun poly(3-hydroxybuty-rate-*co*-3-hydroxyvalerate) (PHBV) nanofibers loaded with TiO_2 (bPHBV + TiO_2 and cPHBV + TiO_2), serving as tissue engineering scaffolds [115]. As illustrated in Fig. 4A, the bPHBV + TiO_2 scaffold was prepared by electrospinning a blended solution of PHBV and TiO_2, while the cPHBV + TiO_2 scaffold was fabricated via coaxial electrospinning of core PHBV fibers coated with TiO_2 NPs. Compared to the bPHBV + TiO_2 scaffold, the cPHBV + TiO_2 scaffold presented better antibacterial performance upon exposure to UV light.

By integrating electrospinning and thermal treatment process, Wang and co-workers developed TiO_2/GDY composite nanofibers [56]. In brief, a solution containing tetrabutyl titanate (TBT) and PVP was electrospun to form the precursor of TiO_2 fibers. Subsequently, the obtained nanofibers were subjected to a 2-h thermal treatment at 550 °C in air, followed by the assembly of GDY onto TiO_2 nanofibers through electrostatic force and calcination at 350 °C for another 2 h. Under UV light irradiation, the obtained TiO_2/GDY nanofibers exhibited superior photocatalytic antibacterial effect due to the enhanced photocatalytic ROS generation (Fig. 4B). The abundant ROSs induced oxidation of cellular components and perforation of bacterial cell walls, leading to membrane leakage, structural damage, and ultimately bacterial death. In addition, the bactericidal activity of TiO_2/GDY was found to be sustained through continuous release of ROS, leading to cell wall perforation and effectively preventing formation by methicillin-resistant

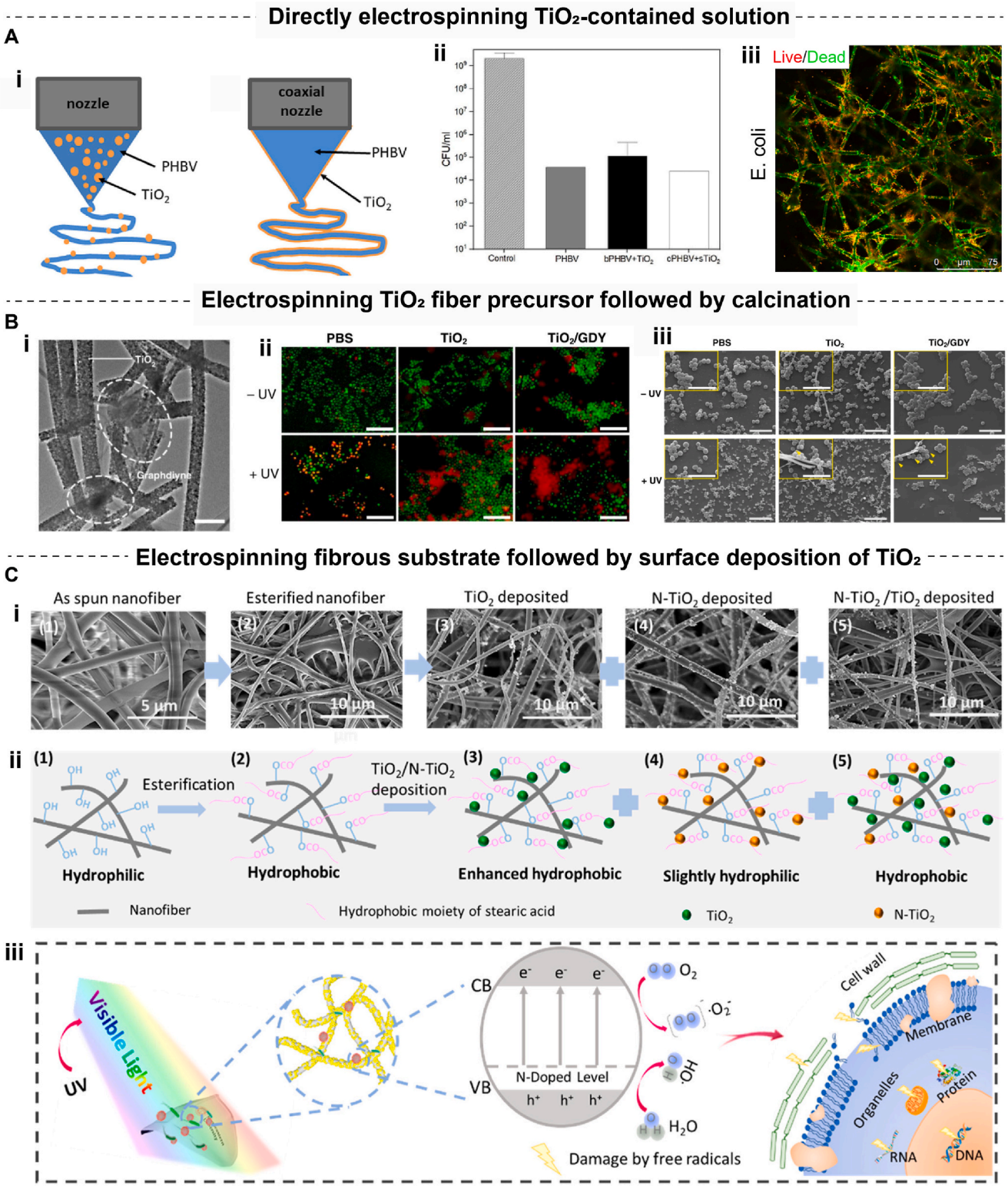

Fig. 4. Three representative routes for incorporating TiO_2 nanomaterials into eNFMs with bactericidal activities. (A) (i) Schematics of blended electrospinning of PHBV and TiO_2 NPs, and co-axial electrospinning with PHBV in the core layer and TiO_2 NPs in shell layer. (ii) The number of *E. coli* after 24 h incubation on the materials. (iii) Live/dead imaging of *E. coli* incubated for 16 h on the core-shell PBHV-TiO_2 scaffold. Reprinted with permission from Ref. [115] Copyright 2023, Elsevier Inc. (B) (i) TEM image of GDY-modified TiO_2 nanofibers. (ii) Live/dead staining images of MRSA biofilms treated by different groups with or without UV irradiation, and (iii) SEM images of MRSA biofilms after photocatalytic treatment with nanofibers. Reprinted with permission from Ref. [56]. Copyright 2020, Nature. (C) (i) SEM images of as-spun nanofibers subjected to various treatment processes. (ii) Schematics of the functionalization process involving hydrophobilization and subsequent deposition of N-TiO_2 onto as-spun nanofibers. (iii) Antibacterial mechanism under light irradiation for a mask containing N-TiO_2. Reprinted with permission from Ref. [118]. Copyright 2021, American Chemical Society.

Staphylococcus aureus (*MRSA*). Approximately 76 % of the biofilm was eradicated after UV irradiation, as confirmed by crystal violet staining results. Notably, the TiO_2/GDY group exhibited significantly reduced biofilm formation compared to other groups.

To further enhance the photo-catalytic antimicrobial effect of TiO_2 composite nanofibers, doping with metals such as Ag or Cu compounds is a commonly employed method. For example, Lee et al. developed Ag NPs-loaded TiO_2 composite nanofibers to argument enhancing antibacterial activity [116]. The pre-electrospun TiO_2 nanofibers were immersed in $AgNO_3$ solutions and then exposed to UV light for Ag NPs formation. The bactericidal rate of the prepared Ag/TiO_2 composite nanofibers was with 83.47 ± 0.87 % in dark for 1 h. Additionally, utilizing an environmentally friendly chemistry method, Ni et al. developed cellulose acetate (CA) nanofibers containing Ag NPs embedded TiO_2 NPs for long-term significant bactericidal activity [117]. In addition to metal ions, heteroatoms also employed as dopants onto the TiO_2 NPs to improve the photo-catalytic antimicrobial effect of the composite nanofibers. Li et al. presented a reusable, biodegradable, and antimicrobial mask by electrospinning PVA, PEO, and cellulose nanofiber, followed by esterifying and deposition of a nitrogen-doped TiO_2 (N-TiO_2) and TiO_2 mixtures [118]. Upon exposure to 0.1 solar illumination or natural sunlight for a duration of only 10 min, the fabricated nanofibers containing photocatalytic N-TiO_2/TiO_2 presented 100 % bactericidal activity. As illustrated in Fig. 4C, the robust photocatalytic antibacterial performance could be attributed to the generation of •OH and $•O_2^-$ by N-TiO_2 containing nanofibers upon light irradiation, which have the ability to impair cell walls, membranes, RNA, proteins, organelles, or deposit pathogen DNA. Particularly, these nanofibers with N-TiO_2 can be used for facial recovery through brief periods of light exposure to effectively sterilize deposited pathogens and enable direct reuse.

In addition, other active metal oxide/sulfide-based nanoparticles such as MgO, WO_3, MoS_2, and CeO_2, have also been investigated for their bactericidal activities in enhancing the functionality of eNFMs [119–121]. For instance, Ma and her colleagues prepared a multifunctional branched PEI and PAA/WO_3/PAN composite membrane using a combination of blow spinning and LbL techniques [122]. The incorporation of hydrophilic PAN fibers decorated with WO_3 nanoparticles exhibited excellent photodegradation behavior against organic pollutants while demonstrating superior bactericidal effect owing to their synergetic electron interactions. Both the WO_3/PAN and PP/WO_3/PAN membranes displayed significant bactericidal activity against *B. subtilis*

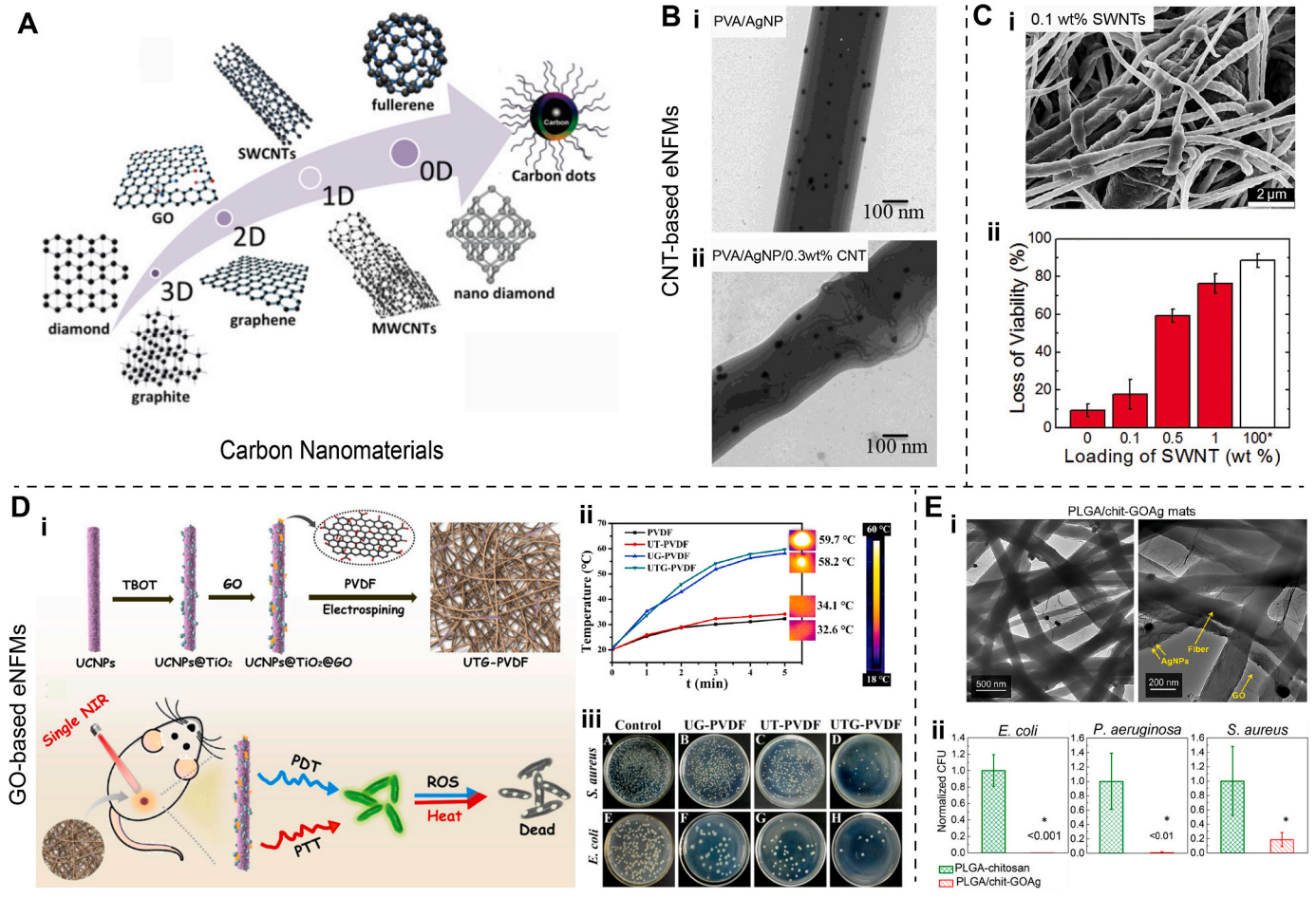

Fig. 5. Representative carbon nanomaterials incorporated into eNFMs with bactericidal activities. (A) Representative carbon-based nanomaterials. Reprinted with permission from Ref. [124]. Copyright 2020, Wiley-VCH. (B) TEM images of electrospun (i) PVA/AgNP composite mat and (ii) PVA/AgNP/CNT composite mat containing 0.3 wt% CNT by electrospinning process. Reprinted with permission from Ref. [134]. Copyright 2020, Elsevier B.V. (C) (i) SEM image of *E. coli* after 1 h incubation on SWNTs-embedded PSf mats. (ii) Fluorescent-based toxicity analysis of electrospun PSf mats with different contents of SWNTs and a commercial filter coated with 100 wt% SWNTs. Reprinted with permission from Ref. [135]. Copyright 2011, American Chemical Society. (D) (i) Schematic illustrations depicting the preparation process of UTG-PVDF nanocomposite membrane and its corresponding antibacterial efficacy under NIR light irradiation. (ii) Temperature monitoring of diverse membranes after NIR illumination. (iii) Photos of *S. aureus* and *E. coli* colonies grown on broth plates on different membranes upon NIR light irradiation, with UTG-PVDF membranes in the dark as control group. Reprinted with permission from Ref. [143]. Copyright 2019, American Chemical Society. (E) (i) TEM images revealed the presence of GO-Ag sheets decorating the surface of electrospun PLGA-CS mats. (ii) Number of viable bacteria cells attached to diverse mats. Reprinted with permission from Ref. [145]. Copyright 2015, American Chemical Society.

and *E. coli*. To further enhance antibacterial efficacy, multi-mode antibacterial eNFMs were developed by incorporating various metal compounds. In another study, Ci and co-workers reported the synthesis of photo-excited antimicrobial PCL@MoS_2/ZnS hybrid nanofibers [123]. The incorporation of MoS_2/ZnS imparted remarkable photothermal and photocatalytic properties to the hybrid nanofibers. Under visible light illumination for 10 min, the obtained PCL@MoS_2/ZnS hybrid nanofibers exhibited high bactericidal rates of up to 96.03 % and 99.09 % against *S. aureus* and *E. coli*, respectively, attributed to the synergistic effect of hyperthermia and ROS generation.

3.2.2. Carbon nanomaterial-loaded eNFMs

Carbon-based nanomaterials, as depicted in Fig. 5A, encompass a range of structures including 3D graphite, 2D graphene, 1D carbon nanotubes (MWCNTs), and 0D carbon dots (C-dots), along with nano diamonds [124]. These materials exhibit numerous appealing characteristics, such as broad light absorption across the UV-Vis-NIR spectrum, near-infrared (NIR) photoluminescence, remarkable photothermal response, and photosensitive ROSs production [125]. Due to their unique physicochemical properties and relative high biosafety, carbon-based nanomaterials such as CNT and GO have demonstrated great potential as antimicrobial nanomaterials for non-antibiotic therapies of infectious diseases [126]. CNT and GO are promising antimicrobial additives for modifying eNFMs to combat bacterial infections in biomedical fields. The following subsection mainly focuses on the fabrication strategies, bactericidal performance, and antibacterial mechanisms of CNT-based eNFMs and GO-based eNFMs.

3.2.2.1. CNT-loaded eNFMs. Carbon nanotubes (CNTs), as one of the allotropes of carbon characterized by cylindrical nanostructures, were first observed by Sumio lijima and co-workers in 1991 [127]. The classification of CNTs is based on the number of graphene sheets rolled on their surface, including single-walled carbon nanotubes (SWNTs) and multi-walled carbon nanotubes (MWNTs) [128]. CNTs possess unique structural and physicochemical properties, along with high electrical conductivity [129]. Additionally, CNTs exhibit bactericidal properties due to their ability to generate ROSs and possess photo-thermal conversion capability [130]. Particularly noteworthy is that incorporating CNTs into eNFMs can enhance both mechanical strength and antimicrobial activity [131].

As an illustrated example, Wang et al. directly incorporated acid-treated CNTs into the PCL spinning solution to prepare eNFMs [132]. The addition of CNTs significantly enhanced the mechanical strength of electrospun PCL fibers. In order to improve the bactericidal activity, Tiu Brylee David B et al. developed multilayer gas barrier films by modifying polystyrene nanofibers with MWNTs [133]. The incorporation of MWNTs into the nanofibers significantly enhanced the bactericidal effect, resulting in up to 97 % inactivation against *B. Subtilis*. Islam and co-workers developed a PVA/AgNP/CNT composite mat by electrospinning incorporating of 0.3 wt% CNT [134]. The inclusion of CNTs improved the thermal, mechanical and bactericidal properties of the mat, while Ag NPs were beneficial for improving its thermal and bactericidal properties (Fig. 5B).

The bactericidal effect of SWNTS is enhanced owing to their superior physicochemical properties, particularly in the case of SWNTs with a small diameter of 0.8 nm. To exploit this property, Schiffman and co-workers developed electrospun PSf-SWNT mats by incorporating varying weight percentages of SWNTs [135]. The longitudinal and axial distribution of SWNTs along the fibers can be observed in Fig. 5C. Notably, an increase in the incorporation of SWNTs from 0.1 wt% to 1.0 wt% resulted in a corresponding decrease in *E. coli* viability within the electrospun PSf-SWNT mat, as shown in Fig. 5C ranging from 18 % to 76 %. Moreover, time-dependent bacterial cytotoxicity tests demonstrated that the antibacterial activity of PSf-SWNTs mats was evident after only a contact time as short as 15 min or less.

3.2.2.2. Graphene-loaded eNFMs. Graphene-based nanomaterials, including graphene, GO, reduced graphene oxide (rGO), nanographene oxide (nGO) and graphene quantum dots (GQDs) [136–138], have gained significant attention in various fields. Among these derivatives, GO stand out as a popular choice due to its straightforward manufacturing process, high specific surface area, inherent optical and photothermal properties, as well as remarkable mechanical stiffness and strength [139]. The antibacterial performance of graphene and GO nanowalls was initially investigated by Akhavan and Ghaderi in 2010 [140]. The underlying mechanism involves the sharp edges of the nanowalls effectively damaging bacterial cell membranes upon direct contact. This leads to the efflux of intracellular matrix components and subsequent bacterial inactivation [141]. Afterwards, GO/rGOs were incorporated into eNFMs for antimicrobial applications.

As an illustration, Wang and co-workers developed silker fiber (SF)/GO blended nanofibers by electrospinning technology [29]. The bactericidal activity of SF/GO fibers was found to be superior to than that of the pristine SF fibers, indicating that the incorporation of GO imparts fibers with enhanced antibacterial capability to the fibers. To further enhance the antimicrobial activity, various polymers such as CS, polyamide, and PEI have been employed for modifying graphene nanosheets. Liu et al. developed PVA-*co*-PE nanofibers containing CS and GO through a melt-phase-separated nanofiber/CS-GO suspension coating method [142]. After modification with CS/GO, the inactivation rate of the nanofibers against *E. coli* and *S. aureus* increased to 97.8 %–99.5 %. A plausible antibacterial mechanism involving the physical attachment of CS and GO onto PVA-*co*-PE nanofibers is proposed. In physiological solutions as this medium, CS exhibits cationic surface charges originating from NH_3^+ groups, which facilitate strong electrostatic interactions with bacterial membrane phospholipids, eventually leading to cell membranes destruction. Simultaneously, GO initially induce displacement of phospholipid molecules from the cell membrane *through* robust van der Waals attractions and subsequently adsorb these extracted lipids via hydrophobic interactions, resulting in damage to the bacterial membrane.

Additionally, GO has been widely regarded as a promising candidate for the development of multi-model antibacterial agents to achieve synergistic sterilization. For instance, Sun and co-workers developed a nanocomposite membrane with synergistic PDT and PTT antibacterial effects [143]. In their study, as presented in Fig. 5D, nanosized GO was encapsulated within core-shell UCNPs@TiO_2 NPs, resulting in UCNPs@TiO_2@GO (UTG). Subsequently, UCNPs@TiO_2@GO was blended with PVDF and electrospun into a UTG-PVDF nanocomposite membrane. Under a single 980 nm NIR light irradiation, the temperature of the UTG-PVDF membrane rapidly increased above 55 °C within 5 min due to the photothermal effect induced by embedded GO under NIR excitation. Simultaneously, the incorporation of GO in nanocomposite membranes not only acts as an electron collector and transporter, effectively preventing photogenerated e^--h^+ recombination and prolonging their lifetime, but also significantly enhances ROS generation through photoactivation. Consequently, this synergistic PDT/PTT bactericidal property, triggered by a sole NIR light source, overcomes limitations associated with restricted UV or visible light penetration depth and eliminates complexities arising from multiple light sources.

In addition to the aforementioned physical antibacterial properties, the incorporation of Ag NPs onto graphene-based nanomaterials surfaces can also improve the performance of antibacterial matrices. The oxidizing groups on GO can serve as anchoring and nucleation sites for Ag NPs growth, thereby enhancing the bactericidal effect of GO/rGO-Ag NP nanocomposites. Meanwhile, GO exhibited high surface area that facilitates cell interaction and deposition [144]. Elimelech et al. prepared PLGA-CS eNFMs functionalized with GO-Ag nanocomposite through an *in-situ* method [145]. The coupling agents *N*-(3-dimethylaminopropyl)-*N*′-ethylcarbodiimide (EDC) and *N*-hydroxysuccinimide (NHS) were used to chemically anchor the GO-Ag nanocomposites on the CS modified PLGA fibers, so that the as-prepared GO-Ag

nanocomposites were uniformly distributed on the upper surface of the fibers. Ultimately, as shown in Fig. 5E, the PLGA/CS-GO-Ag mats exhibited inactivation rates of 99 % for *S. aureus* and 76 % against *E. coli* and *P. aeruginosa*. The antibacterial effects of PLGA/CS-GO-Ag mats were achieved by the synergetic effect of GO sheets and Ag NPs, facilitating effective interaction between bacteria and Ag NPs due to the large surface area provided by GO sheets. Meanwhile, bacterial inactivation was attributed to the direct interaction between released Ag^{+} ions and GO-Ag sheets.

3.2.3. MOF-loaded eNFMs

With the development of nanotechnology, MOFs, as a new type of porous nanomaterials, have exhibited remarkable potential in effectively eradicating bacteria through synergistic mechanisms [146–148]. Particularly, diverse MOFs such as ZIF-8 [149–151], PCN-224 [152], and HKUST-1 [153–155] can be uniformly encapsulated or coated onto electrospun fibrous substrates to mitigate aggregation and introduce abundant bactericidal active sites, producing highly flexible, recyclable, and reusable hybrid membranes with exceptional antibacterial properties [156–158]. Researchers have dedicated their efforts to the integration of MOFs into eNFMs for bactericidal activity, as well as expanding the practical applications of MOFs. Two primary approaches commonly utilized in the preparation of MOFs-incorporated eNFMs include (i) direct electrospinning of blended solutions containing MOFs

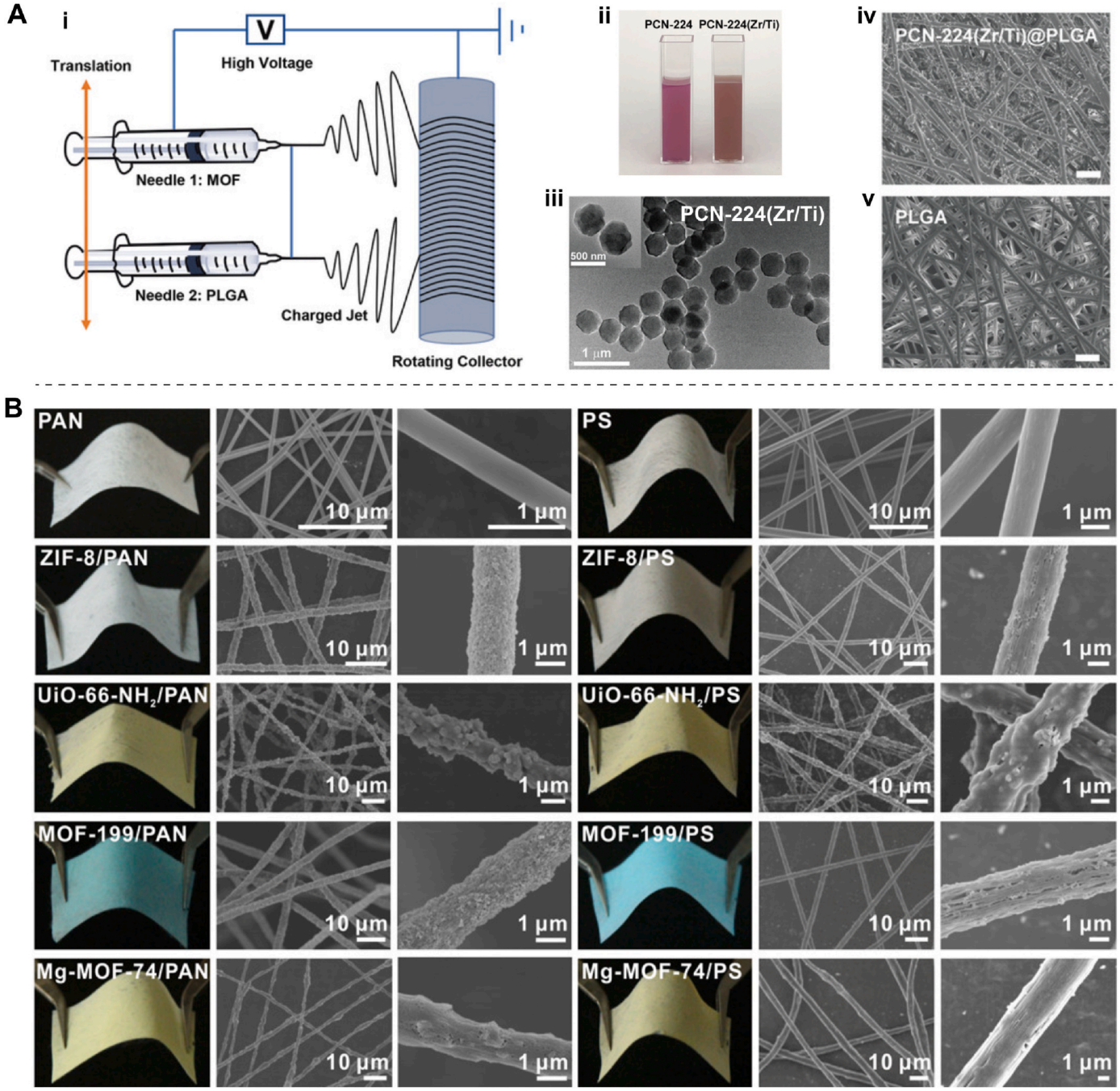

Fig. 6. Various MOFs incorporated into eNFMs by direct electrospinning of MOF/polymer solutions. (A) Preparation of PCN-224(Zr/Ti) NPs loaded PLGA fibrous dressing by electrospinning. Reprinted with permission from Ref. [159]. Copyright 2020, Wiley-VCH. (B) Photographs and SEM images of the different MOFs loaded eNFMs with 60 % wt% MOF loading into PAN or PS polymer matrix. Reprinted with permission from Ref. [160]. Copyright 2016, American Chemical Society.

and polymer, and (ii) *in situ* growth of MOFs on the surface of pre-electrospun nanofibers.

In terms of direct electrospinning of MOFs-polymer blended spinning solutions, a notable example is the development of MOF NPs based electrospun fibers by Chen and co-workers, who loaded titanium-incorporated PCN-224 (PCN-224(Zr/Ti)) NPs onto PLGA nanofibers [159]. In this study, PCN-224, a Zr-based porphyrin MOF, was utilized as a photosensitizer for generating $^1O_2$ upon visible light illumination. The preparation of PCN-224(Zr/Ti)@PLGA fibers involved co-electrospinning a solution of PLGA/HFIP and an HFIP solution containing PCN-224(Zr/Ti) NPs. TEM images demonstrated the homogeneous dispersion of PCN-224(Zr/Ti) NPs onto the resultant PCN-224 (Zr/Ti)@PLGA nanofibers (Fig. 6A). Notably, the incorporation of Ti significantly enhanced ROS generation for combating MDR bacterial infections.

In the study of Zhang and co-workers [160], a series of four MOFs, namely ZIF-8, UiO-66-NH_2, MOF-199 and Mg-MOF-74, were carefully selected and incorporated into three polymers including PAN, polystyrene (PS) and PVP to fabricate nanofibrous filters referred to MOFilter (Fig. 6B). The dispersion of MOF NPs in these polymer solutions exhibited excellent uniformity, with no significant aggregation even at high loading concentrations of 60 wt%. Through precise control of electrospinning parameters such as applied voltage and spinning solution flow rate, the above four MOFs could be successfully converted into fiber mats.

ZIFs, a well-known subset of MOFs, have garnered significant attention in field of biomedicine due to their negligible cytotoxicity, exceptional chemical and thermal stability, as well as pH sensitivity [161]. ZIF-8, a representative subclass of ZIFs, can be utilized to confer bactericidal activities to eNFMs through the coordination between Zn^{2+} and the pyridinic N of 2-methylimidazole (2-MIM). Currently, several approaches have been reported for the fabrication of ZIF-8-based eNFMs with bactericidal properties. For instance, via a stepwise *in situ* growth method, Zhan and co-workers fabricated durable PAN nanofibers loaded with ZIF-8/Ag/AgCl/TiO_2 [162]. In brief, initially, PAN nanofibers containing 2-MIM was prepared via electrospinning. Subsequently, ZIF-8, Ag/AgCl and TiO_2 NPs were successively formed *in situ* on the surfaces of PAN nanofibers. The resulting composite nanofibers presented photocatalytic activity upon both visible light and natural sunlight illumination due to the synergistic effect of ZIF-8, Ag/AgCl and TiO_2. Additionally, these composite nanofibers demonstrated excellent bactericidal properties against *E. coli* and *S. aureus*.

Although ZIF-8-based eNFMs demonstrate satisfactory antibacterial performance, the potential dissolution of ZIF-8 may lead to subsequent inactivation of its antibacterial properties. To address this issue, Zhang and co-workers fabricated the nondissolution-bonded antimicrobial fibers by covalent immobilization and electrospinning techniques [163]. Specially, a mixed solution containing T-ZIF-8, PEG2000 and TPU, as well as the conductive salt $ZnCl_2$ was spun into fibers as depicted in Fig. 7A. The obtained TPU-PEG/$ZnCl_2$/T-ZIF-8 fibers showed effective photocatalytic sterilization against both *E. coli* and *S. aureus*. The bactericidal mechanism can be attributed to the release of Zn^{2+} and the formation of $\bullet O_2^-$ upon visible light irradiation. Interestingly, this system exhibited a superior bactericidal effect against *S. aureus* compared to *E. coli*, which can be attributed to the differential antibacterial mechanisms employed by fibers against Gram-positive *S. aureus* and Gram-negative *E. coli*. The cell wall of Gram-positive bacteria is primarily composed of porous peptidoglycan, enabling direct $\bullet O_2^-$ interaction with internal bacteria components through the pore channel, thereby facilitating rapid bactericidal activity. In contrast, the cell wall of Gram-negative bacteria consists of peptidoglycan, and the outer membrane is mainly composed of lipopolysaccharide, lipoprotein and phospholipid. $\bullet O_2^-$ can only be oxidized by C=C in the outer membrane, leading to DNA oxidation and significantly reducing the penetration rate of $\bullet O_2^-$ through the bacterial cell wall. Consequently, this impairs the bactericidal efficacy against *E. coli*.

By combining electrospinning and electrospray, Zhu and co-workers developed PLA@ZIF-8 NFMs with bactericidal activities [164]. Briefly, PLA spinning solution and ZIF-8 dispersion were respectively loaded into two syringes, and ZIF-8 nanocrystals were electro-sprayed and PLA was electrospun at stable injection speed of 1 mL/h and 0.5 mL/h, respectively. As presented in Fig. 7B, the intact ZIF-8 nanocrystals with varying load contents (from 2 wt% to 6 wt%) were distributed throughout the membrane and firmly embedded in the PLA fiber surface. The antibacterial rates of PLA@ZIF-8 nanofibers against *E. coli* and *S. aureus* were 99.9 % and 100 %, respectively, which can be mainly ascribed to the promotion of ROS production upon light irradiation.

By combining electrospinning and *in-situ* hydrothermal treatment, Ma et al. developed ZIF-8@thiolated graphene composites-based polyimide (ZIF-8@GSH/PI) nanofibrous membranes [165], as presented in Fig. 7C. Briefly, PI eNFM was firstly prepared through the combination of electrospinning and imidization process. Then the PI eNFM was treated with GSH aqueous solution, followed by drying in vacuum. Subsequently, the prepared GSH/PI membrane was soaked into a mixed solution of $Zn(NO_3)_2\bullet 6H_2O$ and 2-MIM, and was hydrothermally reacted at 50 °C for 1 h to form ZIF-8. Due to the released Zn^{2+} from ZIF-8, the obtained ZIF-8@GSH/PI nanofibrous membranes presented enhanced bactericidal effect on *E. coli* and *B. sub* compared with those of GSH/PI membrane. The possible antimicrobial mechanism was proposed: Zn^{2+} released by ZIF-8 reacted with bacteria cell membrane proteins or acted as an antibacterial component directly, destroying the bacterial cell membrane structure by destroying liposomes, leading to the leakage of intracellular molecules, and then leading to cell death. Overall, cellular internalization, ROS production and plasma membrane destruction caused by the released Zn^{2+} were the reasons for its excellent antibacterial properties.

Owning to the unique porous structure of ZIF-8, antibacterial agents were loaded into the ZIF-8 cavity and the antibacterial agents loaded ZIF-8 were incorporated into polymer matrix to prepare MOF-based mixed-matrix electrospinning nanofibers. For example, Qian et al. prepared MOF/PCL hybrid nanofibers by co-electrospinning biodegradable PCL matrix with photosensitive ZIF-8 (RB@ZIF-8 NPs) [166]. The photodynamic antibacterial RB@ZIF-8 NPs was obtained by loading Rose Bengal (RB) as a photosensitizer into ZIF-8 framework, and then RB@ZIF-8 NPs was electrospun with PCL to form hybrid nanofibers. Due to the increase of RB@ZIF-8 NPs (termed as RZXP, and X indicated the loading contents), the morphology of hybrid nanofibers changed significantly, and the color of the nanofibers gradually changed from white to rose red. When the loading content was the lowest (30 %), the surface of RZ30P nanofibers showed sporadic distribution compared with bare PCL, demonstrating that the loaded nanoparticles were mainly distributed in the fiber matrix. For RZ60P and RZ90P, RB@ZIF-8 NPs were uniformly aggregated and distributed on the surfaces, and the surface roughness increased obviously. Systematic bacterial experiments demonstrated that the original membrane did not have any antimicrobial effect, but it could be activated immediately to generate ROS under visible light illumination, which was closely related to the load content of RB@ZIF-8 NPs.

3.2.4. Emerging 2D nanomaterial-loaded eNFMs

Since the first experimental isolation of graphene in 2004 [167], a large number of 2D nanomaterials, such as transition metal carbide/-nitride and carbon nitride (MXene) [168], 2D covalent organic frameworks (COFs) and black phosphorous (BP) NSs [168–172], have become a rich playground for researchers to confer antibacterial properties on eNFMs, and expand the application range of these 2D nanomaterials.

As a new class of multifunctional 2D nanomaterials, MXene with the chemical formula of $M_{n+1}X_nT_x$ (M for early transition metals, X for carbon and/or nitrogen, and T_x for surface functional groups), is broadly utilized in sensors, supercapacitors, electromagnetic interference shielding and photo/electro-catalysis fields [173,174], as well as antibacterial fields [175]. Among various MXenes, $Ti_2C_3T_x$ is a promising

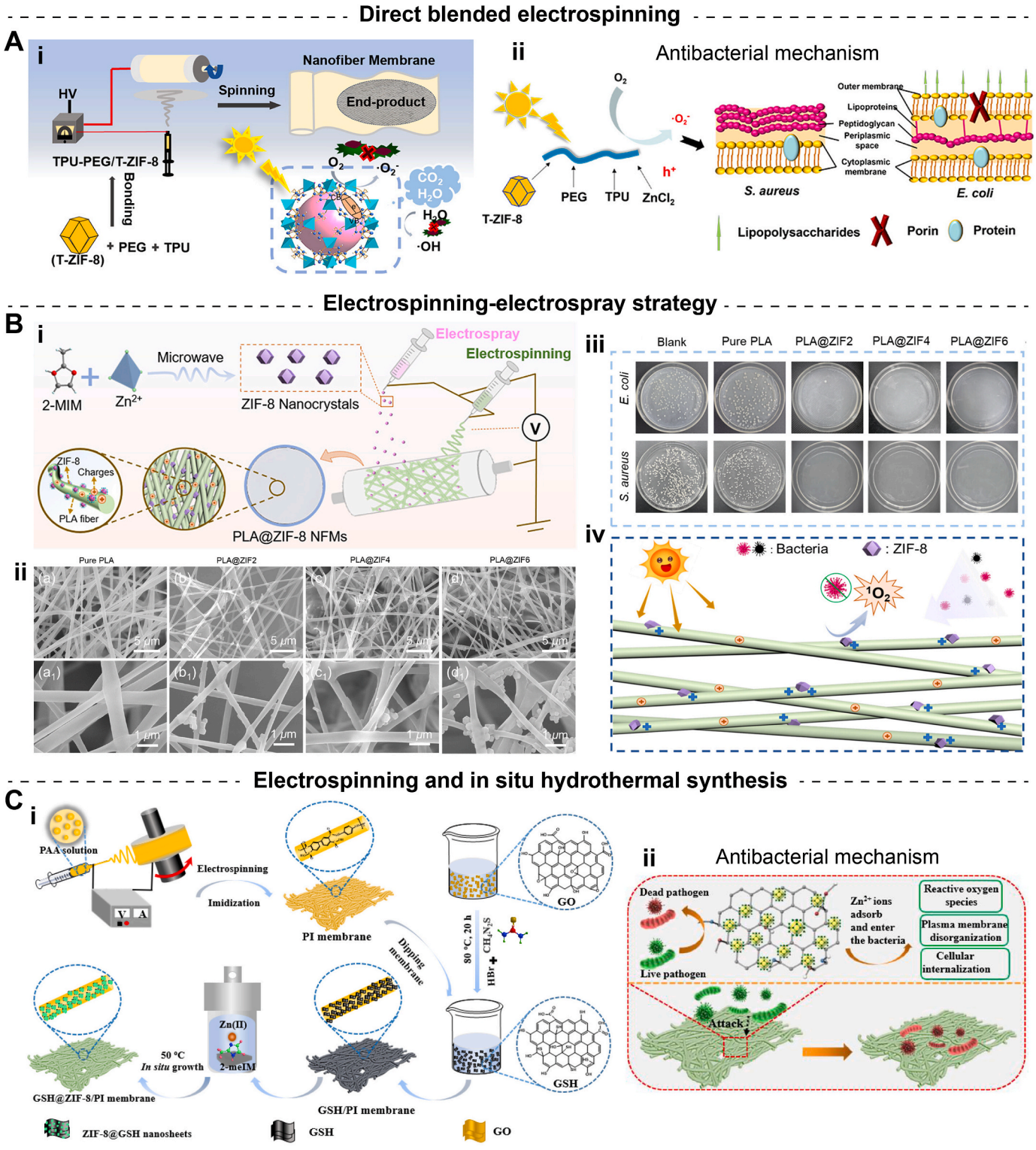

Fig. 7. Different preparation routes for loading ZIF-8 into eNFMs with bactericidal activities. (A) (i) Schematic illustration of TPU-based T-ZIF-8 nanofibers as photocatalytic bactericidal agents. (ii) Antibacterial mechanism diagram of the TPU-PEG/$ZnCl_2$/T-ZIF-8 fiber membrane against *E. coli* and *S. aureus*. Reprinted with permission from Ref. [163]. Copyright 2023, American Chemical Society. (B) (i) Synthetic routes of PLA@ZIF-8 NFMs via electrospinning-electrospray method. (ii) SEM images of pure PLA membrane and PLA@ZIF-8 NFMs with loading different contents of ZIF-8 (from 2 wt% to 6 wt%). (iii) Antibacterial properties and (iv) bacteria-killing mechanism of PLA@ZIF-8 NFMs. Reprinted with permission from Ref. [164]. Copyright 2023, American Chemical Society. (C) (i) Schematic illustration of the preparation routes of ZIF-8@GSH/PI nanofibrous membrane and (ii) the schematic diagram of the corresponding antibacterial mechanism. Reprinted with permission from Ref. [165]. Copyright 2020, American Chemical Society.

candidate for the development of multifunctional eNFMs due to its high electrical conductivity, excellent volumetric capacitance, ease of processing, good cytocompatibility and antibacterial activity [176,177]. Gao et al. prepared titanium carbide $Ti_2C_3T_x$ nanosheet firstly, and the PAN was dissolved in $Ti_2C_3T_x$-containing DMF solution to obtain the precursor solution. Then, the $Ti_2C_3T_x$-modified PAN nanofibers (P@M filters) were obtained via the electrospinning technology [178]. The incorporation of a small amount of $Ti_2C_3T_x$ did not affect the geometry of PAN fibers. As $Ti_2C_3T_x$ loading amount increased, the diameter distribution of P@M filters became wider due to the agglomeration of $Ti_2C_3T_x$. Meanwhile, due to the migration of hydrophilic $Ti_2C_3T_x$ with polar functional groups (O, OH and F) to the surface of PAN fiber, $Ti_2C_3T_x$ were mainly distributed on the surface of the PAN fiber. As expected, P@M filters strongly inhibited the growth of *E. coli* and *S. aureus*, demonstrating the excellent antibacterial activity of $Ti_2C_3T_x$ NSs. In another study, Zhou and co-workers developed infectious microenvironmentally activated nano-catalytic membranes consisting of electrospun PLGA scaffolds, MXene/Ag_2S bio-heterojunctions (MX/AS bio-HJs), and lactate oxidase (LOx) for chronic skin regeneration [179,180]. As illustrated in Fig. 8A, the MX/AS bio-HJs in the membranes not only had a good photothermal effect, but also catalyzed H_2O_2 to produce overwhelming •OH under NIR light irradiation, which had rapid synergistic bactericidal performance.

Carbon nitride (*g*-C_3N_4), as another emerging graphite-like 2D material [181], has also drawn considerable attention in the fabrication of antibacterial eNFMs, due to its inherent merits such as visible light catalytic activity, good chemical stability, moderate band gap, non-toxicity, and easy preparation [182,183]. Song et al. reported that *g*-C_3N_4 modified core-shell nanostructure membranes (termed as CNCT) was an efficient and recyclable photocatalysts for the degradation of antibiotics and inactivation of bacteria by *in-situ* thermal polymerization of gaseous melamine molecules on electrospun Co-TiO_2 nanofibers [184]. Ultrathin *g*-C_3N_4 NSs were synthesized *in situ* and coated on Co-TiO_2 nanofibers to form core-shell quantum heterostructures. By adjusting the content of the precursor (melamine), the thickness and loading capacity of *g*-C_3N_4 NSs could be precisely controlled. Significantly, the resultant CNCT fibrous membranes also showed outstanding photocatalytic degradation and disinfection properties upon visible light irradiation. In the absence of photocatalysts, the photolysis of bacteria was negligible. Similarly, due to the poor visible light response of bare TiO_2 membrane, its antibacterial efficiency was also negligible.

As an emerging class of multifunctional nanomaterials, COFs have presented potential for biomedical applications, such as in PDT and drug delivery. Through condensation reaction and Schiff based reaction, as shown in Fig. 8B, Zou and co-workers proposed a one-pot strategy for preparing a curcumin-embedded COF (CUR@COF) [185]. The CUR@COF showed a loading capacity of up to 27.68 % on CUR. The obtained CUR@COF NPs were further incorporated into PCL NFMs through electrospinning. TEM test confirmed the presence of CUR@COF NPs inside the CUR@COF/PCL fibers. Particularly, the obtained CUR@COF/PCL fibers showed CUR release profile in a pH response through protonation reaction under acidic conditions, indicating that the acidic extracellular microenvironment promoted CUR release from the fibers. Additionally, with the increase of CUR@COF content, the inhibitory rate of the fibers against *E. coli* and *S. aureus* increased.

Among 2D nanomaterials, BP NSs with large specific surface area, efficient photothermal conversion, excellent biocompatibility and antibacterial property have attracted much interest in the biomedical applications. In a recent study, Zhao et al. developed an all-in-one bioactive photothermal nanofibers for promoting diabetic wound healing [186]. Through LbL assembly, BP NSs and hemoglobin (Hb) self-assembled onto electrospun poly-l-lactide (PLLA) nanofibers using positively-charged QCS (a hemostatic and broad-spectrum antibacterial material) and negatively-charged hyaluronic acid (HA). In this system, BP NSs were used to convert NIR radiation into heat and stimulate Hb to release O_2 *in situ* to improve the hypoxic microenvironment of diabetic wounds. Particularly, moderate BP-derived photothermal therapy can increase bacterial susceptibility to QCS. Under NIR light illustration for 5 h, the obtained nanofibers showed high inhibition rates of 98.24 ± 1.68 % and 90.36 ± 1.08 % against MRSA and *E. coli*, respectively. As illustrated in Fig. 8C, the bactericidal polymer of QCS, the nano-knife effect of BP NSs, and local hyperthermia under NIR light irradiation may be potential antibacterial mechanisms. Except the photothermal and nano-knife effect, BP NSs are capable to overcome the shortcoming of Ag NPs easy polymerization for better antibacterial performance.

4. Bio-applications of antibacterial eNFMs

As mentioned above, electrospinning has become a straightforward method to produce ultrafine nanofibers as engineering scaffolds for tissue regenerative therapies. The electrospun scaffolds play a monumental role in cell migration, attach and proliferation [203–205], due to the produced fibers with diameters of 50–200 nm which are very similar to the that of extracellular matrix (ECM) collagen fibrils [206,207]. Additionally, the adjustable porosity and physical-chemical properties of electrospun scaffolds to mimic the fibrillar nature of ECM allow its use as promising 2D or 3D scaffolds for the support and growth of cells.

So far, great efforts have been given to achieve the application of electrospun scaffolds in tissue regeneration and repair. The disinfection/sterilization is an emerging essential step during the manufacturing process and/or before the use of any implantable medical device [207]. However, bacterial infection of electrospun scaffolds as medical implants is one of the main reasons to their failure, and the threat caused by drug-resistant pathogens has prompted the development of more effective antibacterial products for tissue regenerative applications. Treatment of such implant infections usually requires both elimination of bacteria surrounding the implant and accelerated tissue regeneration [208].

With the development in recent decades, a variety of electrospun scaffolds with addition of antibacterial nanomaterials have been presented to inhibit the growth of bacteria, reduce the risk of secondary infection during and after implant surgery, and promote tissue repair and regeneration [209]. The pivotal biological functions exhibited by the eNFMs containing antibacterial nanomaterials for tissue regenerative therapies are summarized in Table 2. The most recent achievements of antibacterial nanomaterials loaded electrospun scaffolds for various tissue regenerative therapies, mainly involving wound healing, bone repair, periodontal repair and tendon repair, are highlighted in the following subsections, which are very helpful for classifying and expanding their biomedical engineering applications.

4.1. Wound healing

Skin, as the largest organ of the human body, has important functions such as protection, immunity, thermoregulation and sensation [8,223]; and skin tissue is the first external environmental barrier against dehydration, chemical/radiological damage, and microbial invasion. Although most skin defect can be normally healed within 1–2 weeks, the extensive full-thickness wounds are hard-to-heal and have serious impact on health even threatening the life of human beings [224–226]. Of particularly note, the open wounds are susceptible to bacterial contamination, resulting in prolonged inflammatory periods and enhanced expression of metalloproteinases. Thus, given high risk incidence of acute and chronic wounds worldwide, the need for wound dressings is greater than ever to block microbial invasion and eradicate colonizing bacteria.

Up to now, many electrospun fibrous dressings have been developed and realized the effectiveness of disinfection on bacterial infected wounds. Typically, two functions of the electrospun fibrous dressings are essential for infected wound healing: (i) protecting wound areas from the bacterial invasion as a physical barrier; and (ii) eradicating the colonizing bacteria in wound sites.

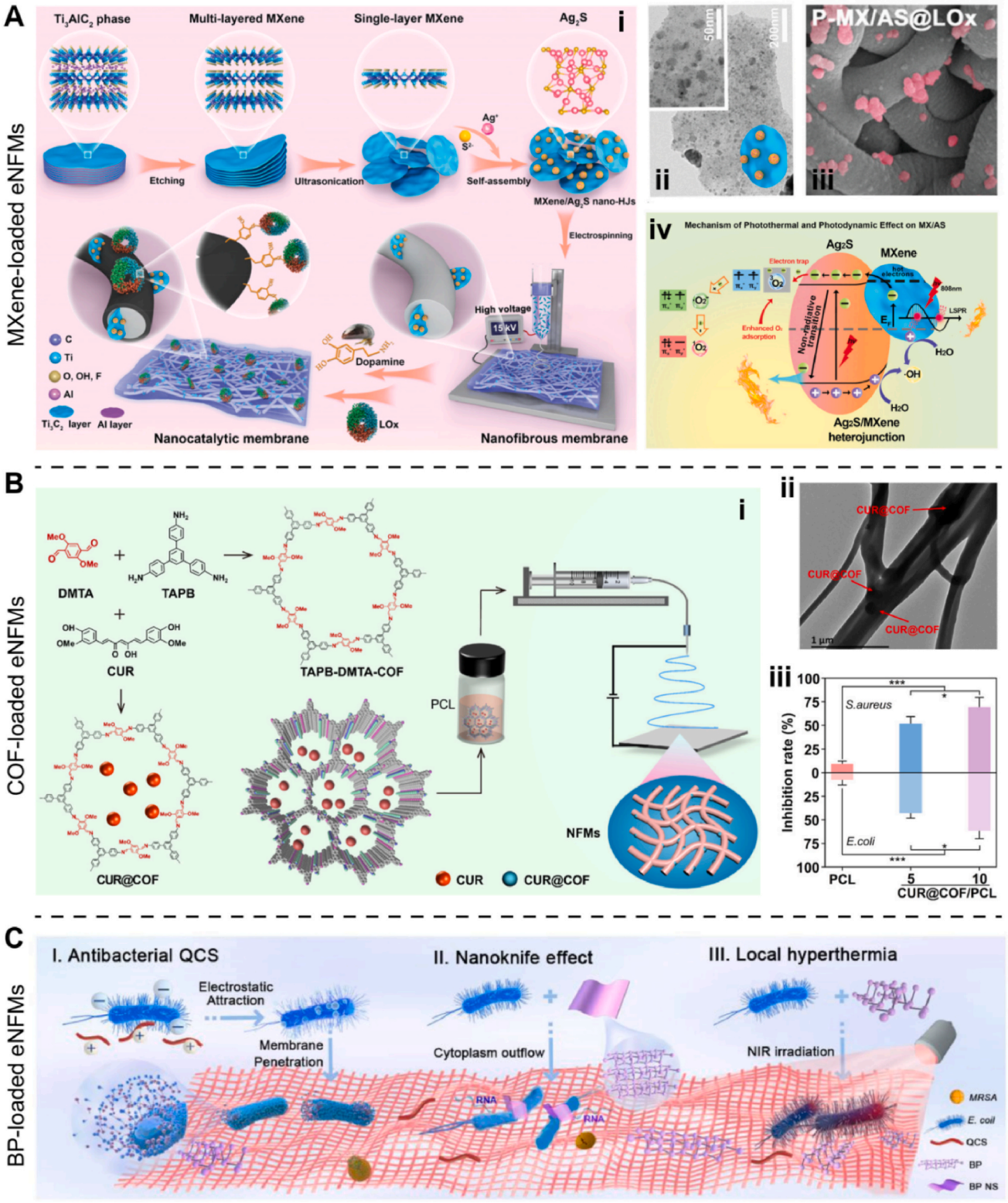

Fig. 8. Representative emerging 2D nanomaterials incorporated eNFMs with bactericidal activity. (A) (i) Schematic illustration of the fabrication of P-MX/AS@LOx membrane. (ii) TEM image of MX/AS. (iii) SEM image of P-MX/AS@LOx membrane. (iv) Mechanism of photothermal and photodynamic effect on MX/AS. Reprinted with permission from Ref. [179]. Copyright 2021, Wiley-VCH. (B) (i) Schematic illustration of the preparation of CUR@COF and PCL NFMs with the loading of CUR@COF. (ii) TEM image of 10CUR@COF/PCL nanofibers with loading 10 wt% CUR@COF mixtures. (iii) Inhibition rates of *S. aureus* and *E. coli* with PCL, 5CUR@COF/PCL, and 10CUR@COF/PCL NFMs. Reprinted with permission from Ref. [185]. Copyright 2022, American Chemical Society. (C) Schematic illustration of antibacterial mechanism of PLLA/QCS composite nanofibers containing QCS and HA/BP/Hb. Reprinted with permission from Ref. [186]. Copyright 2023, Elsevier Ltd.

Table 2
A comprehensive overview of the pivotal biological functions exhibited by eNFMs containing antibacterial nanomaterials for tissue regenerative therapies.

Biological functions	How to achieve the biological function by eNFMs
Antibacterial activity	By immobilizing antibacterial nanomaterials in eNFMs, the functionalized eNFMs can be given direct antibacterial ability, effectively inhibiting or killing bacteria in contact [210–212].
Preventing biofilm formation	The antimaterial nanomaterials-contained eNFMs can prevent bacteria attachment on the surface and biofilm formation by changing their physical and chemical properties, such as size, shape, and surface charge [213–215].
Anti-inflammatory effect	The antibacterial nanomaterials-incorporated Janus nanofiber membranes can inhibit the expression of inflammatory factor (such as IL-6) and upregulate the expression of anti-inflammatory factor (such as TGF-β) [216].
Promoting angiogenesis	Some eNFMs has the function of promoting cell proliferation and migration and promoting angiogenesis, and the specific bioactive molecules contained in eNFMs are essential for the healing of chronic wounds or deep skin defects [217].
Accelerating epithelization	By regulating cell diffusion along the arrangement direction, the eNFMs can prevent nano-directed proliferation of epithelial cells and promote proper epithelialization of the wound [218,219].
Osteogenic activity	The antibacterial nanomaterials-contained eNFMs, such as Janus nanofibrous scaffold, prepared by electrospinning back-to-back layers of PLLA/ZnO and PLLA/barium titanate, with the fiber alignments adjusted from orientation to random by manipulating the rotating speed of the roller, can upregulate the expression of genes associated with osteogenic differentiation, such as Runx2, Col I and OCN [220].
Osteo-immunomodulatory function	The MPNs-functionalized nanofiber membranes can induce macrophages to polarization towards M2 type, manipulate good bone immune environment, and promote bone regeneration [221].
Microenvironment responsiveness	Some antibacterial eNFMs are sensitive to pH, enzymes, reactive oxygen species (ROS), light or temperature, and play a better antibacterial role under specific physiological conditions [222].

The addition of antibacterial nanomaterials into electrospun fibrous dressings is demonstrated to be effective for infected wound healing. The therapy strategies of antibacterial nanomaterial-loaded electrospun fibrous dressings mainly include metal ions therapy (MIT), photothermal therapy (PTT), photodynamic therapy (PDT), chemodynamic therapy (CDT) and their arbitrary combinations. The following subsection mainly summarizes the recent achievements of antibacterial nanomaterial-loaded eNFMs, as well as the corresponding working mechanisms in treatment of bacteria-infected wound.

4.1.1. Single model MIT

Metal ions play a vital role in the daily processes of the human body, including maintaining vital functions, regulating metabolism, and accelerating tissue repair [227]. Many metal ions such as Ag^{+}, Au^{+}, Cu^{2+}, and Zn^{2+} released by metal nanoparticles or metal oxides/sulfides nanomaterials based eNFMs can repair skin by promoting the synthesis and secretion of ECM [228–230], and have been diffusely utilized to treat infected wounds without external intervention due to their remarkable bactericidal properties.

As a typical example, to treat a MDR bacteria wound infection, Yang et al. employed a small molecule (6-aminopenicillanic acid, APA) modified Au NPs as active bactericidal ingredients to PCL/Gel nanofibers to achieve biocompatible and bactericidal wound dressings [80], as presented in Fig. 9A. The distribution of Au_APA NPs in the nanofibers was demonstrated to be homogeneous. Importantly, Au_APA can induce cell membrane destruction and cell lysis, resulting in the effective bactericidal performance of Au_APA nanofibers. It was found that the cumulative release of Au from Au_APA nanofibers was 20.4 % of the original amount after 1 day and up to 65.7 % after 7 days. *In vivo* experiments indicated that Au_APA nanofibers had remarkable ability to treat MDR bacterial wound infection.

Considering to the bacterial infection and insufficient neovascularization of chronic wounds, Yin et al. presented an antimicrobial and proangiogenic fibrous dressing by loading dimethyloxalylglycine (DMOG) into ZIF-8 and electrospinning with Gel-PCL [231]. As illustrated in Fig. 9B, DMOG@ZIF-8 particles in the dressing decomposed with Gel degradation, entered the moist wound environment, released Zn^{2+} and DMOG, which had bactericidal activity and promote angiogenesis, respectively. *In vitro*, the dressing containing 2.5 % DMOG@ZIF-8 eliminated more than 90 % of *E. coli* and *S. aureus* without affecting fibroblast proliferation and adhesion. The bactericidal effect of the dressing was due to the released Zn^{2+} from the breakdown of ZIF-8. *In vivo*, the dressing effectively accelerated the healing of skin wounds in *S. aureus*-infected diabetic rats within 2 weeks.

4.1.2. Single model CDT

CDT has achieved satisfactory efficacy in terms of bactericidal performance, which catalyzes substrates to generate cytotoxic ROS through Fenton reaction or Fenton-like reaction to inactivate bacteria [232,233]. Particularly, the acidity and high level of H_2O_2 in the infected tissue are beneficial to CDT for antibacterial therapy [234]. The addition of nanomaterials with CDT effect into electrospun fibrous dressings have been demonstrated to be useful for killing bacteria and promoting infected wound healing.

Inspired by the cardiac healing of skin wounds, as presented in Fig. 10A, Huang and co-workers presented radially fibrous dressing containing CuO_2 NPs (CPs) for angiogenesis and acceleration healing of diabetic wounds [235]. Due to the incorporation of CuO_2, the fabricated Ran@CP membrane allowed *in situ* production of H_2O_2 under the activation of acidic diabetes microenvironment and the subsequent Fenton-type reaction, achieving 99.4 % elimination of *S. aureus*. Meanwhile, the Cu^{2+} ions release greatly up-regulated the expression of hypoxia-inducible factor 1α (HIF-1α) and vascular endothelial growth factor (VEGF) in HUVECs, promoting angiogenesis *in vitro*. Interestingly, Ran@CP membrane can guide the National Collection of Type Cultures to clone 929 (L929) mouse fibroblasts through the splittering structure of radial arrangement, spreading and directional migration along the fiber distribution. *In vivo* implantation experiments showed that CP-embedded membrane with radial structure could not only greatly promote wound healing in diabetic SD rats at 14 days, but also promoting wound angiogenesis.

Similarly, Qi et al. developed a CuO_2-laden composite membrane for promoting diabetic wound healing [236]. As illustrated in Fig. 10B, the nanofiber presented a unique core/shell structure containing n-CuO_2+PVP/PCL composite shell and a PCL core through coaxial electrospinning technique. The obtained CuO_2-laden nanocomposite membrane presented high antibacterial ratios of 97.3 % and 99.9 % against *E. coli* and *S. aureus*, respectively. Under the conditions of infection and diabetes characterized by weakly acidic pH, n-CuO_2 decomposition released H_2O_2 and Cu^{2+} ions, which were subsequently produced •OH by Fenton reaction, thereby activating ROS-mediated antibacterial activity, inhibiting inflammation and promoting angiogenesis. Simultaneously, the dissolution of PVP presented a unique nanogroove pattern on the surface of nanofibers, which provided the required cell guidance function to accelerating tissue regeneration. *In vitro* and *in vivo* experiments indicated that CuO_2-laden composite membrane can significantly promote wound healing, promote collagen deposition, reduce inflammation and promote wound vascularization.

In another study, by combining electrospinning and electrospray, Xu et al. developed MgO-based NPs composite PCL fibrous dressings for the CDT of wounds with bacterial infection [237]. The composite dressings produced high levels of ROS without the need for external stimulation. Such excellent CDT properties resulted in highly efficient glutathione

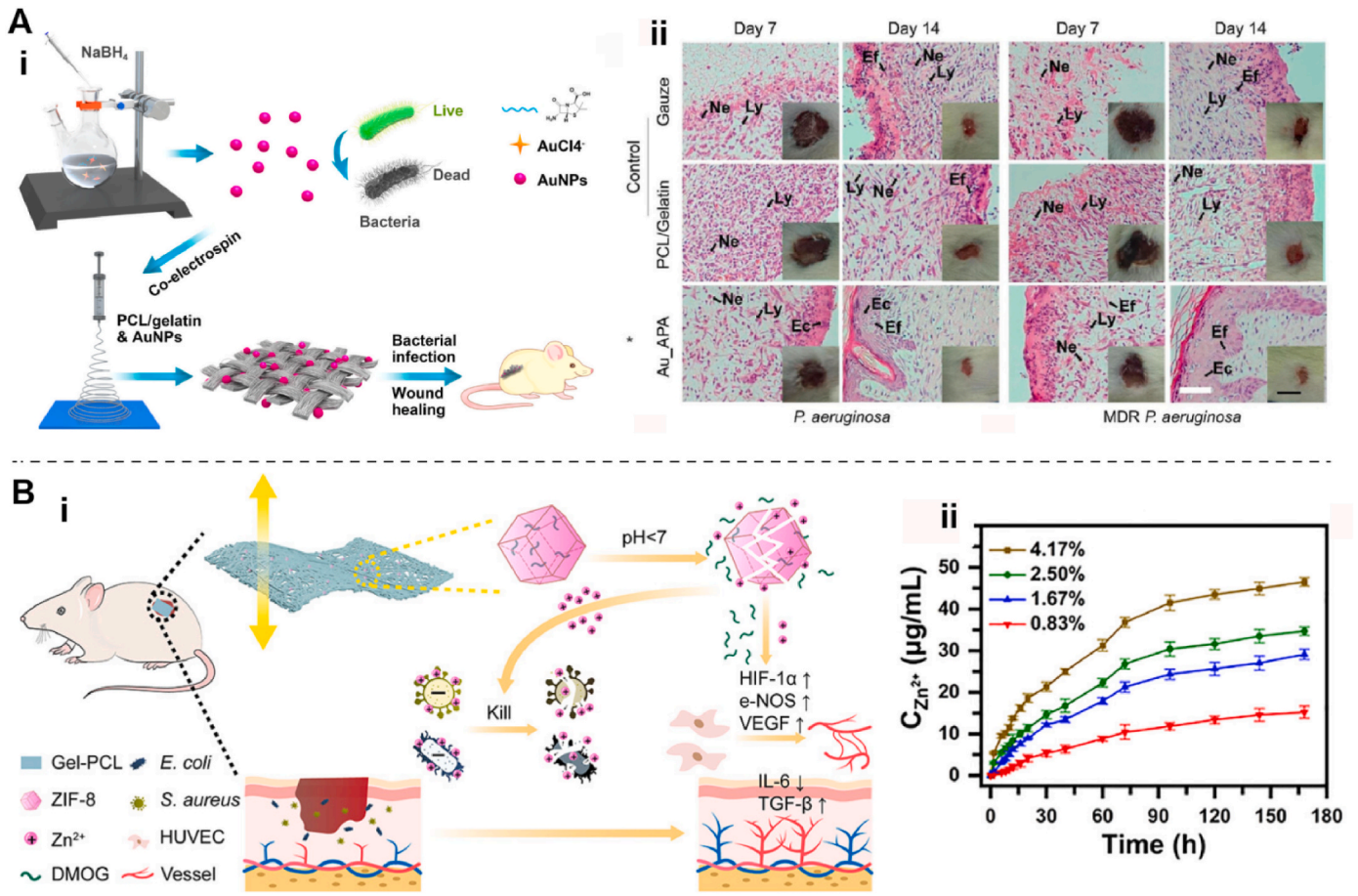

Fig. 9. Representative single model MIT by nanomaterial-loaded eNFMs for infected wound healing. (A) (i) Schematic illustrations of the preparation of AuNPs and AuNPs-doped electrospun PCL/Gel fibers with bactericidal activities and the application for treating wounds infected by MDR bacteria. (ii) H&E staining of the wounds after the postoperative day 7 and day 14. Reprinted with permission from Ref. [80]. Copyright 2017, American Chemical Society. (B) (i) Schematic illustration of DMOG@ZIF-8@Gel-PCL dressing with sequential anti-infection and pro-angiogenesis for chronic wound healing. (ii) Release profile of Zn^{2+} by DMOG@ZIF-8@Gel-PCL dressing with different contents of DMOG@ZIF-8. Reprinted with permission from Ref. [231]. Copyright 2023, American Chemical Society.

oxidation and significant bacteria killing rate against *S. aureus* of approximately 99 %. *In vivo* experiments demonstrated the remarkable ability of the composite dressings to treat *S. aureus*-infected wounds.

4.1.3. Single model PTT

PTT is a clinically promising method for killing bacteria by irradiating photothermal agents with NIR light to produce local hyperthermia [238,239], thus destroying the complete structure of the bacteria by non-invasively generating high temperatures within its bioactive substrates (such as proteins and nucleic acids) [240], making it easier for the antimicrobials to penetrate and destroy the protected bacteria. PTT adds photothermal nanomaterials such as PDA NPs, Cu_2S NPs and BP NSs to electrospun fibrous dressing, providing new possibilities for the effective treatment of bacteria-infected wounds [241,242].

Recently, Zhang and co-workers developed Janus nanofiber membranes with photothermally enhanced biofluid drainage and sterilization functions to promote diabetic wound healing [243], as illustrated in Fig. 11A and **B**. Briefly, PDA NPs with the size of 100 nm were first synthesized and then added into PAN solution. The obtained PAN/PDA spinning solution was then electrospun onto the surface of PP nonwoven membrane, resulting in the formation of Janus nanofiber membrane with PP as hydrophobic inner layer and $PAN_{x\%PDA}$ hydrophilic outer layer. Based on the contact points on the Janus interface, $PP/PAN_{x\%PDA}$ Janus membrane can "pump" water from the hydrophobic PP layer to the hydrophilic $PAN_{x\%PDA}$ layer in 22 s. Upon 808 nm NIR illumination, $PAN_{30\%PDA}$ can evaporate water in 7 min. Due to the incorporation of photothermal nanoagent PDA NPs, the temperature of $PP/PAN_{30\%PDA}$ under NIR illumination increased significantly to 100 °C, suggesting remarkable photothermal properties. To simulate a wet wound environment, the Janus membrane was immersed into PBS for 30 s, followed by NIR irradiation for 900 s. During irradiation, the temperature of $PP/PAN_{30\%PDA}$ Janus membrane rapidly increased to the first platform within 30 s and was maintained at 58 °C. After maintaining the equilibrium temperature for a certain time, the temperature begins to rise again, reaching the second platform, which is due to the complete evaporation of the water on the membrane. As shown in Fig. 11C, the cell membrane of bacteria in $PP/PAN_{30\%PDA}$ group wrinkled or even burst under NIR light irradiation. In addition, living/dead staining results showed that $PP/PAN_{30\%PDA}$ combined with NIR light could lead to bacteria death (Fig. 11D), and the antibacterial efficacies against *E. coli* and *S. aureus* could reach more than 95 %, contributed to the significant photothermal effect. Furthermore, in a *S. aureus*-infected diabetic mouse wound model, $PP/PAN_{30\%PDA}$ Janus membrane achieved a wound closure rate of up to 96.7 % upon NIR light illumination, better than that (59.8 %) of traditional bandages (Fig. 11E); and collagen regeneration was enhanced in the $PP/PAN_{30\%PDA}$ group, while the presence of collagen fibers was limited in the control group (Fig. 11F). Additionally, the bacteria removal effect of $PP/PAN_{30\%PDA}$ Janus membrane combined with NIR laser irradiation was better than that of bandages and $PP/PAN_{30\%PDA}$ alone.

Here, a high temperature of 50 °C or higher is required to effectively kill bacteria by PPT alone [244], and the produced side-effects such as

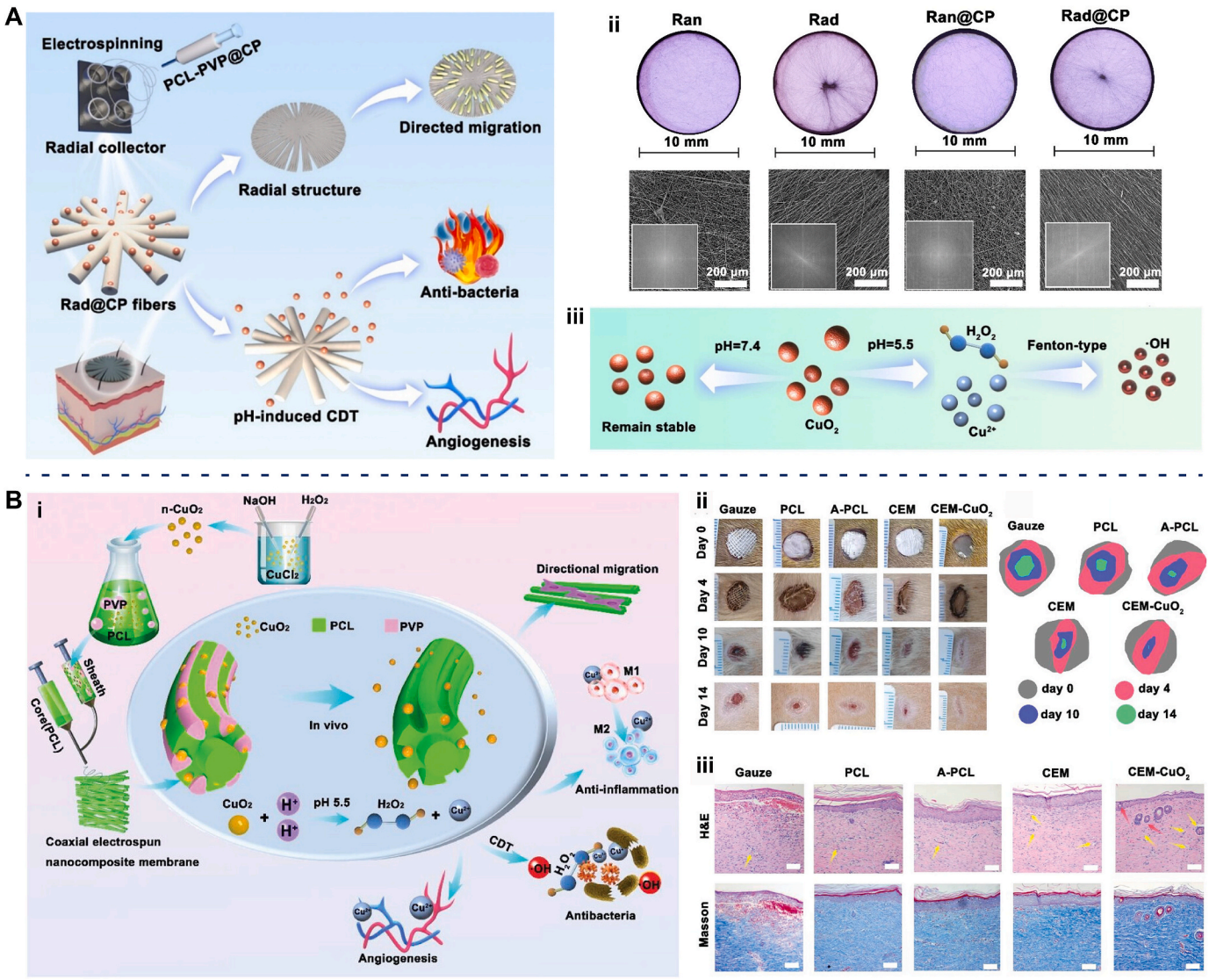

Fig. 10. Representative single mode CDT by nanomaterial-loaded eNFMs for infected wound healing. (A) (i) Schematic illustration for the preparation of Rad@CP for angiogenesis and accelerating wound healing. (ii) Optical microscope of the membranes and SEM images inserted with FFT calculations of the membranes. (iii) Schematic illustration of H_2O_2 self-generation and triggered Fenton-type reaction. Reprinted with permission from Ref. [235]. Copyright 2023, American Chemical Society. (B) (i) Schematic illustration of preparing the coaxial electrospun nanocomposite membrane containing CuO_2 NPs with multifunction for diabetic wound treatment. (ii) Digital images of wounds processed by EUFs within 14 days and the corresponding simulation wound healing traces. (iii) H&E and Masson staining images of the wounds after 14 days. Reprinted with permission from Ref. [236]. Copyright 2023, Wiley-VCH.

inflammation and thermal damage to nearby normal tissues limit the applications of PPT by antibacterial nanomaterial-loaded eNFMs in infected wound healing [245]. Therefore, researchers have made great attempts to achieve lower temperature PTT (<45 °C) based on the inhibitors of heat shock proteins (HSPs) [246–248]. Moreover, the combined therapies of PTT with other antibacterial strategies such as MIT, CDT and PDT have been also developed for infected wound healing.

4.1.4. Single model PDT

PDT is regarded as a non-invasive, clinically approved and safe therapeutic strategy [249]. As a promising antibacterial method, PDT has great potential in fighting bacterial infections. Particularly, bactericidal PDT uses light sources to activate photosensitizers enriched in lesions and generate ROSs through oxidative stress, lipid peroxidation, protein dysfunction, and DNA damage, ultimately inducing bacteria death [250–252]. Here, alone PDT highly dependent on ROSs is a newly developed method for electrospinning fibrous dressings to kill bacteria and even eliminate biofilms, while maintaining high efficiency without developing therapeutic resistance.

For instance, through incorporating MOF NPs alone into eNFMs without any added antibacterial ingredients, Chen and co-workers developed electrospun PLGA nanofibers containing PCN-224(Zr/Ti) NPs for chronic wound healing, as illustrated in Fig. 12A. PCN-224 (Zr/Ti) NPs were synthesized by a facile cation exchange method [159]. Upon visible light illumination, the addition of Ti could significantly improve the photocatalytic performance with more ROSs production, thus effectively eliminating MDR bacteria. The PCN-224(Zr/Ti) @PLGA dressing showed high biocompatibility and minimal cytotoxicity. Importantly, the dressing was effective for PDT healing of chronic wound infected with MDR bacteria.

To improve therapy efficiency, Ma et al. developed a multifunctional dressing for promoting chronic diabetic wound healing [253]. As presented in Fig. 12B, the dressing of UCNPs@SiO_2@CeO_2/PCL was fabricated through the combination of amidation reaction and electrospinning. Under 980 nm NIR illumination, the cells membranes of *E. coli* and *S. aureus* growing on UCNPs@SiO_2@CeO_2/PCL membranes

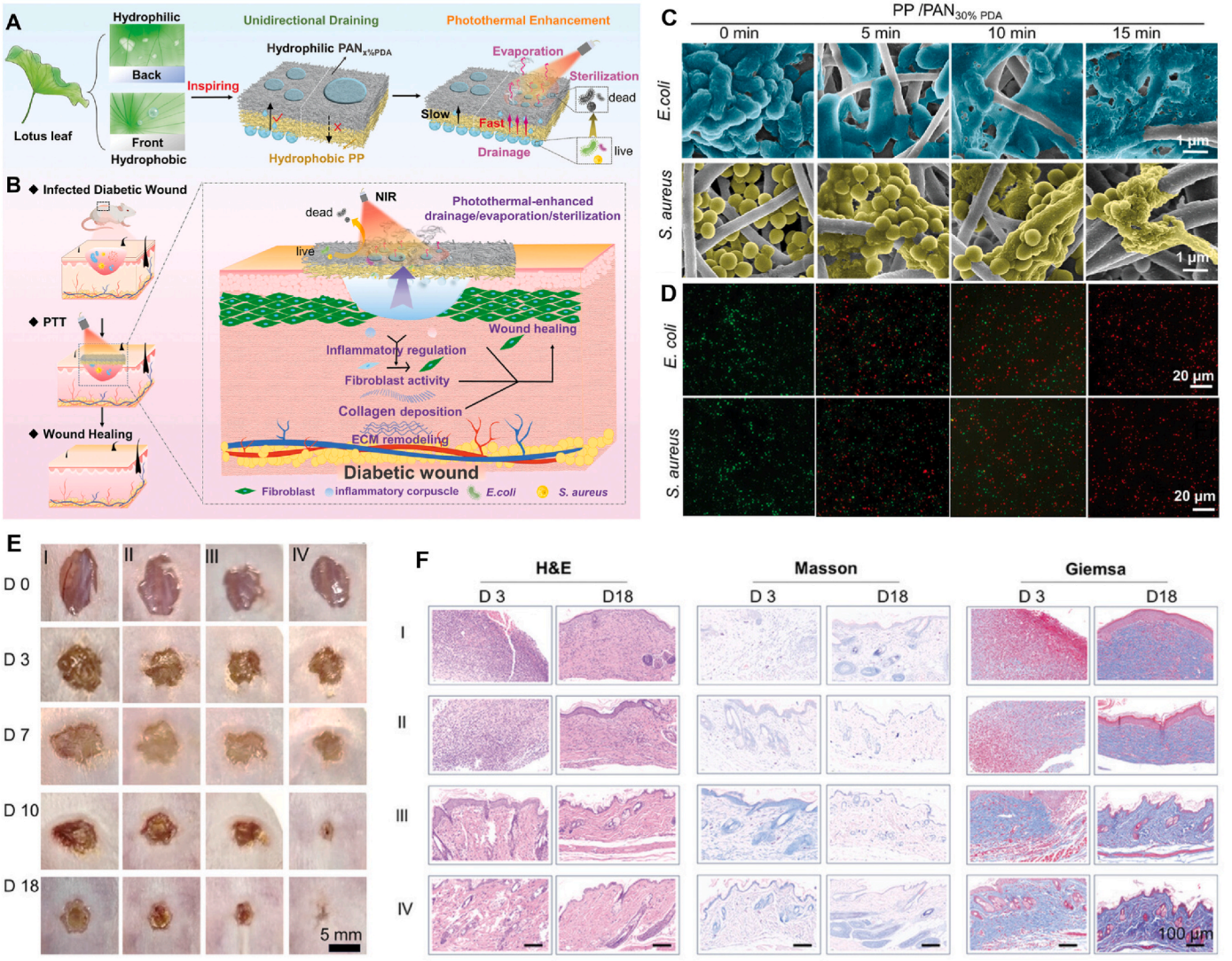

Fig. 11. Representative single model PTT by nanomaterial-loaded eNFMs for accelerating infected wound healing. (A) Schematic illustration of fabricating lotus leaf-inspired Janus PP/PAN$_{x\%PDA}$ fibrous membrane and (B) wound exudate drainage and photothermal evaporation/sterilization to promote chronic wound healing. (C) SEM images and (D) fluorescence images of *E. coli* and *S. aureus* after treatment with PP/PAN$_{x\%PDA}$ after NIR laser irradiation from 0 to 15 min. (E) Representative photographs of wound healing with different treatment groups. (F) H&E, Masson, and Giemsa staining images of the wound. Reprinted with permission from Ref. [243]. Copyright 2024, Wiley-VCH.

were seriously damaged and no complete morphology could be seen, demonstrating the excellent photodynamic antibacterial capability of UCNPs@SiO_2@CeO_2/PCL membranes. One possible mechanism was that the UV light emitted by UCNPs under NIR light illustration was absorbed by CeO_2 on the surface of UCNPs, and the electrons in CeO_2 were excited from the valence band to the conduction band. The remaining electron holes in the valence band can interact with H_2O on the surface of UCNPs@SiO_2@CeO_2 to produce ROS for antibacterial use. Additionally, the reversible transformation of Ce^{3+} and Ce^{4+} in CeO_2 NPs enabled the membrane good ability for relieving oxidative stress around chronic wounds, thus further promoting the transformation of wounds from inflammatory to proliferative stage and promoting the healing of chronic wounds. Both *in vitro* and *in vivo* experiments confirmed that the modified CeO_2 outside UCNPs can enable UCNPs@SiO_2@CeO_2/PCL membranes with very attractive photodynamic bactericidal activity and excellent antioxidant ability, which can effectively promote chronic wound healing.

Although PDT exhibited great potential for combating bacterial infection, its bactericidal effect may be affected due to the shallow penetration of short-wavelength light and the short diffusion length and lifetime of the produced ROSs. To address the issue, Sun et al. developed a nanocomposite PVDF fibrous membrane with NO-assisted PDT bactericidal performances under a single NIR irradiation [152]. The electrospun nanocomposite membrane was prepared by incorporating L-arginine (LA) doped UCNP@PCN NPs (consist of UCNPs and PCN-224) with hierarchical structure into PVDF matrix. Upon 980 nm NIR light irradiation, the produced ROS by UCNP@PCN@LA-PVDF membrane not only played a major antibacterial role in PDT but also induced loaded LA to generate nitric oxide (NO), and finally realized NO-assisted antimicrobial action of PDT. NO-assisted PDT membrane had anti-inflammatory and promoted wound healing effects due to the remarkable synergistic bactericidal properties of NO and its ability to promote keratinocyte proliferation and fibroblast migration.

4.1.5. *Multi model therapy*

Due to the different antibacterial principles, some limitations are along with single model MIT, CDT, PTT and PDT in bacteria inactivation for infected wound healing treatment. For instance, although MIT presents high bactericidal efficiency and broad-spectrum bactericidal property, but the potential toxicity of metal ions to normal mammalian

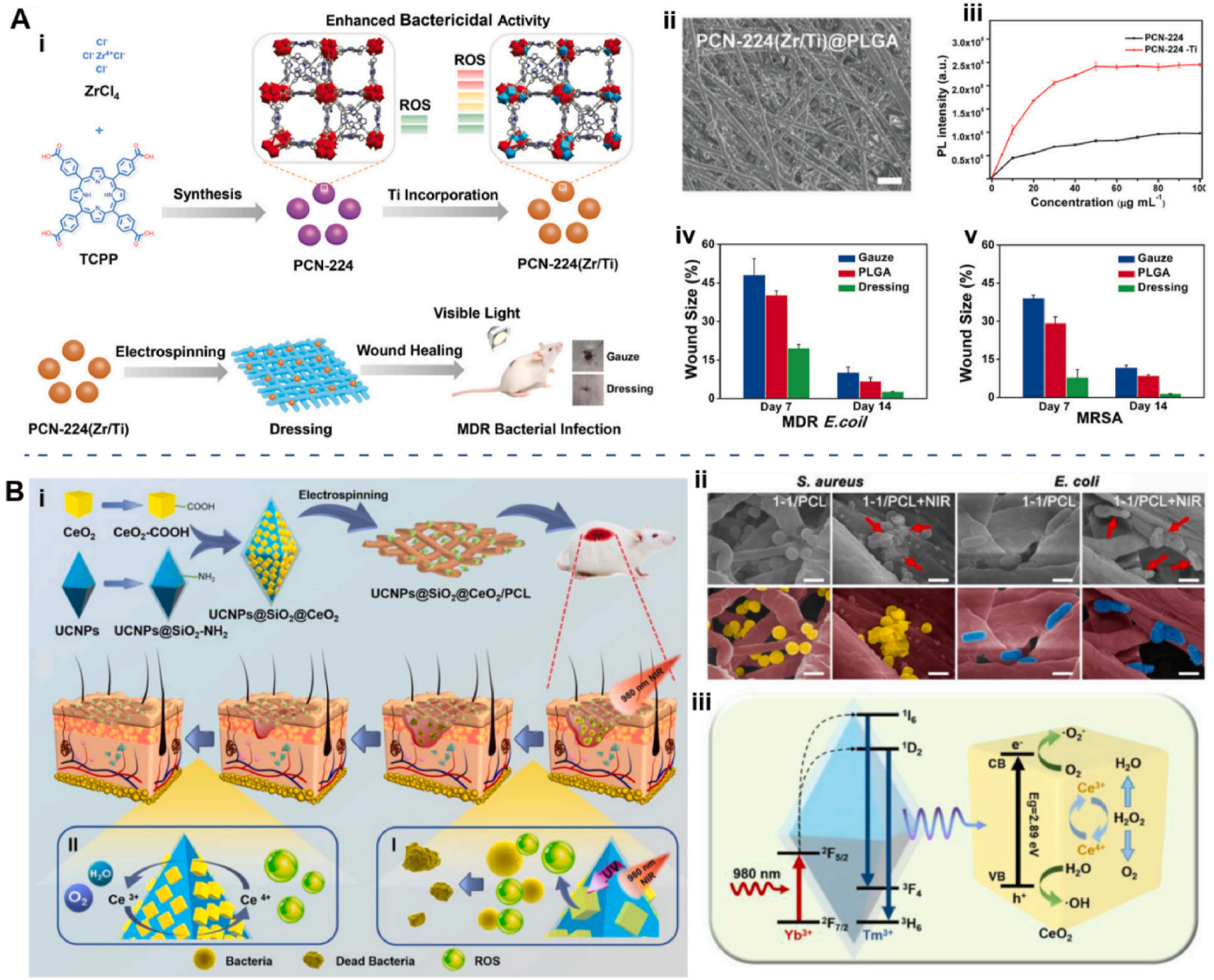

Fig. 12. Representative single model PDT by nanomaterial-loaded eNFMs for infected wound healing. (A) (i) Schematic illustration of the preparation of PCN-224 (Zr/Ti)@PLGA dressing for treating bacterial infection. (ii) SEM image of PCN-224(Zr/Ti)@PLGA fibrous dressing. (iii) PL spectra of DCFH for detecting the generation of ROS by PCN-224 and PCN-224(Zr/Ti) with different concentrations upon visible light illumination. The number counts of bacteria removed from (iv) MDR *E. coli* and (v) MRSA infected wounds. Reprinted with permission from Ref. [159]. Copyright 2020, Wiley-VCH. (B) (i) Schematic illustration of UCNPs@SiO_2@-CeO_2/PCL membranes with multifunction for promoting diabetic wound healing. (ii) FESEM images of *E. coli* and *S. aureus* on UCNPs@SiO_2@CeO_2/PCL (mass ratio between UCNPs@SiO_2-NH_2 and CeO_2-COOH of 1:1) with or without NIR irradiation. (iii) Schematic diagram of the upconversion, ROS formation and antioxidant mechanism of the UCNPs@SiO_2@CeO_2. Reprinted with permission from Ref. [253]. Copyright 2022, Wiley.

cells is a concern [254]. The antibacterial efficacy of CDT is highly dependent on the generation of •OH, but insufficient •OH may limit the therapy efficacy on infected wound healing [255]. Despite PTT and PDT as non-invasive antibacterial strategies, the elevated temperatures (above 50 °C) by PTT can damage surrounding health issues and even produce HSPs to create resistance to PTT [244,256,257], while the generated ROS by PDT has an extremely short lifetime (~3 μs) and short diffusion distance (<0.02 μm) [258]. Particularly, the multi-model therapy of arbitrary combination of MIT, CDT, PTT and PDT by antibacterial nanomaterial-loaded eNFMs can avoid the drawbacks of a single model of antibacterial strategy and generate synergistic effects in infection wound therapy.

Bacterial biofilms are usually formed during wound infections, which greatly increases the bacterial resistance to adaptive host immune responses. Through combining MIT and PTT, Zhao et al. constructed a serious of antibacterial dressings for promoting infected wound healing [259]. The wound dressings were fabricated by encapsulating Ag NPs and BP into PCL nanofibers using electrospinning technique, where BP was used to overcome the shortcoming of Ag NPs easy aggregation, especially the synergistic effect of BP photothermal conversion and NIR can promote the release of Ag NPs. Through the synergistic bactericidal action of PTT and MIT, the obtained PCL/AgNPs/BP nanofiber presented good photothermal capacity and photothermal stability, and had obvious bactericidal and biofilm ablation activities, as well as good biocompatibility. In the presence of NIR irradiation, the thickness of the bacterial biofilm in PL-3 group decreased rapidly and showed obvious burning phenomenon, while the thickness of the bacterial biofilm in PL-0 group was as high as 35.67 ± 2.08 μm with *S. aureus* cells. The synergy of Ag^+ ions release and BP's photothermal effect effectively inhibited bacterial growth and biofilm formation, thus promoting rapid healing of infected wound. Interestingly, the thermal energy generated by stimulating BP promoted the release of Ag^+ ions, bacterial sensitivity, and vascular regeneration.

To reduce the inflammatory response along with PTT, Huang and co-

workers developed a MXene-incorporated engineered fibrous membrane by electrospinning and electrostatic driven assembly for infectious skin regeneration [260]. Upon 10 min NIR light irradiation, the engineered fibrous membrane not only produced hyperthermia but also increased local ROS levels. Through the synergistic bactericidal action of PDT/PTT, the engineered fibrous membrane presented considerable bacterial inactivation. *In vivo* experiments confirmed that the aspirin-loaded engineered fibrous membrane for healing infected skin possessed the ability to kill pathogenic bacteria, promoted wound epithelialization and collagen deposition, promoted angiogenesis and regulated inflammation by regulating NF-kB pathway.

Through the synergistic effect of PTT/PDT/MIT, Yang et al. developed a photoactivated antibacterial nanofiber membrane consisting of an electrospun PCL scaffold and PDA-coated MXene/Ag_3PO_4 (MX@AgP) bioheterojunctions (bio-HJs) [261]. Upon the illumination of 808 nm NIR light, MX@AgP NPs-loaded membranes showed remarkable PTT/PDT properties and released cytotoxic Ag^+ ions for MIT, preventing the reproduction of remaining bacteria in the dark. If the NIR light was removed, the PDA reduced Ag^+ ions to Ag^0 NPs *in situ*, realizing the self-charging of Ag^+ ions and providing enough Ag^+ ions for secondary phototherapy. In addition, under the synergistic action of PTT/PDT/MIT, the self-recharging membranes possessed superior ability to eradicate biofilm. The effect of 5MX@AgP-PCL + NIR group on biofilm integrity was around 10 %. In contrast, the 8MX@AgP-PCL + NIR group effectively eradicated more than 50 % of mature *S. aureus* biofilm, and the biofilm biomass was significantly reduced, which was consistent with the crystal violet (CV) staining results. In addition, *in vivo* experiments showed that photoactivated nanofiber membrane could reshape the wound microenvironment by inactivating bacteria, stopping bleeding, improving epithelization and collagen deposition, and promoting angiogenesis.

To take full advantage of the properties of the infective microenvironment (IME), Zhou et al. developed a novel IME-activated nanocatalytic membrane that orchestrated rapid sterilization and recovery of chronic wounds through synergy of CDT/PTT/PDT/MIT [179]. As shown in Fig. 13A, the IME-activated nanocatalytic membrane consisted of PLGA scaffolds, MXene/Ag_2S (MX/AS) bio-HJs, and lactate oxidase (LOx). Specially, PLGA scaffolds were gradually degraded into lactate acid (LA), and LOx consumed LA to produce more H_2O_2 by microenvironment response. The produced H_2O_2 can be catalyzed by P-MX/AS@LOx membranes to •OH through Fenton-like reaction for killing bacteria. Particularly, as shown in Fig. 13B, CV staining results demonstrated that the P-MX/AS@LOx + NIR group could remove more than 50 % of the biofilm, while the P-MX/AS + NIR group eliminated only a small part of that. Confocal 3D images of LIVE/DEAD staining showed that around 50 % of dead bacteria were present in P-MX/AS@LOx + NIR group, which was consistent with the CV staining results, while live bacteria with dense biofilm architecture covered the PLGA membrane. P-MX/AS@LOx membranes showed both PTT and PDT with more •OH generation upon 808 nm NIR light irradiation, as well as releasing Ag^+, all resulting in the rapid synergistic sterilization. The synergistic treatment of CDT/PTT/PDT/MIT by P-MX/AS@LOx

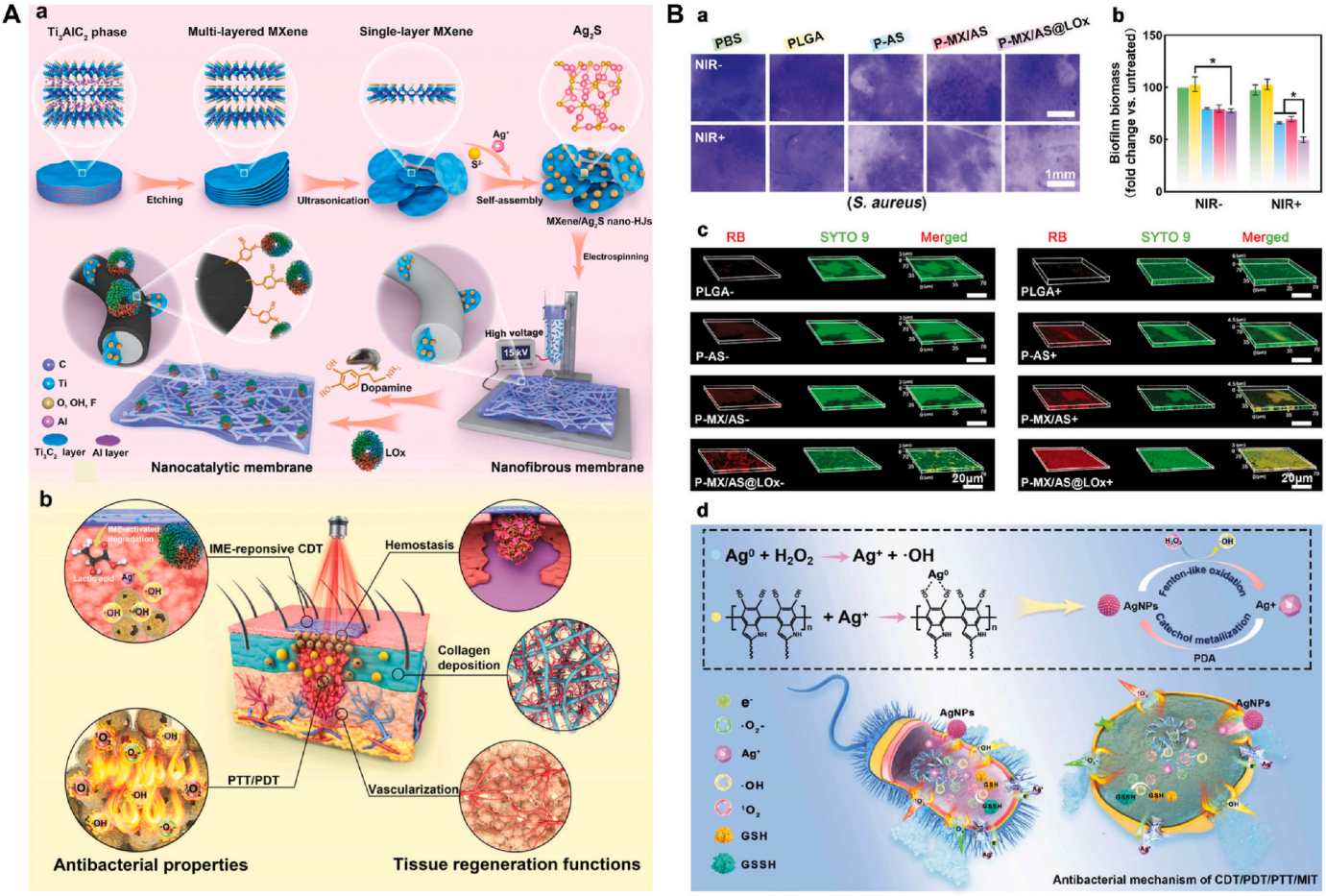

Fig. 13. Representative synergistic antibacterial therapies by antibacterial nanomaterial-loaded eNFMs in infected wound healing. (A) Schematic illustration of the fabrication of P-MX/AS@LOx membrane with antimicrobial properties and tissue regeneration functions. (B) (a) Typical pictures of biofilms visualized by CV staining, (b) quantitative analysis of the CV-stained biofilms, (c) 3D confocal images of residual biofilms treated with the samples for 10 min, and (d) schematic illustration of antibacterial mechanism of CDT/PDT/PTT/MIT. Reprinted with permission from Ref. [179]. Copyright 2021, Wiley-VCH.

membranes caused the highly effective bactericidal efficacy. In addition, the P-MX/AS@LOx membranes showed excellent biocompatibility and remodeled wound microenvironment by killing bacteria, hemostasis, accelerating angiogenesis, promoting epithelialization and collagen deposition.

Similarly, Wang et al. developed a IME-unlocked bio-catalytic fabric which generated O_2 and integrated CDT/PDT/PTT for bacteria-infected wound therapy [262]. The fabric consisted of an electrospun PCL scaffold, MXene/SnS_2 (MX/SnS) bio-HJs and LOx. Based on the acidic microenvironment of the infected area, LOx-loaded fabric can consume LA generated by bacteria at the infected site, producing H_2O_2. Meanwhile, under 808 nm NIR light illumination, MX/SnS bio-HJs not only catalyzed H_2O_2 to promote the generation of •OH by Fenton-like reaction but also generated O_2 to strengthen PDT. Significantly, the bio-catalytic fabrics showed significant phototherapy effects under NIR irradiation, including outstanding PTT and improved PDT efficiency. Additionally, the fabric possessed good biocompatibility/blood compatibility and accelerated wound healing by promoting hemostasis, decreasing inflammatory response, and facilitating collagen deposition and angiogenesis.

Combining PTT and ferroelectric polarization strategies, Wang et al. embedded self-assembled $Bi_4Ti_3O_{12}/Ti_3C_2T_x$ (BTO/$Ti_3C_2T_x$) heterostructures into PVDF nanofibers via electrospinning [263]. Interestingly, $Ti_3C_2T_x$ can enhance the light absorption range and photothermal conversion efficiency of BTO upon visible light exposure, and accelerate oriented electron transfer. More ROSs could be generated by utilizing the trapped e^- and h^+. Additionally, the inhibition rates of PVDF/BTO/$Ti_3C_2T_x$ membrane against *E. coli* and *S. aureus* were 99.71 % ± 0.16 % and 99.61 % ± 0.28 %, respectively, when the membrane was irradiated by sunlight for 20 min, combined with photothermal effect and ferroelectric polarization enhanced photocatalysis. Furthermore, the membrane presented good biocompatibility and significant property on wound healing.

Through a synergistic effect of PTT and photo-thermoelectric catalysis, Wang et al. integrated a highly efficient photo-thermoelectric catalyst rGO-Bi_2Te_3 into PU fibers for bacteria-infected wound therapy [264]. The photo-thermoelectric catalysis of rGO-Bi_2Te_3 significantly improved ROSs yield due to the efficient e^--h^+ separation resulting from the unique thermoelectric field and heterogenerous interface of rGO--Bi_2Te_3. After cycled by 808 nm NIR light illumination, the inhibition rate of 50 % rGO-Bi_2Te_3@PU membrane against *S. aureus* was 91.88 ± 5.34 %. The remarkable antibacterial property was attributed to the synergy of the generated ROSs and heat on bacteria, further accelerating the death of bacteria. In the MRSA-infected wound healing model, the wound temperature of 50 % rGO-Bi_2Te_3@PU group increased to around 55 °C after 1 min of NIR light illumination, while that of PU group was maintained at around 40 °C. Compared to control group, 50 % rGO--Bi_2Te_3@PU membrane showed better disinfection performance with antibacterial efficiency of 99.35 ± 0.29 % against MRSA. Moreover, the tissue repair ability and reliable biosafety of 50 % rGO-Bi_2Te_3@PU membrane were verified *in vivo*. This work provided a new insight on the design of heterogeneous interfaces in photo-thermoelectric catalysis.

Additionally, *in situ* electrospinning technique gains attractive attentions in the preparation of nanofibrous membrane wound dressings by using portable or handheld electrospinning devices [265–267]. Compared to the traditional electrospinning technique, *in situ* electrospinning can deposit nanofibers directly on the wound surface, thus matching the wound site better and more effectively, especially for cases where wound surface is uneven [268–270]. With the development of this type of electrospinning, handheld electrospinning has shown its potential for advanced and personalized wound care.

As a typical example, Zhang and co-workers designed a portable electrospinning device to prepare photodynamic nanocomposite fibers by an *in situ* deposition method [271]. Photodynamic nanofibers were prepared by electrospinning the precursor solution contained PCL, PVP, and hypericin-coated UCNPs (UCNPs@hypericin), as illustrated in Fig. 14A. TEM tests confirmed that UCNPs@hypericin clusters had good dispersity in nanocomposite fibers. Owing to the size of formed UCNPs@hypericin clusters (~55 nm) much greater than that of the uniform eluting pores (~4 nm), the photosensitizer hypericin did not shed or leak into wound tissue. *In vivo* experiments indicated that the rapid hemostasis at the incision site can be achieved within 7 s by UCNPs@hypericin nanocomposite fiber. In MRSA-infected wounds irradiated by 808 nm NIR light, UCNPs@hypericin nanocomposite fibers possessed a superior photodynamic bactericidal effect, promoting collagen deposition and reducing wound healing time from 24 to 16 days.

Similarly, the PTT strategy has been successfully implemented by a handheld electrospinning device. By *in situ* electrospinning technique, Liu et al. prepared CuS-doped composite nanofibers for rapid outdoor hemostasis and ablation of superbacteria at the same time [272,273], as shown in Fig. 14B. Upon 808 nm NIR irradiation, the higher concentration of CuS and the longer irradiation time caused the higher temperature of composite nanofibers. When the CuS content was 0.3 wt%, the temperature of composite nanofibers rose to 56 °C within 5 min, which was basically the same as that when the CuS content was 0.2 wt%. This excellent photothermal performance contributed to the outstanding antibacterial property after PTT against the superbacteria *P. aeruginosa*. In addition, CuS composite nanofibers deposited *in situ* on the wound can accelerate hemostasis (<6 s) and reduce the healing time of superbacteria-infected wounds (18 days).

In another study, Zhang and co-workers reported a multifunctional luminescent MOF-based nanofiber dressing with visual monitoring and bactericidal effect for diabetic wound therapy [274]. As presented in Fig. 14C, the glucose oxidase/carbon dots@Cu-MOF-based (GOx/CDs@MOF) nanofiber dressing was prepared by a handheld electrospinning device driven by 10 kV applied voltage. In the hyperglycemic microenvironment, glucose activated the dressing's cascade catalytic reaction to produce •OH and thereby inactivated bacteria. Meanwhile, during the process of diabetic wound healing, when pH value was in the range of 5~9.5, CDs, as a pH fluorescent indicator, enabled GOx/CDs@MOF dressing with sensitive and reversible fluorescence sensing behavior towards wound pH values. These fluorescence signals were quantified through smart phones to accurately reflect wound status. *In vivo* and *in vitro* experiments showed that GOx/CDs@MOF dressing efficiently killed *E. coli* and *S. aureus* and accelerated wound healing.

4.2. Bone repair

Bone tissue engineering is an alternative therapeutic intervention to repair or regenerate bone defect [275]. The scaffold is one of the three basic components for the bone tissue engineering to mimic ECM [276]. Among various scaffolds such as hydrogels, microneedles, microspheres, electrospun scaffolds have received extensive attentions in bone tissue regeneration due to its further modifications of chemical, biological, and mechanical properties [277,278]. However, despite advances in scaffold design and the application of best surgical practices, bacterial infections have become one of the leading causes of failed bone repair surgeries [279]. Once implanted in the body, the biomaterial induces local tissue reactions, including acute and chronic inflammation, foreign body reaction, granulation tissue formation, and finally fiber embedding [280]. This creates an immunosuppressive pain, leaving the implant vulnerable to microbial colonization and infection [281]. Meanwhile, scaffolds are substrates for bacterial adhesion and biofilm formation, and play a vital role in pathogenesis of implant infection [282]. Therefore, the development of rapidly and effectively sterilized electrospun scaffolds by adding antibacterial to reduce bone infection is an urgent and unmet clinical need [283–285].

Bone infection is an inflammatory bone disease caused by infectious microorganisms that can cause progressive bone destruction and loss [244,286]. By a combination of electrospinning and self-assembly techniques, Amantay et al. prepared NIR light-responsive PDA

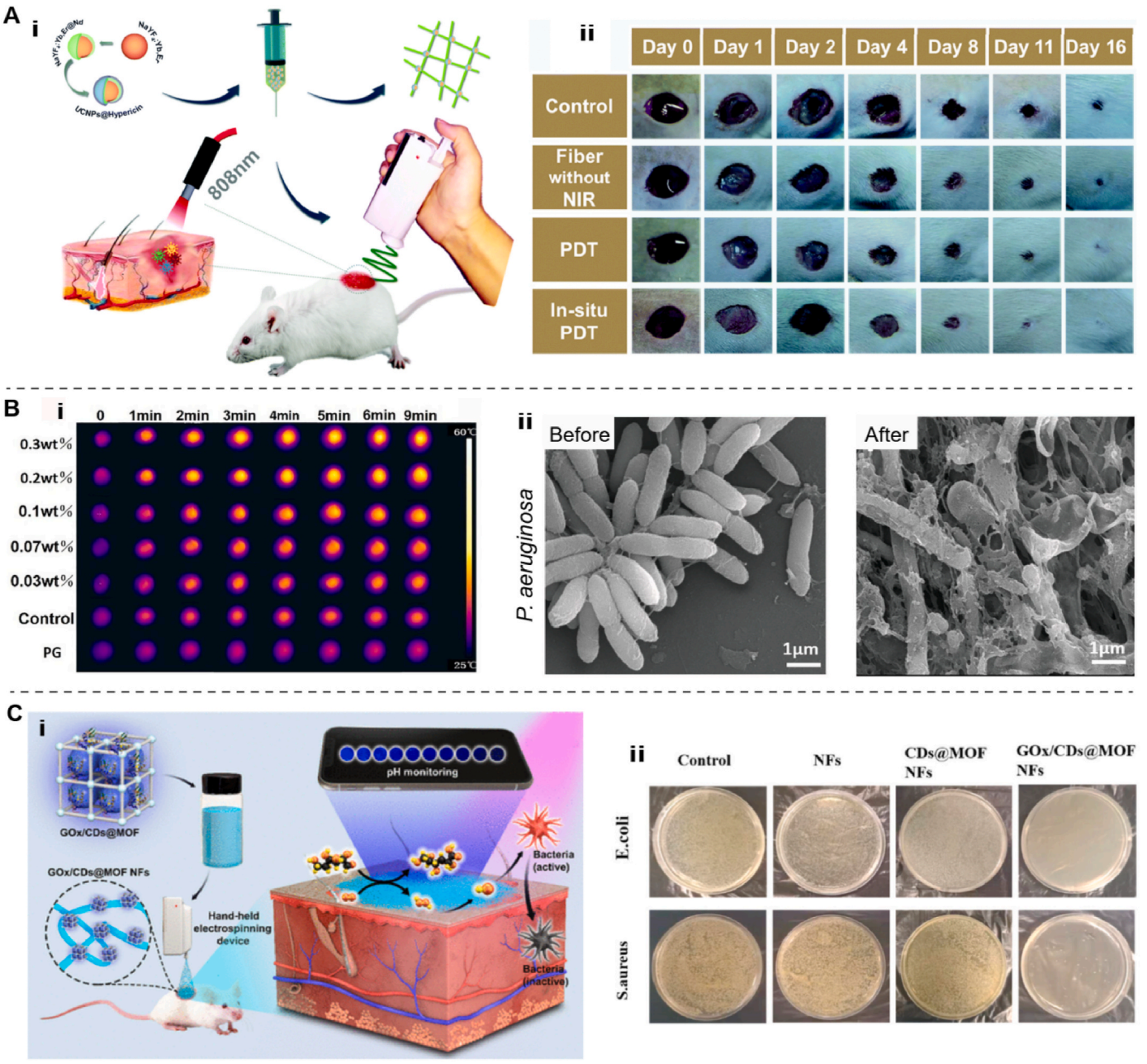

Fig. 14. Representative handheld electrospinning devices for the preparation of nanomaterial-loaded eNFMs for promoting infected wound healing. (A) (i) Schematic illustration of preparation of UCNPs@hypericin NPs loaded PCL/PVP nanocomposite fiber membrane for outdoor hemostasis and superbacteria sterilization. (ii) Photos of MRSA infected trauma after different treatment. Reprinted with permission from Ref. [271]. Copyright 2021, Royal Society of Chemistry. (B) (i) Thermographic images of nanofibers versus time with CuS concentration under 808 nm NIR irradiation (PG refers to nanofibers without loading CuS NPs). (ii) SEM images of *P. aeruginosa* before and after PTT. Reprinted with permission from Ref. [272]. Copyright 2020, Elsevier B.V. (C) (i) Schematic illustration of preparation of GOx/CDs@MOF NF dressing for visual monitoring of wound pH and inhibiting bacterial infection. (ii) Agar plate photographs of bacteria of *E. coli* and *S. aureus* after various treatments. Reprinted with permission from Ref. [274]. Copyright 2023, American Chemical Society.

adherent Cu NPs contained PLLA composite fibers (PLLA@PDA/Cu) for antibacterial and bone regeneration [200]. Due to the photothermal property of Cu NPs, PLLA@PDA/Cu composite fibers can produce abundant ROSs under the irradiation of 808 nm NIR light, with 23.7 % photothermal conversion efficiency. After being irradiated by NIR light, PLLA@PDA/Cu composite fibers showed 99 % and 94 % antibacterial rates against *E. coli* and *S. aureus*, indicating the rapid and powerful bactericidal efficacy of composite fibers. In addition, PLLA@PDA/Cu composite fibers were beneficial to cell adhesion and diffusion, and had good cytocompatibility, osteogenic and angiogenesis properties. Overall, the composite PLLA@PDA/Cu fiber was a promising photothermal antibacterial material.

The periosteum is rich in osteoprogenitor cells, osteoblasts, and capillary networks, which play a crucial role in bone development, formation, remodeling and fracture healing. To accelerate repair of periosteum, Liu et al. prepared an artificial tissue-engineered periosteum composed of PCL doped with tantalum (Ta) NPs and ZnO NPs by electrospinning technology [287]. The electrospun PCL/Ta/ZnO nanofiber membrane can slowly release Zn^{2+}. *In vitro* antibacterial experiment and subcutaneous anti-infection model of SD rats validated that the PCL/Ta/ZnO nanofiber membrane had good bactericidal ability against *E. coli* and *S. aureus*. The unique antibacterial mechanism of TA

NPs and the released Zn^{2+} enhanced the synergistic bactericidal effect, thus achieving the best efficacy. Additionally, the osteogenic properties of PCL/Ta/ZnO nanofiber membrane were significant stronger than those of PCL and PCL/Ta groups, which was related to the expression of osteogenic-related genes such as alkaline phosphatase (ALP), bone morphogenetic protein-2 (BMP-2), osteocalcin (OCN), runt-related transcription factor-2 (Runx-2). Moreover, PCL/Ta/ZnO nanofiber membrane had the best ability to promote the migration of endothelial progenitor cells (EPCs) to the injury site, the best ability to promote tubule formation of EPCs, and the strongest ability to promote the expression of angiogenesis-associated genes such as angiopoietin-1 (Ang-1), VEGF, and endothelial nitric oxide synthase (eNOS). In a critical-size skull defect model, PCL/Ta/ZnO demonstrated significant infection control and good immunomodulatory effect, thus achieving rapid vascularized bone repair.

To achieve long-term immunomodulatory and bactericidal functions, He and co-workers incorporated TA/Zn^{2+}-based metal-phenolic networks (MPNs) nanocomposites into PCL nanofibers for accelerating bone regeneration [221]. Briefly, TA/Zn^{2+}-based MPNs nanocomposites were obtained by simply mixing TA solution and $ZnCl_2$ solution, followed by adjusting pH value of the mixed solution to 8.0. Then the obtained nanocomposites were dispersed into PCL spinning solution, followed by blending electrospinning. The resulting PCL/TA/Zn fibrous membrane presented pH-responsive Zn^{2+} release behavior, which was beneficial to the long-term bactericidal property. Additionally, TA molecules could be released from the fibrous membrane, resulting in intracellular ROS scavenging to relieve oxidative stress of surrounding cells. Moreover, the favorable osteogenesis property was achieved by the fibrous membrane, mainly due to the manipulated beneficial anti-inflammatory and osteoimmune microenvironment.

To overcome the limited mechanical properties or biological activity of repairing bone defects, Wang and co-workers developed dual Mg reinforced Janus structural composite membrane (Mg-MgO/PCL) by casting and electrospinning combined processing technique [288]. The incorporation of Mg sheets and MgO NPs improved the composite membrane's mechanical properties, especially the tensile strength and compression force, through the enhancement of Mg sheet and the improvement of crystallization. Compared to porous microfibers, the

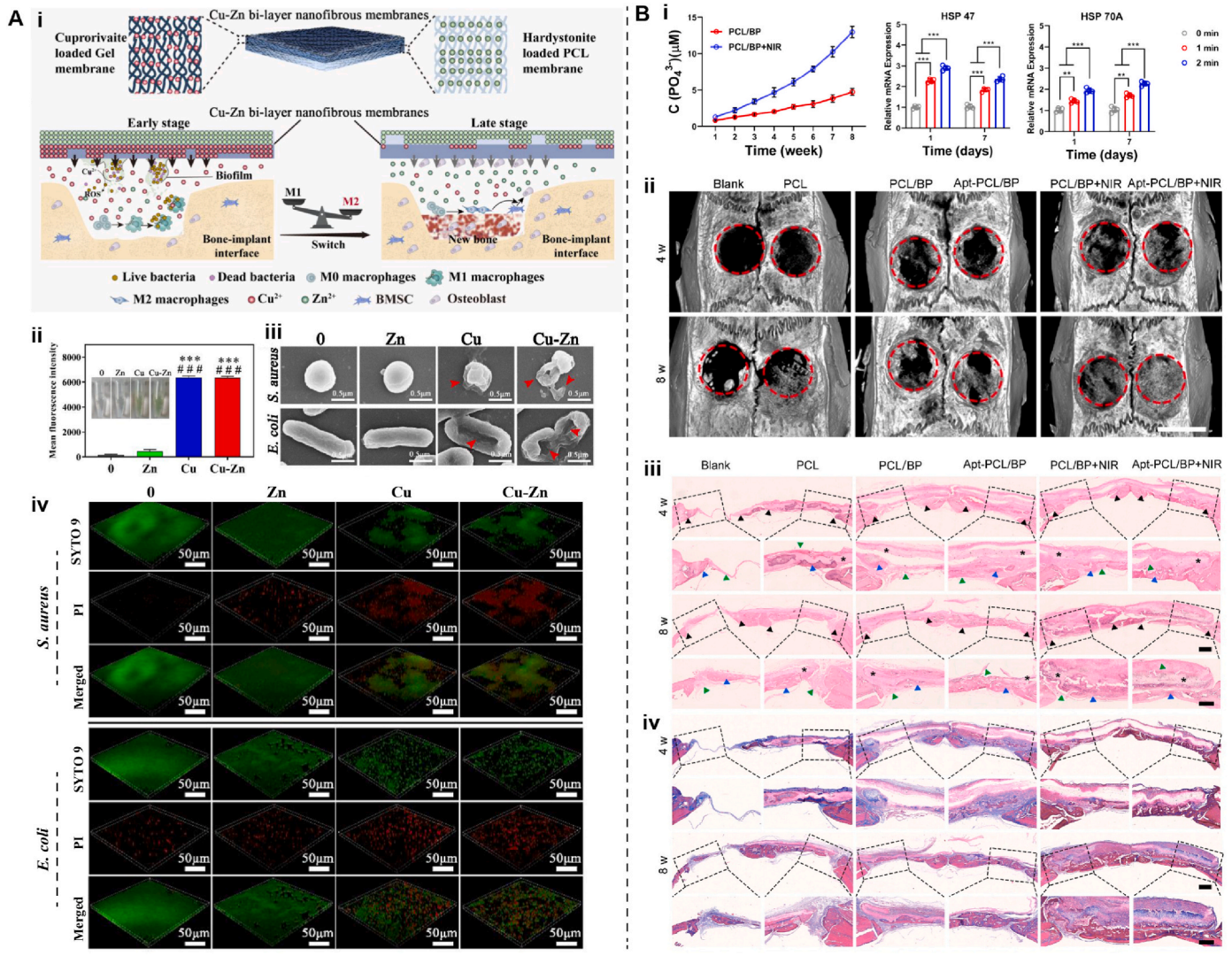

Fig. 15. Representative antimicrobial nanomaterial-incorporated eNFMs for guiding bone regeneration. (A) (i) Schematic illustration of the basic structures and dual-temporal bidirectional immunomodulatory effects of Cu-Zn bi-layer nanofibrous membranes. (ii) ROS levels produced by various membranes in aqueous solutions. (iii) SEM images of bacteria morphology after different treatments. (iv) Confocal laser scanning microscopy results of biofilm structure of two strains. Reprinted with permission from Ref. [289]. Copyright 2020, Elsevier Ltd. (B) (i) Release of PO_4^{3-} from the PL/BP scaffold with or without irradiation by NIR light and the relative expression of HSP 47 and HSP 70A without illumination (0 min) or with 1 min and 2 min illumination. (ii) Micro-CT 3D reconstruction of the repaired bone tissues at 4 weeks and 8 weeks post-operation, respectively. (iii) H&E staining and (iv) Masson's Trichrome staining of the repaired bone tissues at 4 weeks and 8 weeks post-operation. Reprinted with permission from Ref. [194]. Copyright 2023, American Chemical Society.

Janus structure design of the membrane improved protection against fibroblast penetration towing to its good shielding capability, osteogenic potential, and *in vitro* and *in vivo* angiogenic properties. The porous microfiber side supported pre-osteoblast cell adhesion by the biomimetic ECM and sustained Mg^{2+} release, enhancing osteogenesis and angiogenesis. After adding 2 wt% MgO NPs, Mg-MgO/PCL membrane presented significant antibacterial effect and induced the apoptosis rate of *S. aureus* to exceed 88.75 %. In a rat skull defect model, Mg-MgO/PCL membrane can greatly promote the new bone formation after surgery *in vivo*.

In order to adapt to the immune characteristics of implant-associated infection and implant-bone integration disorder, Guo et al. reported Cu-Zn bi-layer NFMs by combining electrospinning technology and hot-pressing method [289]. As shown in Fig. 15A, Cu-Zn bi-layer NFMs presented excellent biofilm resistance and transient resistance to floating bacteria regardless of bacterial species. In contrast, Cu bi-layer NFMs could briefly suppress infection at an early stage, while Zn bi-layer NFMs not only had no obvious bactericidal activity, but also promoted infection development, suggesting that the Cu component in the NFMs was directly responsible for the antibacterial activity. The underlying antimicrobial mechanism was that Cu and Cu-Zn bi-layer NFMs generated more ROSs in aqueous solution, causing bacterial death by damaging the cell wall or membrane, and inhibiting biofilm formation by cutting biomacromolecules (eDNA) in the biofilm matrix. Additionally, Cu-Zn bi-layer NFMs showed good controlled releases of Cu^{2+} and Zn^{2+}, and could sequentially adjust the transfer of macrophage phenotype from M1 to M2 by alternating activating MAPK and mTOR signaling pathways. In sum, the dual-temporal bidirectional immunomodulatory effect of Cu-Zn bi-layer NFMs showed good disinfection and osteogenic ability both *in vitro* and *in vivo*.

The strong photothermal bactericidal properties alone might cause thermal damage to nearby tissues, leading to further deterioration of tissues. To overcome the issues of strong photothermal bactericidal properties and thermal damage to nearby tissues, Zhang and co-workers in a recent study [194] constructed a multifunctional nanofiber scaffold with biomimetic mild photothermal effect enhancement to achieve bacteria-free and efficient bone regeneration. Briefly, BP NSs as photothermal agents were first doped into the electrospun PCL fiber scaffold, and then the PCL/BP scaffold was treated with O_2 plasma, and then soaked in PBS solution containing MSC-specific aptamer (Apt 19S). Subsequently, a layer of PCM particles containing vancomycin (an antibiotic) and BP NSs was sprayed on Apt-PCL/BP scaffold surface by a coaxial electrospray process. Due to the incorporation of PCM/BP microparticles, the temperature of Apt-PCL/PCM/BP scaffold was as high as 40.2 °C upon low intensity of NIR illumination, higher than the melting point of PCM (39 °C). The vancomycin release was achieved by the conversion from solid to liquid of PCM microparticles. As show in Fig. 15B, the PTT effect of PCL/BP scaffold can enhance the expression of HSP (HSP 47 and HSP 70A) after irradiation by NIR light, accelerate the release of PO_4^{3-} in the scaffold, and promote the osteogenic differentiation and biomineralization of MSCs. In the rat model of critical size cranial bone defect, at 4 and 8 weeks after implantation, new bone tissues were formed at both the edge and center of the defect in the NIR irradiation group, while only a small quantity of bone tissue was found in the blank group. Additionally, the BV/TV and BMD of the regenerated bone in Apt-PCL/BP + NIR group were greatly larger than those in BP-encapsulated scaffold with frequent irradiation of NIR light. In addition, H&E and Masson's trichrome staining results showed that NIR irradiation combined with BP-encapsulated scaffolds resulted in faster and better healing of wounds with bone-like structures. In sum, this work demonstrated the ability of nanofibers to eliminate bacteria, recruit MSCs, and promote bone repair under the help of PTT both *in vitro* and *in vivo*.

4.3. Periodontal repair

Periodontitis was reported as the 11th global pandemic disease in 2016 [290], and is one of the most common diseases caused by oral pathogens [291]. Periodontitis as an oral infection caused by bacteria can cause severe degradation of periodontal tissue and has a high prevalence of 42.2 % in adults aged 30 years and older. Serious periodontitis is an inflammation caused by oral bacterial biofilms that can cause serious damage to the soft and hard tissues of the periodontal tissue and lead to impaired tooth function and aesthetics [292]. To repair periodontal tissue, guided bone regeneration (GBR) membrane as a physical barrier is typically required to isolate soft tissue from invading bone defects and preserve space for infiltration of bone cells for optimal results [293–295]. One of the major goals of periodontal therapy is to alter or inhibit the periodontal microbiota to ablate subgingival infection and periodontal pockets and to prevent the recurrence of periodontitis [296]. The development of eNFMs combined with antibacterial nanomaterials for periodontal regeneration is motivated by current clinical practice that utilizes eNFMs to maintain space within defects and facilitating the bone formation of periodontal defect.

As a typical example, Liu and co-workers integrated MgO NPs (nMgO) into PLA/Gel fibrous membranes with considerable biodegradable, antibacterial and osteogenic properties for periodontal repair [297]. In this system, the acidic degradation products of PLA can be neutralized by Mg^{2+} ions generated by the hydrolysis of nMgO, improving the pH microenvironment conductive to cell proliferation. The results showed that nMgO-loaded membranes had excellent bactericidal effect against both *E. coli* and *S. aureus* in a dose-dependent manner. Meanwhile, the nMgO-loaded membranes can simultaneously promote osteogenic differentiation of rBMSCs and effectively guide periodontal tissue regeneration. In the periodontal defect repair model, nMgO-loaded membranes greatly promoted the *in-situ* osteogenesis of periodontal defects and formed a large number of new bones, as shown in Fig. 16A. This bone promoting effect was more obvious in nMgO-1.5 membrane, and the newly formed bone tissue almost filled the defect.

The hypoxia environment of periodontal disease can promote the proliferation of anaerobic bacteria. In this regard, Danilo and co-workers developed composite bead-on-string PLA nanofibers containing CaO_2 NPs and MnO_2 NSs, as O_2-release system for the treatment of periodontitis [298]. CaO_2 NPs were used as the precursor of O_2 production, and MnO_2 NSs were used as the nanozyme to catalyze the decomposition of H_2O_2 into the final O_2 product. The composite membranes showed continuous O_2 release for more than 7 days, and its level was adjusted by CaO_2 NPs content. This structure presented suitable physicochemical performance and antibacterial effects against some bacteria commonly related to aggressive and chronic periodontitis, such as *Porphyromonas gingivalis* (*P. gingivalis*) and *Treponema denticola* (*T. denticola*). *In vitro* studies also indicated that the membranes were non-cytotoxic to human oral keratinocyte and could enhance cell viability, while high contents of CaO_2 NPs and MnO_2 NSs were embedded into the fiber.

Additionally, ZnO NPs are regarded with a wide-spectrum antibacterial property against a variety of pathogenic microorganisms and can be used as antimicrobial additive to eNFMs to enhance the antimicrobial ability of dental implant materials [299,300]. In order to overcome the limited application of barrier membrane in bacteria-supported microenvironments and stratification of soft and hard tissues, Xiang and co-workers developed a nanocomposite multifunctional sandwich-like GBR membrane (termed as SGM) by sequential electrospinning nZnO-doped SF pure SF, and hydroxyapatite nanoparticle-doped SF (nHA/SF) [301]. In this system, the surface layer of SGM containing nZnO had good antibacterial effect against *E. coli* and *S. aureus*. The interlayer of SGM with dense structure had good biocompatibility and suitable mechanical properties, which made the GBR membrane play a barrier role. The inner layer containing nHA was conductive to differentiation and matrix mineralization of MC3T3-E1. SGM promoted bone formation in periodontal defect model of rats. *In vivo* experiments

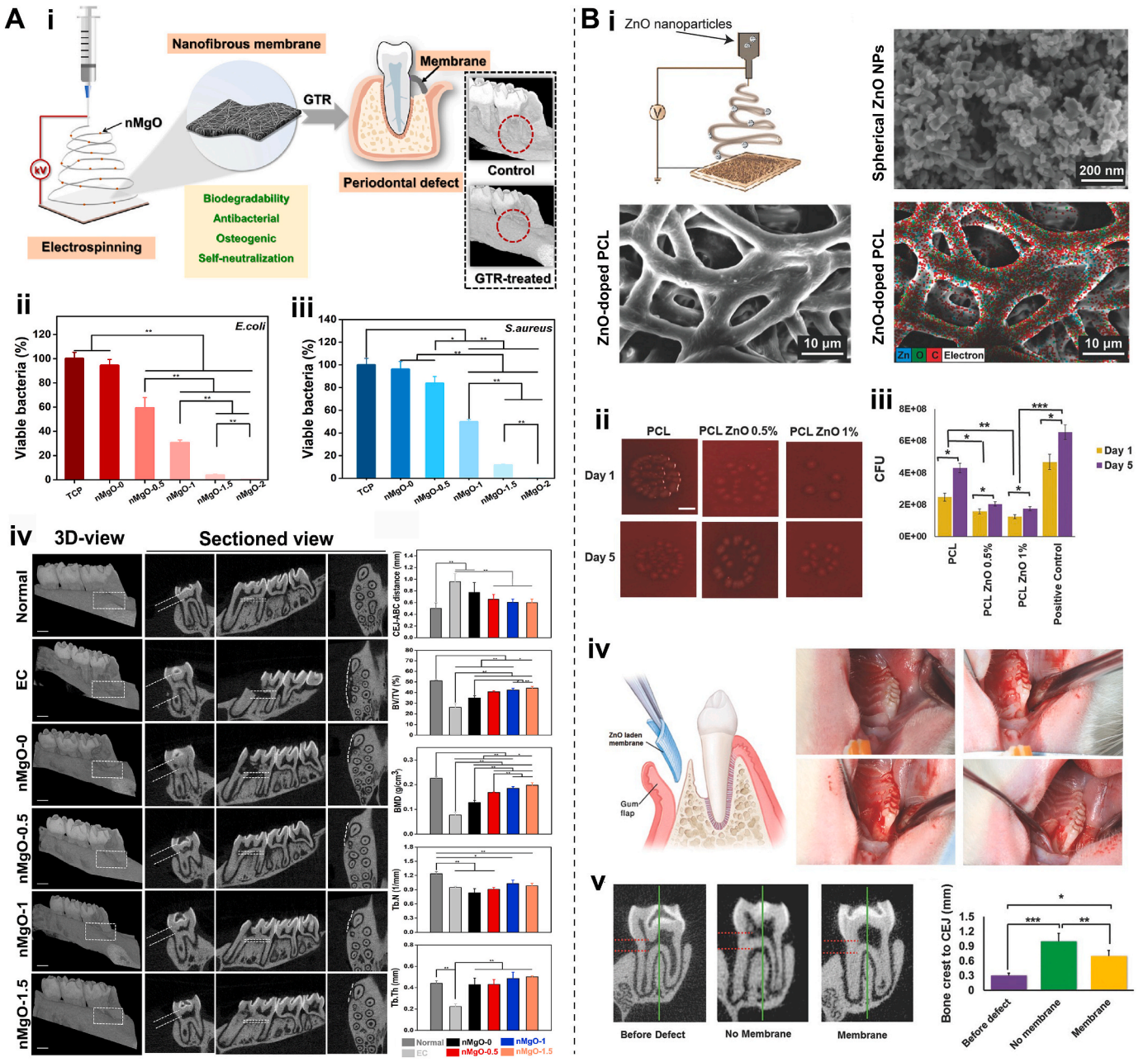

Fig. 16. Representative antimicrobial nanomaterial-loaded eNFMs for periodontal tissue repair. (A) (i) Schematic illustration of nMgO-doped PLA composite membrane for periodontal tissue regeneration. Quantitative bacterial survival rates of tissue culture plate (TCP) and nMgO-loaded membranes against (ii) *E. coli* and (iii) *S. aureus*. (iv) 3D reconstructed digitized images and sectioned images of periodontal defects analyzed by Micro-CT 6 weeks post-surgery and corresponding quantitative analyses of bone related parameters including CEJ-ABC distance, BV/TV, BMD, Tb.N and Tb. Th 6 weeks post-surgery. Reprinted with permission from Ref. [297]. Copyright 2020, Elsevier Ltd. (B) (i) Schematic illustration of the preparation of ZnO-loaded PCL membrane, SEM image of spherical ZnO NPs, and SEM image of ZnO-loaded PCL membrane with 1 % (w/v) ZnO and corresponding EDAX elemental imaging. (ii) CFUs on the membrane surfaces and (iii) corresponding quantified data against *P. gingivalis*. (iv, v) *In vivo* experiments in a rat periodontal defect model. Reprinted with permission from Ref. [302]. Copyright 2017, Wiley-VCH.

showed that SGM can promote bone repair in rat skull defect model and periodontal defect model.

To improve the limited bioactivity and regenerative potential of the existing periodontal membranes, Nasajpour et al. developed an osteoconductive and antibacterial PCL composite membrane by electrospinning of PCL and spherical ZnO NPs [302]. Fig. 16B showed that ZnO NPs were evenly distributed on the fabricated membranes and fiber surfaces. The engineered membranes with 0.5 % and 1 % (w/v) of ZnO NPs showed significant bactericidal property against *P. gingivalis* after 1 and 5 days, respectively, while bare PCL showed no bactericidal effect at either time interval. Particularly, loading 0.5 % (w/v) ZnO NPs enabled the engineered membrane to be bactericidal and osteoconductive responses without negatively affecting its biocompatibility. Additionally, the incorporation of ZnO NPs can regulate the mechanical strength and degradation characteristic of the engineered membrane. In a rat periodontal defect model, the engineered membrane had antibacterial property with good osteoconductive performance, which demonstrated its promise for periodontal repair.

In another study, in order to improve the repair effectiveness of existing GBR membranes, Lian and co-workers prepared a novel

multifunctional electro-written bi-layered GBR scaffold by a combination of solution electrospinning writing (SEW) and solution electrospinning (SES) techniques [303]. Cu-loaded MSNs were incorporated into the PLGA/Gel fiber matrix to prepare a composite PLGA/Gel-Cu@MSNs scaffold. The loose porous SEW layer supported and promoted bone ingrowth, while the dense and compact SES layer prevented non-osteoblast penetration. Therapeutic Cu^{2+} ions were released in a controlled manner, giving the composite scaffold effective osteogenic and bactericidal properties. Importantly, the composite PLGA/Gel-Cu@MSNs fibrous scaffold showed promising bone regeneration effect in a rat periodontal defect model.

In addition, the microbial persistence and reinfection often lead to the treatment failure for endodontic infection and concurrent inflammation. To address the issues, Chachlioutaki and co-workers developed electrospun nanofiber films containing ZnO NPs (a bactericidal agent) and ketoprofen (an anti-inflammatory agent), along with polymer matrix of PVA, hydroxypropyl methylcellulose (HPMC) and carboxymethylcellulose (CMC) [304]. ZnO NPs were loaded within the polymer matrix of nanofiber films and distributed uniformly in the center and surface of the fiber core. *In vivo* antibacterial properties of the ZnO-contained nanofiber films were verified in a human tooth culture model infected with *Enterobacter faecalis* (*E. faecalis*). The combination of anti-inflammation and bactericidal activity of ZnO nanofiber films directly acted on the site of action, which was of great attraction in the endodontic treatment of non-vital infected teeth.

4.4. Tendon repair

Tendons are dense connective tissue with the function of transferring force from muscles to bones [305,306], carrying loads and performing biomechanical functions by supporting, stabilizing and strengthening joints to avoid bone dislocation and fracture [307]. Tendon repair requires an environment that promotes cell proliferation and collagen synthesis. Electrospun nanofibrous membranes have been promising biomaterials for the support and growth of cells due to the similarity of fiber diameter and structure to the that of extracellular matrix (ECM) collagen fibrils, as well as the adjustable porosity and physical-chemical properties of electrospun scaffolds. In addition, by regulating the chemical composition and physical structure, the electrospun scaffolds can regulate the migration, attachment and proliferation of cells.

Tendon sheath infection and tendon adhesion are the main complications after tendon injury. In tendon surgery, existing surgical options include the utilization of antibiotics to prevent infection and physical barriers to reduce adhesion formation [308]. Nevertheless, the ability of antibiotics to produce better anti-adhesion effect is limited, and physical barriers may increase the risk of postoperative infection. Antibacterial materials are very important in the field of medicine, especially in surgery and wound treatment where infection prevention is required. The primary justifications for employing antibacterial materials composed of electrospun nanofiber scaffolds in tendon repair are summarized in Table S1. Researchers have been developing novel antibacterial materials such as antibacterial nanomaterials combined electrospinning scaffolds that not only effectively fight infection, but also promote the repair process of tendon, which have been considered as promising candidates for anti-adhesion, anti-inflammatory and antibacterial activities in tendon repair [52].

As a typical example, Liu et al. prepared Ag NPs/PLLA electrospun membranes by incorporating Ag NPs without significant effects on the physical and chemical properties [309]. The Ag NPs/PLLA fibrous membranes can prevent cell proliferation via a synergistic anti-proliferative effect on the hydrophobicity of the electrospun structure. Due to the incorporation of Ag NPs, the fibrous membranes showed initial potential as bactericidal and anti-adhesion barriers for tendon repair. To manage post-surgical tendon adhesion, Shalumon et al. prepared core-shell nanofibrous membranes (CSNMs) with Ag NPs-contained PEG/PCL as shell layer and HA/ibuprofen as core layer by co-axial electrospinning method [52]. HA had a lubricating effect to smooth tendon sliding and decreased fibroblast adhesion, while Ag NPs and ibuprofen showed anti-infection and anti-inflammation effects, respectively. The core-shell structure could satisfy the requirements for an anti-adhesion barrier by ibuprofen and Ag NPs to lessen infection and inflammation, while HA can reduce the fibroblasts adhesion. Additionally, histological and functional analyses in rabbit flexor tendon rupture models indicated the enhanced effects of the CSNMs in lessening inflammation and tendon adhesion.

Similarly, Chen et al. developed dual functional core-shell electrospun HA/PCL fibrous membranes containing Ag NPs for prevention of peritendinous adhesion and bacterial infection after tendon surgery [310], as shown in Fig. 17A. While PCL and HA/PCL fibrous membranes were without inhibition zones, Ag NPs-contained HA/PCL fibrous membranes showed inhibition zone against *E. coli* (2.21 ± 0.14 cm^2) higher than that against *S. aureus* (1.66 ± 0.02 cm^2), ascribed to the structure difference of bacteria cell wall. Meanwhile, Ag releasing from Ag NPs-contained HA/PCL fibrous membranes stabilized after 4 days, conformed the short-term antibacterial activity, while HA release was prolonged to 21 days, producing lubrication around the healed tendon and exerting long-term anti-adhesion properties. Additionally, due to the synergistic effect of Ag and HA, Ag NPs-contained HA/PCL fibrous membranes showed the highest inhibition effect on the adhesion and proliferation of fibroblasts without obvious cytotoxicity. Importantly, based on gross observation, histological analysis, joint flexion, tendon slip, and biomechanical tests, Ag NPs-contained HA/PCL fibrous membranes showed better peritendinous anti-adhesion properties compared to PCL and HA/PCL fibrous membranes in rabbit models of deep flexor tendons.

Inspired by the pathophysiology of tendon anatomy and adhesion development, as presented in Fig. 17B, Zhang and co-workers developed an adhesive and robust dual-layer Janus patch with antioxidative, anti-inflammatory, and anti-bacterial activities for tendon repair, where a multifunctional electrospun hydrogel patch (MEHP) served as the inner layer (surgical oriented tendon) and PLLA fibrous membrane served as the outer layer (facing the surrounding tissue) [311]. Specially, MEHP was fabricated from gelatin methacryloyl (GelMA) and ZnO NPs by co-electrospinning, followed by treating with tannic acid (TA). *In vitro* antibacterial experiments, compared to the ZnO-loaded GelMA nanofiber membrane without TA treatment, MEHP with 2 % weight ratio of ZnO to GelMA showed the best inhibition effect on bacterial growth and bigger inhibition zone diameters of 15.96 ± 4.81 mm and 25.47 ± 6.81 mm against *E. coli* and *S. aureus*, respectively. Additionally, MEHP presented the best antibacterial activity with around 90 % antibacterial ratios against both *E. coli* and *S. aureus* using plate count method. Here, TA had the capability to scavenge ROS generated by ZnO, so the potential bactericidal mechanism of MEHP may involve the interplay between ZnO NPs with the membrane, as well as the release of Zn^{2+} and TA. Moreover, the MEHP can be tightly attached to the finger surface even if the finger was severely bent without significant structural damage or detachment, indicating good flexibility. Additionally, MEHP exhibited excellent *in vitro* H_2O_2 scavenging capacity and obvious inhibition on the overexpression of pro-inflammatory factors including tumor necrosis factor α (TNF-α), cyclooxygenase-2 (Cox-2) and interleukin 6 (IL-6), indicating its good tissue adhesion strength, superior antioxidative and anti-inflammatory abilities. After the development of MEHP, the Janus patch was constructed using PLLA fibrous membrane. The tensile strength of Janus patch was ~2 MPa, and the mechanical strength was much higher than that of commercially available products. In an Achilles tendon rupture animal model, the Janus patch showed the slightest adhesion score of 1.58 ± 0.67 across all groups based on the quantitative analysis of gross observation, and the breaking force of Janus patch (52.62 ± 5.17 N) was greatly higher that of other groups, indicating a better recovery effect of injured tendon. Overall, Janus patch had goof anti-inflammatory and anti-adhesion abilities, could promote tendon healing and repair, and possessed great potential in the

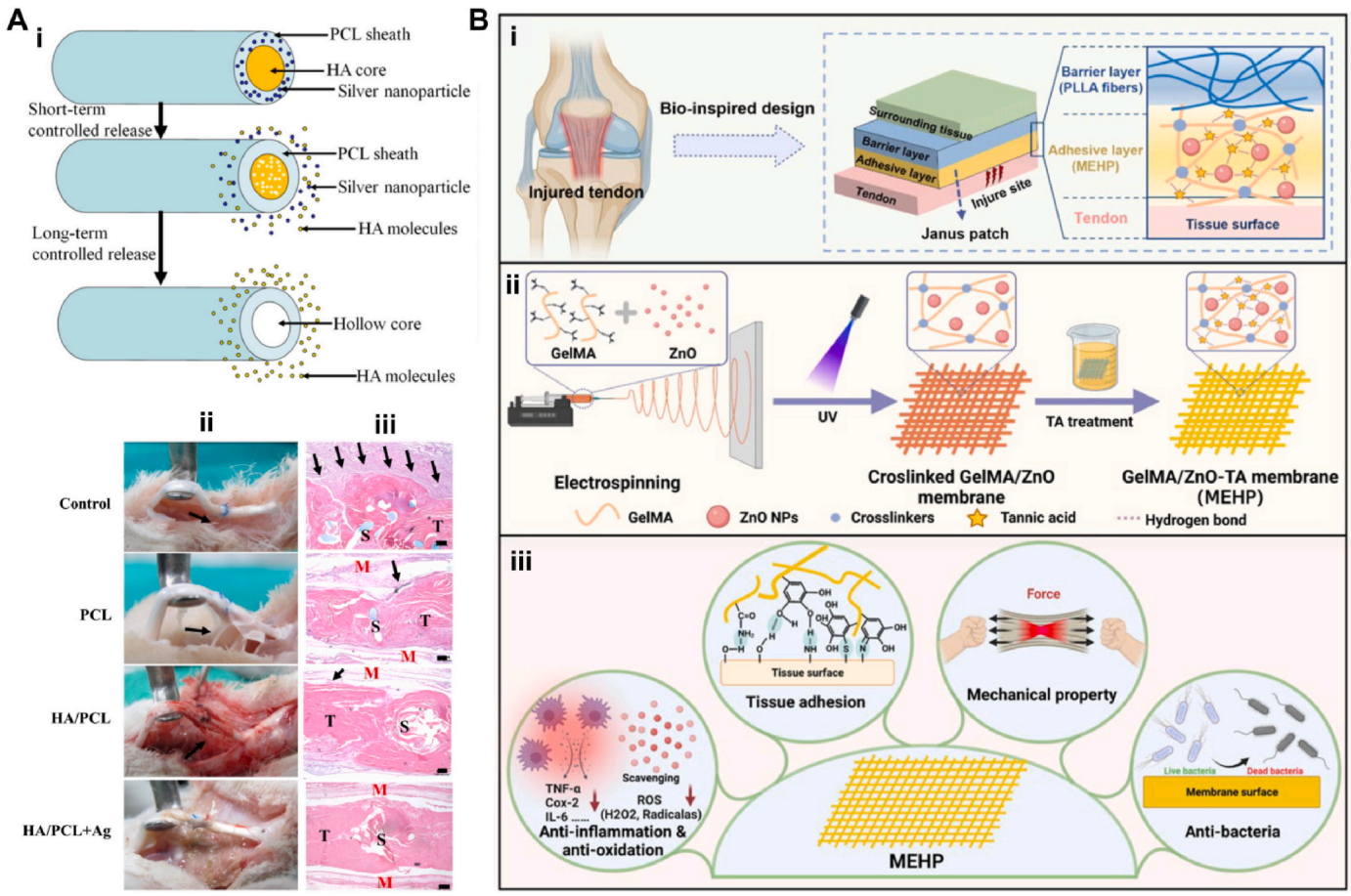

Fig. 17. Representative antimicrobial nanomaterial-loaded eNFMs for tendon tissue repair. (A) (i) Schematic illustration of short-term controlled release of Ag and long-term controlled release of HA from Ag NPs-embedded HA/PCL NFMs. (ii) Gross observation of adhesion occurred in a rabbit model of flexor digitorum profundus tendon repair in different groups 3 weeks post-operation and (iii) corresponding H&E staining images of tissue section at the tendon repair site. Reprinted with permission from Ref. [310]. Copyright 2015, Elsevier Ltd. (B) (i) A dual-layer Janus patch that comprised a MEHP on the inner side and a PLLA fibrous membrane on the outer surface for tendon regeneration. (ii) MEHP prepared by electrospinning GelMA and ZnO, and further reinforced by TA treatment. (iii) Multifunctions of MEHP for providing an advantageous microenvironment for tendon healing. Reprinted with permission from Ref. [311]. Copyright 2023, American Chemical Society.

treatment of tendon injury.

Herein, it should be pointed out that the surface design, chemical composition and physical form of antibacterial materials can affect their antibacterial effect and tissue repair ability. By precisely controlling the dose and release characteristics of the antibacterial agent, it is possible to improve the antibacterial efficiency of the material while promoting the repair and regeneration of damaged tissues. Moreover, in clinical applications, when selecting the right antibacterial material, physicians need to weigh its antibacterial effect against its potential impact on tissue repair. Sometimes, a combination of treatments may be required, such as the use of a temporary antibacterial dressing followed by a change to a material that more promotes tendon healing. In addition, the individual treatment plan and the specific situation of the patient are also factors that need to be considered when selecting the right material.

4.5. Other bio-applications of antibacterial eNFMs

In addition to the abovementioned applications, the antibacterial nanomaterial-incorporated eNFMs also present potential in other bio-applications such as nerve tissue repair and spinal cord injury (SCI) recovery.

Nerve tissue repair directly affects the quality of life and is a valuable therapeutic concept in human healthcare [312,313]. The electrospun scaffolds have been shown to be effective in nerve tissue repair, and the addition of antibacterial nanomaterials into electrospun scaffolds can effectively decrease the risk of bacterial infection after implantation surgery, which contributed to nerve repair and regeneration. For instance, Heidari and co-workers reported a smart electrospun GO-incorporated PCL/Gel nanofibrous mat for application in nerve tissue repair [192]. The bactericidal rate of the mat against *E. coli* and *S. aureus* was more than 99 %, and the corresponding antibacterial mechanism was mainly due to the presence of GO. The sharp edge of GO NSs caused not only the bacterial cell structure disorder, leading to cell death, but also physical damage to bacterial cell membrane, resulting in the loss of the integrity of bacterial membrane. In addition, cell culture experiments indicated that the mats provided a suitable microenvironment for migration, adhesion, and proliferation of PC12 cells. In another study, to promote peripheral nerve injury regeneration, Zhang et al. developed a SF/poly(vinylidene fluoride-*co*-hexafluoropropylene)/$Ti_3C_2T_x$ (SF/PVDF-HFP/MXene) composite scaffold by electrospinning [314]. The composite scaffold presented significant bactericidal activity with over 90 % inhibition rates for all three representative bacteria, *E. coli*, *S. aureus*, and *Candida albicans* (*C. albicans*). This good bactericidal property was mainly ascribed to the addition of MXene whose sharp edge can damage bacteria cell wall, leading to DNA release and occasionally bacteria dispersion. Importantly, upon external mechanical stimulation, the composite scaffold can produce a continuous output voltage. This piezoelectric effect was beneficial to the growth and

proliferation of Schwann cells (SCs) on the composite scaffold. In rat sciatic nerve injury model, the composite scaffold could induce SCs proliferation, enhance axon elongation, and promote axon myelination. Moreover, due to the piezoelectric effect, the regenerated nerve rats showed good motor and sensory function recovery.

The possibility of infection during and after SCI recovery surgery is also a concern. To treat SCI, Kong et al. developed a novel multifunctional hydrogel containing MXene-Au composites, neural stem cells (NSCs) and combined with electrical stimulation [315]. Briefly, the patterned PLGA nanofibers were prepared by electrospinning through the patterned fiberboard. Then, the surfaces of PLGA nanofibers were evenly covered by GelMA solution containing 1 % MXene-Au composites, followed by solidifying under the irradiation of UV for 30 s, resulting in the formation of MAu-GelMA hydrogel. Due to the additions of MXene and Au NPs, the MAu-GelMA hydrogel possessed good bactericidal properties against *E. coli* and *S. aureus*, which could inhibit the growth of bacteria and lower the infection risk of secondary SCI. Moreover, by combining electrical stimulation, MAu-GelMA hydrogel loading of NSCs can lower the formation of cavity and glial scars, improve neuronal differentiation and myelin regeneration of NSCs in the injured area, and accelerate the motor function recovery after SCI in rats.

In sum, because of its ability to simulate the structure and scale of native tissues, electrospun fiber membrane has been attracting much attention as an innovative construct in tissue engineering and regenerative medicine research. However, only five electrospinning fiber products (NCT03690960, NCT06063694, NCT06014437, NCT05944250 and NCT02409628) are ongoing clinical trials as innovative therapeutic options, as shown in Table S2. The main reason why it is difficult to quickly put into clinical application is that the nanofibers produced during electrospinning are usually weak, difficult to use alone, and need to be combined with other materials to improve their application value. Additionally, electrospinning technology is sensitive to the viscosity of the used solution and difficult to control the trajectory of the jet, which has certain requirements on the spinning environment and limits its large-scale production. Moreover, some antibacterial materials can have adverse effects on the environment or the human body. However, electrospinning is moving from laboratory to clinical trials, constantly expanding its application potential in biomedical fields, with the advancement of technology and the expansion of demand, it is expected that more electrospinning fiber products will meet the needs of the medical industry.

5. Conclusion and perspectives

With the development of antibacterial technology and the increase of antibacterial demand, antibacterial eNFMs have received more and more attention. In this review, the recent progress of eNFMs combined with a diverse range of antibacterial nanomaterials in tissue regenerative fields is reviewed. From our limited knowledge, antibacterial eNFMs has made impressive progress over the past few decades, but there is still much to explore and the journey towards the ultimate goal of clinical trial application continues. The limitations of the current strategies are as follows:

(1) **Antibacterial mechanism**: Although electrospinning technology has been widely used in the preparation of antibacterial materials, the antibacterial mechanism still needs to be further studied at the cellular and molecular levels. Understanding how antibacterial materials physically or chemically inhibit or kill bacteria is critical to optimizing the design and preparation of electrospinning antibacterial products.
(2) **Stability and durability of antibacterial membranes**: Antibacterial membranes need to maintain a stable antibacterial effect under various environmental conditions, at present, but some antibacterial materials may lose antibacterial activity in long-term use or under different environmental conditions. Indeed, most nanomaterials are formed and/or deposited on eNFMs via non-covalent bonds, which leads to some characteristics. Weak bonding makes antibacterial ingredients have the ability to release slowly, thus ensuring the bactericidal ability to a certain extent. The stability and durability of antibacterial eNFMs need to be further studied, which is closely related to the composition, structure and fabrication strategy of eNFMs.
(3) **Environmental and health safety**: The safety of antibacterial materials is an important factor that must be considered in their application. Some antibacterial materials can have adverse effects on the environment or human body, and their potential cumulative damage and carcinogenicity should not be ignored, including the long-term toxic and side effects of antibacterial nanomaterials on normal tissues, the fate of nanomaterials in the body, and the toxicity and metabolism of their products. Therefore, its safety must be ensured during use.
(4) **Nanofiber mechanical strength:** Nanofibers produced during electrospinning are usually weak, difficult to use alone, and need to be combined with other materials to improve their application value. The processing of nanofibers into nanofiber yarn may be a prerequisite for subsequent processing such as weaving and upgrading the level of high-end products in the textile industry. Researchers are exploring how to improve the mechanical properties and yarn formation methods of nanofibers.
(5) **Multifunction integration**: In addition to antibacterial properties, electrospinning membranes may also need to integrate other functions during tissue repair process, such as water resistance, moisture permeability, microenvironment responsiveness, *etc.* But the integration of multiple functions into a single electrospun membrane can conflict and requires fine tuning to ensure optimal performance for all functions. Therefore, how to realize multifunctional integration without sacrificing antibacterial properties is a challenge in current research.
(6) **Industrialization and clinical application**: At present, most electrospinning equipment is still in the laboratory stage of small batch production, and the market demand for electrospinning products is increasing. Electrospinning technology is sensitive to the viscosity of the used solution, and the trajectory of the jet is difficult to control, which has certain requirements on the spinning environment and limits its large-scale production. Currently, only a few electrospinning fiber products are ongoing clinical trials. Through the continuous optimization of materials, processes and equipment, electrospinning antibacterial membranes are expected to overcome these challenges in future applications and achieve a wider range of medical applications.

In summary, antibacterial eNFMs serve as a powerful tool for tissue regenerative therapies and exhibit significant potential in wound healing, bone repair, periodontal repair, tendon repair, *etc*. Despite encountering certain challenges, substantial efforts have been dedicated to meticulously designing and integrating antibacterial nanomaterials into eNFMs for their high activity and great application potential. We hope that biosafety issues can be gradually addressed and the next generation eNFMs with biosafety constructed on the basis of a better understanding of their intrinsic antibacterial mechanisms. Meanwhile, we hope that this review will help researchers understand the current situation of antibacterial eNFMs, and further promote the development and clinical application of antibacterial eNFMs in the medical industry.

Declaration of competing interest

The authors declare no competing interests.

Ethics approval and consent to participate

Our submission is a review article, which does not include a clinical study and not involve experimentation on animals and human subjects.

CRediT authorship contribution statement

Shengqiu Chen: Writing – original draft, Investigation, Funding acquisition, Formal analysis, Data curation, Conceptualization. **Yi Xie:** Writing – original draft, Supervision, Funding acquisition, Conceptualization. **Kui Ma:** Investigation, Formal analysis, Data curation. **Zhiwei Wei:** Investigation, Formal analysis. **Xingwu Ran:** Writing – review & editing, Supervision, Conceptualization. **Xiaobing Fu:** Writing – review & editing, Supervision, Funding acquisition, Conceptualization. **Cuiping Zhang:** Writing – review & editing, Supervision, Funding acquisition, Conceptualization. **Changsheng Zhao:** Writing – review & editing, Visualization, Supervision, Conceptualization.

Acknowledgments

This work was supported by the National Natural Science Foundation of China (82172211, 92268206), the National Key Research and Development Programs of China (2022YFA1104300), the CAMS Innovation Fund for Medical Sciences (CIFMS, 2019-I2M-5-059), the Military Medical Research Projects (2022-JCJQ-ZB-09600, 2023-JSKY-SSQG-006), the Natural Science Foundation of Sichuan Province (2023NSFSC0339), the 1·3·5 Project for Disciplines of Excellence of West China Hospital, Sichuan University (ZYGD22008), the China Postdoctoral Science Foundation (2022TQ0223, 2022M722256), and the Post-Doctor Research Project of West China Hospital, Sichuan University (2023HXBH031). The authors gratefully acknowledge Jiangrong Deng, Jiayi Xu and Jinhan Zhou from Core Facilities of West China Hospital, Sichuan University for their assistance in this work.

Appendix A. Supplementary data

Supplementary data to this article can be found online at https://doi.org/10.1016/j.bioactmat.2024.09.003.

References

[1] J. Ding, J. Zhang, J. Li, D. Li, C. Xiao, H. Xiao, H. Yang, X. Zhuang, X. Chen, Electrospun polymer biomaterials, Prog. Polym. Sci. 90 (2019) 1–34, https://doi.org/10.1016/j.progpolymsci.2019.01.002.

[2] Y. Ding, H. Hou, Y. Zhao, Z. Zhu, H. Fong, Electrospun polyimide nanofibers and their applications, Prog. Polym. Sci. 61 (2016) 67–103, https://doi.org/10.1016/j.progpolymsci.2016.06.006.

[3] F. Wang, Y. Si, J. Yu, B. Ding, Tailoring nanonets-engineered superflexible nanofibrous aerogels with hierarchical cage-like architecture enables renewable antimicrobial air filtration, Adv. Funct. Mater. (2021) 2107223, https://doi.org/10.1002/adfm.202107223.

[4] J. Zhang, L. Liu, Y. Si, J. Yu, B. Ding, Electrospun nanofibrous membranes: an effective arsenal for the purification of emulsified oily wastewater, Adv. Funct. Mater. 30 (25) (2020) 202002192, https://doi.org/10.1002/adfm.202002192.

[5] S. Shi, Y. Si, Y. Han, T. Wu, M.I. Iqbal, B. Fei, R.K.Y. Li, J. Hu, J. Qu, Recent progress in protective membranes fabricated via electrospinning: advanced materials, biomimetic structures, and functional applications, Adv. Mater. 34 (17) (2022) 2107938, https://doi.org/10.1002/adma.202107938.

[6] L. Wei, S. Wu, W. Shi, A.L. Aldrich, T. Kielian, M.A. Carlson, R. Sun, X. Qin, B. Duan, Large-scale and rapid preparation of nanofibrous meshes and their application for drug-loaded multilayer mucoadhesive patch fabrication for mouth ulcer treatment, ACS Appl. Mater. Interfaces 11 (32) (2019) 28740–28751, https://doi.org/10.1021/acsami.9b10379.

[7] V. Mayandi, A.C. Wen Choong, C. Dhand, F.P. Lim, T.T. Aung, H. Sriram, N. Dwivedi, M.H. Periayah, S. Sridhar, M.H.U.T. Fazil, Multifunctional antimicrobial nanofiber dressings containing ε-polylysine for the eradication of bacterial bioburden and promotion of wound healing in critically colonized wounds, ACS Appl. Mater. Interfaces 12 (14) (2020) 15989–16005, https://doi.org/10.1021/acsami.9b21683.

[8] M.A. Khan, Z. Hussain, S. Ali, Z. Qamar, M. Imran, F.Y. Hafeez, Fabrication of electrospun probiotic functionalized nanocomposite scaffolds for infection control and dermal burn healing in a mice model, ACS Biomater. Sci. Eng. 5 (11) (2019) 6109–6116, https://doi.org/10.1021/acsbiomaterials.9b01002.

[9] S. Currie, F.J. Shariatzadeh, H. Singh, S. Logsetty, S. Liu, Highly sensitive bacteria-responsive membranes consisting of core–shell polyurethane polyvinylpyrrolidone electrospun nanofibers for in situ detection of bacterial infections, ACS Appl. Mater. Interfaces 12 (41) (2020) 45859–45872, https://doi.org/10.1021/acsami.0c14213.

[10] J. Han, L. Xiong, X. Jiang, X. Yuan, Y. Zhao, D. Yang, Bio-functional electrospun nanomaterials: from topology design to biological applications, Prog. Polym. Sci. 91 (2019) 1–28, https://doi.org/10.1016/j.progpolymsci.2019.02.006.

[11] M. Rahmati, D.K. Mills, A.M. Urbanska, M.R. Saeb, J.R. Venugopal, S. Ramakrishna, M. Mozafari, Electrospinning for tissue engineering applications, Prog. Mater. Sci. 117 (2021) 100721, https://doi.org/10.1016/j.pmatsci.2020.100721.

[12] K.M. Kennedy, A. Bhaw-Luximon, D. Jhurry, Cell-matrix mechanical interaction in electrospun polymeric scaffolds for tissue engineering: implications for scaffold design and performance, Acta Biomater. 50 (2017) 41–55, https://doi.org/10.1016/j.actbio.2016.12.034.

[13] S. Agarwal, J.H. Wendorff, A. Greiner, Progress in the field of electrospinning for tissue engineering applications, Adv. Mater. 21 (32–33) (2009) 3343–3351, https://doi.org/10.1002/adma.200803092.

[14] F. Gao, W. Li, J. Deng, J. Kan, T. Guo, B. Wang, S. Hao, Recombinant human hair keratin nanoparticles accelerate dermal wound healing, ACS Appl. Mater. Interfaces 11 (20) (2019) 18681–18690, https://doi.org/10.1021/acsami.9b01725.

[15] J. He, Y. Liang, M. Shi, B. Guo, Anti-oxidant electroactive and antibacterial nanofibrous wound dressings based on poly (ε-caprolactone)/quaternized chitosan-graft-polyaniline for full-thickness skin wound healing, Chem. Eng. J. 385 (2020) 123464, https://doi.org/10.1016/j.cej.2019.123464.

[16] H. Singh, W. Li, M.R. Kazemian, R. Yang, C. Yang, S. Logsetty, S. Liu, Lipase-responsive electrospun theranostic wound dressing for simultaneous recognition and treatment of wound infection, ACS Appl. Bio Mater. 2 (5) (2019) 2028–2036, https://doi.org/10.1021/acsabm.9b00076.

[17] Z. Tu, G. Guday, M. Adeli, R. Haag, Multivalent interactions between 2D nanomaterials and biointerfaces, Adv. Mater. 30 (33) (2018) 1706709, https://doi.org/10.1002/adma.201706709.

[18] X. Fan, F. Yang, C. Nie, L. Ma, C. Cheng, R. Haag, Biocatalytic nanomaterials: a new pathway for bacterial disinfection, Adv. Mater. (2021) e2100637, https://doi.org/10.1002/adma.202100637.

[19] J.M.V. Makabenta, A. Nabawy, C.-H. Li, S. Schmidt-Malan, R. Patel, V.M. Rotello, Nanomaterial-based therapeutics for antibiotic-resistant bacterial infections, Nat. Rev. Microbiol. 19 (1) (2021) 23–36.

[20] D. Annur, Z.-K. Wang, J.-D. Liao, C. Kuo, Plasma-synthesized silver nanoparticles on electrospun chitosan nanofiber surfaces for antibacterial applications, Biomacromolecules 16 (10) (2015) 3248–3255, https://doi.org/10.1021/acs.biomac.5b00920.

[21] N. Radacsi, F.D. Campos, C.R. Chisholm, K. Giapis, Spontaneous formation of nanoparticles on electrospun nanofibres, Nat. Commun. 9 (1) (2018) 4740, https://doi.org/10.1038/s41467-018-07243-5.

[22] P. Henke, K. Kirakci, P. Kubat, M. Fraiberk, J. Forstova, J. Mosinger, Antibacterial, antiviral, and oxygen-sensing nanoparticles prepared from electrospun materials, ACS Appl. Mater. Interfaces 8 (38) (2016) 25127–25136, https://doi.org/10.1021/acsami.6b08234.

[23] J. Xue, T. Wu, Y. Dai, Y. Xia, Electrospinning and electrospun nanofibers: methods, materials, and applications, Chem. Rev. 119 (8) (2019) 5298–5415, https://doi.org/10.1021/acs.chemrev.8b00593.

[24] E.N. Zare, R. Jamaledin, P. Naserzadeh, E. Afjeh-Dana, B. Ashtari, M. Hosseinzadeh, R. Vecchione, A. Wu, F.R. Tay, A. Borzacchiello, Metal-based nanostructures/PLGA nanocomposites: antimicrobial activity, cytotoxicity, and their biomedical applications, ACS Appl. Mater. Interfaces 12 (3) (2019) 3279–3300, https://doi.org/10.1021/acsami.9b19435.

[25] D.P. Linklater, V.A. Baulin, X. Le Guevel, J.B. Fleury, E. Hanssen, T.H.P. Nguyen, S. Juodkazis, G. Bryant, R.J. Crawford, P. Stoodley, E.P. Ivanova, Antibacterial action of nanoparticles by lethal stretching of bacterial cell membranes, Adv. Mater. (2020) e2005679, https://doi.org/10.1002/adma.202005679.

[26] Y. Wang, Y. Yang, Y. Shi, H. Song, C. Yu, Antibiotic-free antibacterial strategies enabled by nanomaterials: progress and perspectives, Adv. Mater. (2019) e1904106, https://doi.org/10.1002/adma.201904106.

[27] Q. Xin, H. Shah, A. Nawaz, W. Xie, M.Z. Akram, A. Batool, L. Tian, S.U. Jan, R. Boddula, B. Guo, Q. Liu, J.R. Gong, Antibacterial carbon-based nanomaterials, Adv. Mater. 31 (45) (2019) e1804838, https://doi.org/10.1002/adma.201804838.

[28] J. Wang, P. Zhang, B. Liang, Y. Liu, T. Xu, L. Wang, B. Cao, K. Pan, Graphene oxide as an effective barrier on a porous nanofibrous membrane for water treatment, ACS Appl. Mater. Interfaces 8 (9) (2016) 6211–6218, https://doi.org/10.1021/acsami.5b12723.

[29] S.-D. Wang, Q. Ma, K. Wang, H.-W. Chen, Improving antibacterial activity and biocompatibility of bioinspired electrospinning silk fibroin nanofibers modified by graphene oxide, ACS Omega 3 (1) (2018) 406–413, https://doi.org/10.1021/acsomega.7b01210.

[30] D.-N. Phan, N. Dorjjugder, Y. Saito, M.Q. Khan, A. Ullah, X. Bie, G. Taguchi, I.-S. Kim, Antibacterial mechanisms of various copper species incorporated in polymeric nanofibers against bacteria, Mater. Today Commun. 25 (2020) 101377, https://doi.org/10.1016/j.mtcomm.2020.101377.

[31] K.A. Rieger, N.P. Birch, J.D. Schiffman, Designing electrospun nanofiber mats to promote wound healing–a review, J. Mater. Chem. B 1 (36) (2013) 4531–4541, https://doi.org/10.1039/C9TB01733J.

[32] Y. Liu, P. Cheng, Q. Guo, N. Liu, Y. Wan, W. Zhong, Z. Lu, K. Liu, G. Sun, D. Wang, Ag nanoparticles decorated PVA-co-PE nanofibrous microfiltration membrane with antifouling surface for efficient sterilization, Compos. Commun. 21 (2020) 100379, https://doi.org/10.1016/j.coco.2020.100379.

[33] J. He, W. Wang, W. Shi, F. Cui, La_2O_3 nanoparticle/polyacrylonitrile nanofibers for bacterial inactivation based on phosphate control, RSC Adv. 6 (101) (2016) 99353–99360, https://doi.org/10.1039/C6RA22374E.

[34] K. Wu, X. Wu, M. Chen, H. Wu, Y. Jiao, C. Zhou, H_2O_2-responsive smart dressing for visible H2O2 monitoring and accelerating wound healing, Chem. Eng. J. 387 (2020) 124127, https://doi.org/10.1016/j.cej.2020.124127.

[35] K. Gold, B. Slay, M. Knackstedt, A.K. Gaharwar, Antimicrobial activity of metal and metal-oxide based nanoparticles, Adv. Ther. 1 (3) (2018) 1700033, https://doi.org/10.1002/adtp.201700033.

[36] S. Meghana, P. Kabra, S. Chakraborty, N. Padmavathy, Understanding the pathway of antibacterial activity of copper oxide nanoparticles, RSC Adv. 5 (16) (2015) 12293–12299, https://doi.org/10.1039/c4ra12163e.

[37] G. Guan, L. Zhang, J. Zhu, H. Wu, W. Li, Q. Sun, Antibacterial properties and mechanism of biopolymer-based films functionalized by CuO/ZnO nanoparticles against Escherichia coli and Staphylococcus aureus, J. Hazard Mater. 402 (2021) 123542, https://doi.org/10.1016/j.jhazmat.2020.123542.

[38] S. Cheng, M. Qi, W. Li, W. Sun, M. Li, J. Lin, X. Bai, Y. Sun, B. Dong, L. Wang, Dual-responsive nanocomposites for synergistic antibacterial therapies facilitating bacteria-infected wound healing, Adv. Healthcare Mater. 12 (6) (2022) 2202652, https://doi.org/10.1002/adhm.202202652.

[39] T. Dutta, R. Sarkar, B. Pakhira, S. Ghosh, R. Sarkar, A. Barui, S. Sarkar, ROS generation by reduced graphene oxide (rGO) induced by visible light showing antibacterial activity: comparison with graphene oxide (GO), RSC Adv. 5 (98) (2015) 80192–80195, https://doi.org/10.1039/c5ra14061g.

[40] X. Dai, H. Liu, W. Du, J. Su, L. Kong, S. Ni, J. Zhan, Biocompatible carbon nitride quantum dots nanozymes with high nitrogen vacancies enhance peroxidase-like activity for broad-spectrum antibacterial, Nano Res. 16 (5) (2023) 7237–7247, https://doi.org/10.1007/s12274-022-5367-2.

[41] P. Yadav, S.T. Nishanthi, B. Purohit, A. Shanavas, K. Kailasam, Metal-free visible light photocatalytic carbon nitride quantum dots as efficient antibacterial agents: an insight study, Carbon 152 (2019) 587–597, https://doi.org/10.1016/j.carbon.2019.06.045.

[42] Z. Yang, H. Zheng, H. Yin, L. Zhou, Q. Zhang, B. Zhang, Niobium carbide doped ROS/temperature dual-responsive multifunctional hydrogel for facilitating MRSA-infected wound healing, Chem. Eng. J. 471 (2023) 144634, https://doi.org/10.1016/j.cej.2023.144634.

[43] L. Zhu, A. Huo, Y. Chen, X. Bai, C. Cao, Y. Zheng, W. Guo, A ROS reservoir based on a polyoxometalate and metal-organic framework hybrid for efficient bacteria eradication and wound healing, Chem. Eng. J. 476 (2023) 146613, https://doi.org/10.1016/j.cej.2023.146613.

[44] R. Li, T. Chen, X. Pan, Metal–organic-framework-based materials for antimicrobial applications, ACS Nano 15 (3) (2021) 3808–3848, https://doi.org/10.1021/acsnano.0c09617.

[45] G. Yim, C.Y. Kim, S. Kang, D.-H. Min, K. Kang, H. Jang, Intrinsic peroxidase-mimicking Ir nanoplates for nanozymatic anticancer and antibacterial treatment, ACS Appl. Mater. Interfaces 12 (37) (2020) 41062–41070, https://doi.org/10.1021/acsami.0c10981.

[46] F. Wei, X. Cui, Z. Wang, C. Dong, J. Li, X. Han, Recoverable peroxidase-like Fe_3O_4@MoS_2-Ag nanozyme with enhanced antibacterial ability, Chem. Eng. J. 408 (2021) 127240, https://doi.org/10.1016/j.cej.2020.127240.

[47] S. Li, Y. Zhang, H. Jin, H. Gao, S. Liu, W. Shi, W. Sun, Y. Liu, H. Zhang, Biomimetic dual-nanozymes with catalytic cascade reactions against diabetic wound infection, J. Colloid Interface Sci. 651 (2023) 319–333, https://doi.org/10.1016/j.jcis.2023.07.139.

[48] A.D. Sekar, V. Kumar, H. Muthukumar, P. Gopinath, M. Matheswaran, Electrospinning of Fe-doped ZnO nanoparticles incorporated polyvinyl alcohol nanofibers for its antibacterial treatment and cytotoxic studies, Eur. Polym. J. 118 (2019) 27–35, https://doi.org/10.1016/j.eurpolymj.2019.05.038.

[49] C. Lv, S. Chen, Y. Xie, Z. Wei, L. Chen, J. Bao, C. He, W. Zhao, S. Sun, C. Zhao, Positively-charged polyethersulfone nanofibrous membranes for bacteria and anionic dyes removal, J. Colloid Interface Sci. 556 (2019) 492–502, https://doi.org/10.1021/acsami.2c08784.

[50] R. Wang, Y. Li, Y. Si, F. Wang, Y. Liu, Y. Ma, J. Yu, X. Yin, B. Ding, Rechargeable polyamide-based N-halamine nanofibrous membranes for renewable, high-efficiency, and antibacterial respirators, Nanoscale Adv. 1 (5) (2019) 1948–1956, https://doi.org/10.1039/C9NA00103D.

[51] X. Cai, L. Gao, J. Wang, D. Li, MOF-integrated hierarchical composite fiber for efficient daytime radiative cooling and antibacterial protective textiles, ACS Appl. Mater. Interfaces 15 (6) (2023) 8537–8545, https://doi.org/10.1021/acsami.2c21832.

[52] K. Shalumon, C. Sheu, C.-H. Chen, S.-H. Chen, G. Jose, C.-Y. Kuo, J.-P. Chen, Multi-functional electrospun antibacterial core-shell nanofibrous membranes for prolonged prevention of post-surgical tendon adhesion and inflammation, Acta Biomater. 72 (2018) 121–136, https://doi.org/10.1016/j.actbio.2018.03.044.

[53] D. Xing, W. Zuo, J. Chen, B. Ma, X. Cheng, X. Zhou, Y. Qian, Spatial delivery of triple functional nanoparticles via an extracellular matrix-mimicking coaxial scaffold synergistically enhancing bone regeneration, ACS Appl. Mater. Interfaces 14 (33) (2022) 37380–37395, https://doi.org/10.1021/acsami.2c08784.

[54] K. Ko, D. Yoon, S.C. Yang, H.S. Lee, Brush-painted superhydrophobic silica coating layers for self-cleaning solar panels, J. Ind. Eng. Chem. 106 (2022) 460–468, https://doi.org/10.1016/j.jiec.2021.11.023.

[55] H.R. Pant, P. Pokharel, M.K. Joshi, S. Adhikari, H.J. Kim, C.H. Park, C.S. Kim, Processing and characterization of electrospun graphene oxide/polyurethane composite nanofibers for stent coating, Chem. Eng. J. 270 (2015) 336–342, https://doi.org/10.1016/j.cej.2015.01.105.

[56] R. Wang, M. Shi, F. Xu, Y. Qiu, P. Zhang, K. Shen, Q. Zhao, J. Yu, Y. Zhang, Graphdiyne-modified TiO2 nanofibers with osteoinductive and enhanced photocatalytic antibacterial activities to prevent implant infection, Nat. Commun. 11 (1) (2020) 4465, https://doi.org/10.1038/s41467-020-18267-1.

[57] S. Chen, C. Lv, K. Hao, L. Jin, Y. Xie, W. Zhao, S. Sun, X. Zhang, C. Zhao, Multifunctional negatively-charged poly (ether sulfone) nanofibrous membrane for water remediation, J. Colloid Interface Sci. 538 (2019) 648–659, https://doi.org/10.1016/j.jcis.2018.12.038.

[58] H.-T. Lu, G.-Y. Huang, W.-J. Chang, T.-W. Lu, T.-W. Huang, M.-H. Ho, F.-L. Mi, Modification of chitosan nanofibers with CuS and fucoidan for antibacterial and bone tissue engineering applications, Carbohydr. Polym. 281 (2022) 119035, https://doi.org/10.1016/j.carbpol.2021.119035.

[59] S. Chen, Y. Xie, T. Xiao, W. Zhao, J. Li, C. Zhao, Tannic acid-inspiration and post-crosslinking of zwitterionic polymer as a universal approach towards antifouling surface, Chem. Eng. J. 337 (2018) 122–132, https://doi.org/10.1016/j.cej.2017.12.057.

[60] Y. Xu, J. Hu, X. Zhang, D. Yuan, G. Duan, Y. Li, Robust and multifunctional natural polyphenolic composites for water remediation, Mater. Horiz. (2022) 2496–2517, https://doi.org/10.1039/d2mh00768a.

[61] Y. Liu, K. Ai, L. Lu, Polydopamine and its derivative materials: synthesis and promising applications in energy, environmental, and biomedical fields, Chem. Rev. 114 (9) (2014) 5057–5115, https://doi.org/10.1021/cr400407a.

[62] Y. Qian, X. Zhou, F. Zhang, T.G.H. Diekwisch, X. Luan, J. Yang, Triple PLGA/PCL scaffold modification including silver impregnation, collagen coating, and electrospinning significantly improve biocompatibility, antimicrobial, and osteogenic properties for orofacial tissue regeneration, ACS Appl. Mater. Interfaces 11 (41) (2019) 37381–37396, https://doi.org/10.1021/acsami.9b07053.

[63] Q. Zhang, Q. Tu, M.E. Hickey, J. Xiao, B. Gao, C. Tian, P. Heng, Y. Jiao, T. Peng, J. J.C. Wang, S.B. Biointerfaces, Preparation and study of the antibacterial ability of graphene oxide-catechol hybrid polylactic acid nanofiber mats, Colloids Surf. B Biointerfaces 172 (2018) 496–505, https://doi.org/10.1016/j.colsurfb.2018.09.003.

[64] R. Shi, J. Ye, W. Li, J. Zhang, J. Li, C. Wu, J. Xue, L. Zhang, Infection-responsive electrospun nanofiber mat for antibacterial guided tissue regeneration membrane, Mater. Sci. Eng. C 100 (2019) 523–534, https://doi.org/10.1016/j.msec.2019.03.039.

[65] S. Kang, D.h. Park, J. Hwang, Hierarchical ZnO nano-spines grown on a carbon fiber seed layer for efficient VOC removal and airborne virus and bacteria inactivation, J. Hazard Mater. 424 (2022) 127262, https://doi.org/10.1016/j.jhazmat.2021.127262.

[66] K. Song, Q. Wu, Z. Zhang, S. Ren, T. Lei, I.I. Negulescu, Q. Zhang, Porous carbon nanofibers from electrospun biomass tar/polyacrylonitrile/silver hybrids as antimicrobial materials, ACS Appl. Mater. Interfaces 7 (27) (2015) 15108–15116, https://doi.org/10.1021/acsami.5b04479.

[67] Y. Yang, Z. Zhang, M. Wan, Z. Wang, X. Zou, Y. Zhao, L. Sun, A facile method for the fabrication of silver nanoparticles surface decorated polyvinyl alcohol electrospun nanofibers and controllable antibacterial activities, Polymers 12 (11) (2020) 2486, https://doi.org/10.3390/polym12112486.

[68] M. Wan, H. Zhao, L. Peng, Y. Zhao, L. Sun, Facile one-step deposition of Ag nanoparticles on SiO2 electrospun nanofiber surfaces for label-free SERS detection and antibacterial dressing, ACS Appl. Bio Mater. 4 (8) (2021) 6549–6557, https://doi.org/10.1021/acsabm.1c00674.

[69] Y. Wang, R. Cao, C. Wang, X. Song, R. Wang, J. Liu, M. Zhang, J. Huang, T. You, Y. Zhang, D. Yan, W. Han, L. Yan, J. Xiao, P. Li, In situ embedding hydrogen-bonded organic frameworks nanocrystals in electrospinning nanofibers for ultrastable broad-spectrum antibacterial activity, Adv. Funct. Mater. 33 (20) (2023) 2214388, https://doi.org/10.1002/adfm.202214388.

[70] Q. Wang, S. Ji, S. Li, X. Zhou, J. Yin, P. Liu, W. Shi, M. Wu, L. Shen, Electrospinning visible light response Bi2MoO6/Ag3PO4 composite photocatalytic nanofibers with enhanced photocatalytic and antibacterial activity, Appl. Surf. Sci. 569 (2021) 150955, https://doi.org/10.1016/j.apsusc.2021.150955.

[71] H. Shan, Y. Si, J. Yu, B. Ding, Flexible, mesoporous, and monodispersed metallic cobalt-embedded inorganic nanofibrous membranes enable ultra-fast and high-efficiency killing of bacteria, Chem. Eng. J. 382 (2020) 122909, https://doi.org/10.1016/j.cej.2019.122909.

[72] L. Chen, D. Zhang, K. Cheng, W. Li, Q. Yu, L. Wang, Photothermal-responsive fiber dressing with enhanced antibacterial activity and cell manipulation towards promoting wound-healing, J. Colloid Interface Sci. 623 (2022) 21–33, https://doi.org/10.1016/j.jcis.2022.05.013.

[73] A.B. Ali, D. Slawig, A. Schlosser, J. Koch, N.C. Bigall, F. Renz, C. Tegenkamp, R. Sindelar, Polyacrylonitrile (PAN) based electrospun carbon nanofibers (ECNFs): probing the synergistic effects of creep assisted stabilization and CNTs addition on graphitization and low dimensional electrical transport, Carbon 172 (2021) 283–295, https://doi.org/10.1016/j.carbon.2020.10.033.

[74] Y. Xia, X. Fan, H. Yang, L. Li, C. He, C. Cheng, R. Haag, ZnO/Nanocarbons-Modified fibrous scaffolds for stem cell-based osteogenic differentiation, Small (2020) e2003010, https://doi.org/10.1002/smll.202003010.

[75] H. Wang, Y. Ma, J. Qiu, J. Wang, H. Zhang, Y. Li, C. Wang, Multifunctional PAN/Al–ZnO/Ag nanofibers for infrared stealth, self-cleaning, and antibacterial

applications, ACS Appl. Nano Mater. 5 (1) (2021) 782–790, https://doi.org/10.1021/acsanm.1c03518.
[76] C. Kinnear, T.L. Moore, L. Rodriguez-Lorenzo, B. Rothen-Rutishauser, A. Petri-Fink, Form follows function: nanoparticle shape and its implications for nanomedicine, Chem. Rev. 117 (17) (2017) 11476–11521, https://doi.org/10.1021/acs.chemrev.7b00194.
[77] M. Xie, M. Gao, Y. Yun, M. Malmsten, V.M. Rotello, R. Zboril, O. Akhavan, A. Kraskouski, J. Amalraj, X. Cai, J. Lu, H. Zheng, R. Li, Antibacterial nanomaterials: mechanisms, impacts on antimicrobial resistance and design principles, Angew. Chem. Int. Ed. 62 (17) (2023) e202217345, https://doi.org/10.1002/anie.202217345.
[78] Z. Xing, J. Guo, Z. Wu, C. He, L. Wang, M. Bai, X. Liu, B. Zhu, Q. Guan, C. Cheng, Nanomaterials-enabled physicochemical antibacterial therapeutics: toward the antibiotic-free disinfections, Small 19 (50) (2023) 202303594, https://doi.org/10.1002/smll.202303594.
[79] H. Zhu, S. Wang, Y. Wang, C. Song, Q. Yao, X. Yuan, J. Xie, Gold nanocluster with AIE: a novel photodynamic antibacterial and deodorant molecule, Biomaterials 288 (2022) 121695, https://doi.org/10.1016/j.biomaterials.2022.121695.
[80] X. Yang, J. Yang, L. Wang, B. Ran, Y. Jia, L. Zhang, G. Yang, H. Shao, X. Jiang, Pharmaceutical intermediate-modified gold nanoparticles: against multidrug-resistant bacteria and wound-healing application via an electrospun scaffold, ACS Nano 11 (6) (2017) 5737–5745, https://doi.org/10.1021/acsnano.7b01240.
[81] L. Wang, J. Yang, X. Yang, Q. Hou, S. Liu, W. Zheng, Y. Long, X. Jiang, Mercaptophenylboronic acid-activated gold nanoparticles as nanoantibiotics against multidrug-resistant bacteria, ACS Appl. Mater. Interfaces 12 (46) (2020) 51148–51159, https://doi.org/10.1021/acsami.0c12597.
[82] X. Zhao, Y. Jia, J. Li, R. Dong, J. Zhang, C. Ma, H. Wang, Y. Rui, X. Jiang, Indole derivative-capped gold nanoparticles as an effective bactericide in vivo, ACS Appl. Mater. Interfaces 10 (35) (2018) 29398–29406, https://doi.org/10.1021/acsami.8b11980.
[83] S. Zhang, J. Ye, Y. Sun, J. Kang, J. Liu, Y. Wang, Y. Li, L. Zhang, G. Ning, Electrospun fibrous mat based on silver (I) metal-organic frameworks-polylactic acid for bacterial killing and antibiotic-free wound dressing, Chem. Eng. J. 390 (2020) 124523, https://doi.org/10.1016/j.cej.2020.124523.
[84] C.A. Ballesteros, D.S. Correa, V. Zucolotto, Polycaprolactone nanofiber mats decorated with photoresponsive nanogels and silver nanoparticles: slow release for antibacterial control, Mater. Sci. Eng. C 107 (2020) 110334, https://doi.org/10.1016/j.msec.2019.110334.
[85] S.-F. Pan, X.-X. Ke, T.-Y. Wang, Q. Liu, L.-B. Zhong, Y.-M.J.I. Zheng, E. C. Research, Synthesis of silver nanoparticles embedded electrospun PAN nanofiber thin-film composite forward osmosis membrane to enhance performance and antimicrobial activity, Ind. Eng. Chem. Res. 58 (2) (2018) 984–993.
[86] J.D. Schiffman, Y. Wang, E.P. Giannelis, M. Elimelech, Biocidal activity of plasma modified electrospun polysulfone mats functionalized with polyethyleneimine-capped silver nanoparticles, Langmuir 27 (21) (2011) 13159–13164, https://doi.org/10.1021/la202605z.
[87] G. Pagnotta, G. Graziani, N. Baldini, A. Maso, M.L. Focarete, M. Berni, F. Biscarini, M. Bianchi, C. Gualandi, Nanodecoration of electrospun polymeric fibers with nanostructured silver coatings by ionized jet deposition for antibacterial tissues, Mater. Sci. Eng. C 113 (2020) 110998, https://doi.org/10.1016/j.msec.2020.110998.
[88] A. Soroush, W. Ma, M. Cyr, M.S. Rahaman, B. Asadishad, N. Tufenkji, In situ silver decoration on graphene oxide-treated thin film composite forward osmosis membranes: biocidal properties and regeneration potential, Environ. Sci. Technol. Lett. 3 (1) (2016) 13–18, https://doi.org/10.1021/acs.estlett.5b00304.
[89] M. Farooq, M. Khalid, Y. Yoshinori, F. Wang, M.A. Iqbal, M.N. Sarwar, G. Mayakrishnan, I.S. Kim, Ag and MoO3 nanoparticle-containing polyacrylonitrile nanofiber membranes for wound dressings, ACS Appl. Nano Mater. 6 (18) (2023) 17171–17178, https://doi.org/10.1021/acsanm.3c03435.
[90] A. GhavamiNejad, A. Rajan Unnithan, A. Ramachandra Kurup Sasikala, M. Samarikhalaj, R.G. Thomas, Y.Y. Jeong, S. Nasseri, P. Murugesan, D. Wu, C. Hee Park, Mussel-inspired electrospun nanofibers functionalized with size-controlled silver nanoparticles for wound dressing application, ACS Appl. Mater. Interfaces 7 (22) (2015) 12176–12183, https://doi.org/10.1021/acsami.5b02542.
[91] S.-F. Pan, X.-X. Ke, T.-Y. Wang, Q. Liu, L.-B. Zhong, Y.-M. Zheng, Synthesis of silver nanoparticles embedded electrospun PAN nanofiber thin-film composite forward osmosis membrane to enhance performance and antimicrobial activity, Ind. Eng. Chem. Res. 58 (2) (2018) 984–993, https://doi.org/10.1021/acs.iecr.3c00214.
[92] J. Dong, Y. Peng, J. Long, Y. Zhang, Z. Wang, S. Park, Y. Huang, T. Liu, An all-stretchable, ultraviolet protective, and electromagnetic-interference-free E-textile, Adv. Funct. Mater. 33 (45) (2023) 2308426, https://doi.org/10.1002/adfm.202308426.
[93] M. El-Aassar, O.M. Ibrahim, M.M. Fouda, N.G. El-Beheri, M.M. Agwa, Wound healing of nanofiber comprising Polygalacturonic/Hyaluronic acid embedded silver nanoparticles: in-vitro and in-vivo studies, Carbohydr. Polym. 238 (2020) 116175, https://doi.org/10.1016/j.carbpol.2020.116175.
[94] S. Jiji, S. Udhayakumar, K. Maharajan, C. Rose, C. Muralidharan, K. Kadirvelu, Bacterial cellulose matrix with in situ impregnation of silver nanoparticles via catecholic redox chemistry for third degree burn wound healing, Carbohydr. Polym. 245 (2020) 116573, https://doi.org/10.1016/j.carbpol.2020.116573.
[95] J. He, A. Li, W. Wang, C. Cui, S. Jiang, M. Chen, W. Qin, H. Tang, R. Guo, Multifunctional wearable device based on an antibacterial and hydrophobic silver nanoparticles/Ti3C2Tx MXene/thermoplastic polyurethane fibrous membrane for electromagnetic shielding and strain sensing, Ind. Eng. Chem. Res. 62 (23) (2023) 9221–9232, https://doi.org/10.1021/acs.iecr.3c00214.
[96] H. Shi, H. Liu, S. Luan, D. Shi, S. Yan, C. Liu, R.K. Li, J. Yin, Antibacterial and biocompatible properties of polyurethane nanofiber composites with integrated antifouling and bactericidal components, Compos. Sci. Technol. 127 (2016) 28–35, https://doi.org/10.1016/j.compscitech.2016.02.031.
[97] B. Zhou, Y. Li, H. Deng, Y. Hu, B. Li, Antibacterial multilayer films fabricated by layer-by-layer immobilizing lysozyme and gold nanoparticles on nanofibers, Colloids Surf. B Biointerfaces 116 (2014) 432–438, https://doi.org/10.1016/j.colsurfb.2014.01.016.
[98] X. Yang, Q. Wei, H. Shao, X. Jiang, Multivalent aminosaccharide-based gold nanoparticles as narrow-spectrum antibiotics in vivo, ACS Appl. Mater. Interfaces 11 (8) (2019) 7725–7730, https://doi.org/10.1021/acsami.8b19658.
[99] G. Prado-Prone, P. Silva-Bermudez, M. Bazzar, M.L. Focarete, S.E. Rodil, X. Vidal-Gutiérrez, J.A. García-Macedo, V.I. García-Pérez, C. Velasquillo, A. Almaguer-Flores, Antibacterial composite membranes of polycaprolactone/gelatin loaded with zinc oxide nanoparticles for guided tissue regeneration, Biomed. Mater. 15 (3) (2020) 035006, https://doi.org/10.1088/1748-605X/ab70ef.
[100] W. Ma, L. Li, X. Lin, Y. Wang, X. Ren, T.-S. Huang, Novel ZnO/N-halamine-mediated multifunctional dressings as quick antibacterial agent for biomedical applications, ACS Appl. Mater. Interfaces 11 (34) (2019) 31411–31420, https://doi.org/10.1021/acsami.9b10857.
[101] J.H. Kim, M.K. Joshi, J. Lee, C.H. Park, C.S. Kim, Polydopamine-assisted immobilization of hierarchical zinc oxide nanostructures on electrospun nanofibrous membrane for photocatalysis and antimicrobial activity, J. Colloid Interface Sci. 513 (2018) 566–574, https://doi.org/10.1016/j.jcis.2017.11.061.
[102] P.P. Mahamuni-Badiger, P.M. Patil, M.V. Badiger, P.R. Patel, B.S. Thorat- Gadgil, A. Pandit, R.A. Bohara, Biofilm formation to inhibition: role of zinc oxide-based nanoparticles, Mater. Sci. Eng. C 108 (2020) 110319, https://doi.org/10.1016/j.msec.2019.110319.
[103] R. Augustine, P. Dan, A. Sosnik, N. Kalarikkal, N. Tran, B. Vincent, S. Thomas, P. Menu, D. Rouxel, Electrospun poly (vinylidene fluoride-trifluoroethylene)/zinc oxide nanocomposite tissue engineering scaffolds with enhanced cell adhesion and blood vessel formation, Nano Res. 10 (2017) 3358–3376, https://doi.org/10.1007/s12274-017-1549-8.
[104] Y. Liu, Y. Li, L. Deng, L. Zou, F. Feng, H. Zhang, Hydrophobic ethylcellulose/gelatin nanofibers containing zinc oxide nanoparticles for antimicrobial packaging, J. Agric. Environ. Ethics 66 (36) (2018) 9498–9506, https://doi.org/10.1021/acs.jafc.8b03267.
[105] H. Rodríguez-Tobías, G. Morales, D. Grande, Improvement of mechanical properties and antibacterial activity of electrospun poly (d, l-lactide)-based mats by incorporation of ZnO-graft-poly (d, l-lactide) nanoparticles, Mater. Chem. Phys. 182 (2016) 324–331, https://doi.org/10.1016/j.matchemphys.2016.07.039.
[106] S.Y.H. Abdalkarim, H.-Y. Yu, C. Wang, L. Yang, Y. Guan, L. Huang, J. Yao, Sheet-like cellulose nanocrystal-ZnO nanohybrids as multifunctional reinforcing agents in biopolyester composite nanofibers with ultrahigh UV-shielding and antibacterial performances, ACS Appl. Bio Mater. 1 (3) (2018) 714–727, https://doi.org/10.1021/acsabm.8b00188.
[107] Z. Hadisi, M. Farokhi, H.R. Bakhsheshi-Rad, M. Jahanshahi, S. Hasanpour, E. Pagan, A. Dolatshahi-Pirouz, Y.S. Zhang, S.C. Kundu, M. Akbari, Hyaluronic acid (HA)-based silk fibroin/zinc oxide core–shell electrospun dressing for burn wound management, Macromol. Biosci. 20 (4) (2020) 1900328, https://doi.org/10.1002/mabi.201900328.
[108] A. Nasajpour, S. Mandla, S. Shree, E. Mostafavi, R. Sharifi, A. Khalilpour, S. Saghazadeh, S. Hassan, M.J. Mitchell, J. Leijten, Nanostructured fibrous membranes with rose spike-like architecture, Nano Lett. 17 (10) (2017) 6235–6240, https://doi.org/10.1021/acs.nanolett.7b02929.
[109] J. Chen, Y. Rao, J. Huang, N. Cheng, G. Zhou, S. Feng, Z. Zhong, W. Xing, Multi-functional nanofiber membranes with asymmetric wettability and pine-needle-like structure for enhanced moisture-wicking, Chem. Eng. J. 468 (2023) 143709, https://doi.org/10.1016/j.cej.2023.143709.
[110] H.-H. Qu, C. Wang, Y.-X. Guo, Z.-Y. Zhao, L. Qiao, J.-B. Yang, H.-X. Wu, Q.-S. Li, A. Dong, Electrospun N-halamine/ZnO-based platform eradicates bacteria through multimodal antimicrobial mechanism of action, Rare Met. 42 (1) (2022) 222–233, https://doi.org/10.1007/s12598-022-02116-9.
[111] L. Mascia, W. Zhang, F. Gatto, A. Scarpellini, P.P. Pompa, E. Mele, In situ generation of ZnO nanoparticles within a polyethyleneimine matrix for antibacterial zein fibers, ACS Appl. Polym. Mater. 1 (7) (2019) 1707–1716, https://doi.org/10.1021/acsapm.9b00276.
[112] M. Hashmi, S. Ullah, I.S. Kim, Copper oxide (CuO) loaded polyacrylonitrile (PAN) nanofiber membranes for antimicrobial breath mask applications, Curr. Res. Biotechnol. 1 (2019) 1–10, https://doi.org/10.1016/j.crbiot.2019.07.001.
[113] J.M. Cordeiro, V.A.R. Barão, E.D. de Avila, J.F.A. Husch, F. Yang, J.J.J.P. van den Beucken, Tailoring Cu2+-loaded electrospun membranes with antibacterial ability for guided bone regeneration, Biomater. Adv. 139 (2022) 212976, https://doi.org/10.1016/j.bioadv.2022.212976.
[114] T. Toniatto, B. Rodrigues, T. Marsi, R. Ricci, F. Marciano, T. Webster, A. Lobo, Nanostructured poly (lactic acid) electrospun fiber with high loadings of TiO_2 nanoparticles: insights into bactericidal activity and cell viability, Mater. Sci. Eng. C 71 (2017) 381–385, https://doi.org/10.1016/j.msec.2016.10.026.
[115] J.E. Karbowniczek, K. Berniak, J. Knapczyk-Korczak, G. Williams, J.A. Bryant, N. D. Nikoi, M. Banzhaf, F. de Cogan, U. Stachewicz, Strategies of nanoparticles integration in polymer fibers to achieve antibacterial effect and enhance cell proliferation with collagen production in tissue engineering scaffolds, J. Colloid

Interface Sci. 650 (2023) 1371–1381, https://doi.org/10.1016/j.jcis.2023.07.066.
[116] W.S. Lee, Y.-S. Park, Y.-K. Cho, Significantly enhanced antibacterial activity of TiO_2 nanofibers with hierarchical nanostructures and controlled crystallinity, Analyst 140 (2) (2015) 616–622, https://doi.org/10.1039/C4AN01682C.
[117] A.W. Jatoi, I.S. Kim, Q.-Q. Ni, Cellulose acetate nanofibers embedded with AgNPs anchored TiO_2 nanoparticles for long term excellent antibacterial applications, Carbohydr. Polym. 207 (2019) 640–649, https://doi.org/10.1016/j.carbpol.2018.12.029.
[118] Q. Li, Y. Yin, D. Cao, Y. Wang, P. Luan, X. Sun, W. Liang, H. Zhu, Photocatalytic rejuvenation enabled self-sanitizing, reusable, and biodegradable masks against COVID-19, ACS Nano 15 (7) (2021) 11992–12005, https://doi.org/10.1021/acsnano.1c03249.
[119] Z. Zhang, Q. Dai, Y. Zhang, H. Zhuang, E. Wang, Q. Xu, L. Ma, C. Wu, Z. Huan, F. Guo, Design of a multifunctional biomaterial inspired by ancient Chinese medicine for hair regeneration in burned skin, ACS Appl. Mater. Interfaces 12 (11) (2020) 12489–12499, https://doi.org/10.1021/acsami.9b22769.
[120] M. Liu, X. Wang, H. Li, C. Xia, Z. Liu, J. Liu, A. Yin, X. Lou, H. Wang, X. Mo, J. Wu, Magnesium oxide-incorporated electrospun membranes inhibit bacterial infections and promote the healing process of infected wounds, J. Mater. Chem. B 9 (17) (2021) 3727–3744, https://doi.org/10.1039/d1tb00217a.
[121] M. Naseri-Nosar, S. Farzamfar, H. Sahrapeyma, S. Ghorbani, F. Bastami, A. Vaez, M. Salehi, Cerium oxide nanoparticle-containing poly (ε-caprolactone)/gelatin electrospun film as a potential wound dressing material: in vitro and in vivo evaluation, Mater. Sci. Eng. C 81 (2017) 366–372, https://doi.org/10.1016/j.msec.2017.08.013.
[122] W. Ma, Y. Li, S. Gao, J. Cui, Q. Qu, Y. Wang, C. Huang, G. Fu, Self-healing and superwettable nanofibrous membranes with excellent stability toward multifunctional applications in water purification, ACS Appl. Mater. Interfaces 12 (20) (2020) 23644–23654, https://doi.org/10.1021/acsami.0c05701.
[123] H. Ci, L. Ma, X. Liu, Y. Liang, Y. Zheng, Z. Li, S. Zhu, Z. Cui, S. Wu, Photo-excited antibacterial poly (Ɛ-caprolactone)@ MoS_2/ZnS hybrid nanofibers, Chem. Eng. J. 434 (2022) 134764, https://doi.org/10.1016/j.cej.2022.134764.
[124] Z. Peng, T. Zhao, Y. Zhou, S. Li, J. Li, R.M. Leblanc, Bone tissue engineering via carbon-based nanomaterials, Adv. Healthcare Mater. 9 (5) (2020) 1901495, https://doi.org/10.1002/adhm.201901495.
[125] Q. Xin, H. Shah, A. Nawaz, W. Xie, M.Z. Akram, A. Batool, L. Tian, S.U. Jan, R. Boddula, B. Guo, Antibacterial carbon-based nanomaterials, Adv. Mater. 31 (45) (2019) 1804838.
[126] K.D. Patel, T.-H. Kim, N. Mandakhbayar, R.K. Singh, J.-H. Jang, J.-H. Lee, H.-W. Kim, Coating biopolymer nanofibers with carbon nanotubes accelerates tissue healing and bone regeneration through orchestrated cell-and tissue-regulatory responses, Acta Biomater. 108 (2020) 97–110, https://doi.org/10.1016/j.actbio.2020.03.012.
[127] A. Aqel, K.M.M.A. El-Nour, R.A.A. Ammar, A. Al-Warthan, Carbon nanotubes, science and technology part (I) structure, synthesis and characterisation, Arab. J. Chem. 5 (1) (2012) 1–23, https://doi.org/10.1016/j.arabjc.2010.08.022.
[128] M.-S. Choi, T. Park, W.-J. Kim, J. Hur, High-performance ultraviolet photodetector based on a zinc oxide Nanoparticle@Single-walled carbon nanotube heterojunction hybrid film, Nanomaterials 10 (2) (2020), https://doi.org/10.3390/nano10020395.
[129] W. Zhou, X. Bai, E. Wang, S. Xie, Synthesis, structure, and properties of single-walled carbon nanotubes, Adv. Mater. 21 (45) (2009) 4565–4583, https://doi.org/10.1002/adma.200901071.
[130] X. Gao, S. Han, R. Zhang, G. Liu, J. Wu, Progress in electrospun composite nanofibers: composition, performance and applications for tissue engineering, J. Mater. Chem. B 7 (45) (2019) 7075–7089, https://doi.org/10.1039/C9TB01730E.
[131] X. Hu, X. Wang, Y. Xu, L. Li, J. Liu, Y. He, Y. Zou, L. Yu, X. Qiu, J. Guo, Electric conductivity on aligned nanofibers facilitates the transdifferentiation of mesenchymal stem cells into schwann cells and regeneration of injured peripheral nerve, Adv. Healthcare Mater. 9 (11) (2020) 1901570, https://doi.org/10.1002/adhm.201901570.
[132] S. Wang, Y. Li, R. Zhao, T. Jin, L. Zhang, X. Li, Chitosan surface modified electrospun poly (ε-caprolactone)/carbon nanotube composite fibers with enhanced mechanical, cell proliferation and antibacterial properties, Int. J. Biol. Macromol. 104 (2017) 708–715, https://doi.org/10.1016/j.ijbiomac.2017.06.044.
[133] B.D.B. Tiu, H.N. Nguyen, D.F. Rodrigues, R.C. Advincula, Electrospinning superhydrophobic and antibacterial PS/MWNT nanofibers onto multilayer gas barrier films, Macromol. Symp. (2017) 1600138. Wiley Online Library.
[134] M.S. Islam, A.N. Naz, M.N. Alam, A.K. Das, J.H. Yeum, Electrospun poly(vinyl alcohol)/silver nanoparticle/carbon nanotube multi-composite nanofiber mat: fabrication, characterization and evaluation of thermal, mechanical and antibacterial properties, Colloid Interface Sci. Commun. 35 (2020) 100247, https://doi.org/10.1016/j.colcom.2020.100247.
[135] J.D. Schiffman, M. Elimelech, Antibacterial activity of electrospun polymer mats with incorporated narrow diameter single-walled carbon nanotubes, ACS Appl. Mater. Interfaces 3 (2) (2011) 462–468, https://doi.org/10.1021/am101043y.
[136] K.S. Novoselov, A.K. Geim, S.V. Morozov, D.-e. Jiang, Y. Zhang, S.V. Dubonos, I. V. Grigorieva, A.A. Firsov, Electric field effect in atomically thin carbon films, Science 306 (5696) (2004) 666–669, https://doi.org/10.1126/science.1102896.
[137] K. Li, P. Li, Y. Fan, The assembly of silk fibroin and graphene-based nanomaterials with enhanced mechanical/conductive properties and their biomedical applications, J. Mater. Chem. B 7 (44) (2019) 6890–6913, https://doi.org/10.1039/C9TB01733J.
[138] H. Sun, N. Gao, K. Dong, J. Ren, X. Qu, Graphene quantum dots-band-aids used for wound disinfection, ACS Nano 8 (6) (2014) 6202–6210, https://doi.org/10.1021/nn501640q.
[139] A. Ghaffar, L. Zhang, X. Zhu, B. Chen, Porous PVdF/GO nanofibrous membranes for selective separation and recycling of charged organic dyes from water, Environ. Sci. Technol. 52 (7) (2018) 4265–4274, https://doi.org/10.1021/acs.est.7b06081.
[140] S. Sajjad, S.A. Khan Leghari, A. Iqbal, Study of graphene oxide structural features for catalytic, antibacterial, gas sensing, and metals decontamination environmental applications, ACS Appl. Mater. Interfaces 9 (50) (2017) 43393–43414, https://doi.org/10.1021/acsami.7b08232.
[141] J. Zhao, B. Deng, M. Lv, J. Li, Y. Zhang, H. Jiang, C. Peng, J. Li, J. Shi, Q. Huang, C. Fan, Graphene oxide-based antibacterial cotton fabrics, Adv. Healthcare Mater. 2 (9) (2013) 1259–1266, https://doi.org/10.1002/adhm.201200437.
[142] K. Liu, P. Cheng, Y. Wang, W. Zhong, Z. Lu, M. Li, Q. Liu, W. Wang, Q. Zhu, D. Wang, Concurrent filtration and inactivation of bacteria using poly (vinyl alcohol-co-ethylene) nanofibrous membrane facilely modified using chitosan and graphene oxide, Environ. Sci.: Nano 4 (2) (2017) 385–395, https://doi.org/10.1039/C6EN00364H.
[143] J. Sun, L. Song, Y. Fan, L. Tian, S. Luan, S. Niu, L. Ren, W. Ming, J. Zhao, Synergistic photodynamic and photothermal antibacterial nanocomposite membrane triggered by single NIR light source, ACS Appl. Mater. Interfaces 11 (30) (2019) 26581–26589, https://doi.org/10.1021/acsami.9b07037.
[144] S. Szunerits, R. Boukherroub, Antibacterial activity of graphene-based materials, J. Mater. Chem. B 4 (43) (2016) 6892–6912, https://doi.org/10.1039/C6TB01647B.
[145] A.F. De Faria, F. Perreault, E. Shaulsky, L.H. Arias Chavez, M. Elimelech, Antimicrobial electrospun biopolymer nanofiber mats functionalized with graphene oxide–silver nanocomposites, ACS Appl. Mater. Interfaces 7 (23) (2015) 12751–12759, https://doi.org/10.1021/acsami.5b01639.
[146] M. Liu, L. Wang, X. Zheng, Z. Xie, Zirconium-based nanoscale metal–organic framework/poly (ε-caprolactone) mixed-matrix membranes as effective antimicrobials, ACS Appl. Mater. Interfaces 9 (47) (2017) 41512–41520, https://doi.org/10.1021/acsami.7b15826.
[147] M.D. Firouzjaei, A.A. Shamsabadi, M. Sharifian Gh, A. Rahimpour, M.J.A.M. I. Soroush, A novel nanocomposite with superior antibacterial activity: a silver-based metal organic framework embellished with graphene oxide, Adv. Mater. Interfac. 5 (11) (2018) 1701365, https://doi.org/10.1002/admi.201701365.
[148] J. Zhang, T. Yan, J. Fang, J. Shen, L. Shi, D. Zhang, Enhanced capacitive deionization of saline water using N-doped rod-like porous carbon derived from dual-ligand metal–organic frameworks, Environ. Sci.: Nano 7 (3) (2020) 926–937, https://doi.org/10.1039/C9EN01216H.
[149] M.A. Al-Baadani, L. Xu, K. Hii Ru Yie, A. Sun, X. Gao, K. Cai, B.A. Al-Shaaobi, A. M. Al-Bishari, L. Cai, X. Shen, J. Liu, P. Ma, In situ preparation of alendronate-loaded ZIF-8 nanoparticles on electrospun nanofibers for accelerating early osteogenesis in osteoporosis, Mater. Des. 217 (2022) 110596, https://doi.org/10.1016/j.matdes.2022.110596.
[150] F. Doustdar, M. Ghorbani, ZIF-8 enriched electrospun ethyl cellulose/polyvinylpyrrolidone scaffolds: the key role of polyvinylpyrrolidone molecular weight, Carbohydr. Polym. 291 (2022), https://doi.org/10.1016/j.carbpol.2022.119620.
[151] C. Hang, Z. Wei, X. Jieyu, L. Man, Y. Ye, Z. Ling, W. Min, C. Danyang, G. Liang, ZIF-8/Curcumin-Loaded electrospun nanofiber membrane for wound healing, ACS Appl. Nano Mater. 6 (17) (2023) 15620–15631, https://doi.org/10.1021/acsanm.3c02443.
[152] J. Sun, Y. Fan, W. Ye, L. Tian, S. Niu, W. Ming, J. Zhao, L. Ren, Near-infrared light triggered photodynamic and nitric oxide synergistic antibacterial nanocomposite membrane, Chem. Eng. J. 417 (2021) 128049, https://doi.org/10.1016/j.cej.2020.128049.
[153] Y. Zhu, D. Yang, J. Li, Z. Yue, J. Zhou, X. Wang, The preparation of ultrathin and porous electrospinning membranes of HKUST-1/PLA with good antibacterial and filtration performances, J. Porous Mater. 30 (3) (2022) 1011–1019, https://doi.org/10.1007/s10934-022-01394-z.
[154] Z. Liu, J. Ye, A. Rauf, S. Zhang, G. Wang, S. Shi, G. Ning, A flexible fibrous membrane based on copper(ii) metal–organic framework/poly(lactic acid) composites with superior antibacterial performance, Biomater. Sci. 9 (10) (2021) 3851–3859, https://doi.org/10.1039/d1bm00164g.
[155] H. Wu, Z. Hu, Q. Geng, Z. Chen, Y. Song, J. Chu, X. Ning, S. Dong, D. Yuan, Facile preparation of CuMOF-modified multifunctional nanofiber membrane for high-efficient filtration/separation in complex environments, Colloids Surf. Physicochem. Eng. Aspects 651 (2022) 129656, https://doi.org/10.1016/j.colsurfa.2022.129656.
[156] K. Kirakci, D. Bůžek, P. Peer, V. Liška, J. Mosinger, I. Křížová, M. Kloda, S. Ondrušová, K. Lang, J. Demel, Polymeric membranes containing iodine-loaded UiO-66 nanoparticles as water-responsive antibacterial and antiviral surfaces, ACS Appl. Nano Mater. 5 (1) (2021) 1244–1251, https://doi.org/10.1021/acsanm.1c03832.
[157] J. Zhu, W. Qiu, C. Yao, C. Wang, D. Wu, S. Pradeep, J. Yu, Z. Dai, Water-stable zirconium-based metal-organic frameworks armed polyvinyl alcohol nanofibrous membrane with enhanced antibacterial therapy for wound healing, J. Colloid Interface Sci. 603 (2021) 243–251, https://doi.org/10.1016/j.jcis.2021.06.084.
[158] J. Wang, S. Chen, Q. Zeng, H. Jiang, H. Chang, T.C. Zhang, X. Tian, Y. Li, Y. Liang, K. Wang, Polydopamine/UiO-66-NH2 induced photothermal antibacterial electrospun membrane for efficient point-of-use drinking water treatment, Colloids Surf. Physicochem. Eng. Aspects 658 (2023) 130640, https://doi.org/10.1016/j.colsurfa.2022.130640.

[159] M. Chen, Z. Long, R. Dong, L. Wang, J. Zhang, S. Li, X. Zhao, X. Hou, H. Shao, X. Jiang, Titanium incorporation into Zr-porphyrinic metal-organic frameworks with enhanced antibacterial activity against multidrug-resistant pathogens, Small 16 (7) (2020) e1906240, https://doi.org/10.1002/smll.201906240.
[160] Y. Zhang, S. Yuan, X. Feng, H. Li, J. Zhou, B. Wang, Preparation of nanofibrous metal–organic framework filters for efficient air pollution control, J. Am. Chem. Soc. 138 (18) (2016) 5785–5788, https://doi.org/10.1021/jacs.6b02553.
[161] Z. Song, Y. Wu, Q. Cao, H. Wang, X. Wang, H. Han, pH-responsive, light-triggered on-demand antibiotic release from functional metal–organic framework for bacterial infection combination therapy, Adv. Funct. Mater. 28 (23) (2018) 1800011, https://doi.org/10.1002/adfm.201800011.
[162] Y. Zhan, J. Lan, J. Shang, L. Yang, X. Guan, W. Li, S. Chen, Y. Qi, S. Lin, Durable ZIF-8/Ag/AgCl/TiO2 decorated PAN nanofibers with high visible light photocatalytic and antibacterial activities for degradation of dyes, J. Alloys Compd. 822 (2020) 153579, https://doi.org/10.1016/j.jallcom.2019.153579.
[163] A. Zhang, Q. Qiao, Z. Pei, Z. Wang, J. Guo, Y. Li, G. Zhai, P. Fei, J. Lu, H. Jia, Polyurethane-based T-ZIF-8 nanofibers as photocatalytic antibacterial materials, ACS Appl. Nano Mater. 6 (23) (2023) 22173–22184, https://doi.org/10.1021/acsanm.3c04400.
[164] G. Zhu, X. Li, X.-P. Li, A. Wang, T. Li, X. Zhu, D. Tang, J. Zhu, X. He, H. Li, S. Li, Y. Zhang, B. Wang, S. Zhang, H. Xu, Nanopatterned electroactive polylactic acid nanofibrous MOFilters for efficient PM0.3 filtration and bacterial inhibition, ACS Appl. Mater. Interfaces 15 (40) (2023) 47145–47157, https://doi.org/10.1021/acsami.3c11941.
[165] W. Ma, Y. Li, M. Zhang, S. Gao, J. Cui, C. Huang, G. Fu, Biomimetic durable multifunctional self-cleaning nanofibrous membrane with outstanding oil/water separation, photodegradation of organic contaminants, and antibacterial performances, ACS Appl. Mater. Interfaces 12 (31) (2020) 34999–35010, https://doi.org/10.1021/acsami.0c09059.
[166] S. Qian, L. Song, L. Sun, X. Zhang, Z. Xin, J. Yin, S. Luan, Metal-organic framework/poly (ε-caprolactone) hybrid electrospun nanofibrous membranes with effective photodynamic antibacterial activities, J. Photochem. Photobiol., A: Chem 400 (2020) 112626, https://doi.org/10.1016/j.jphotochem.2020.112626.
[167] L. Chen, Y. Hernandez, X. Feng, K. Müllen, From nanographene and graphene nanoribbons to graphene sheets: chemical synthesis, Angew. Chem. Int. Ed. 51 (31) (2012) 7640–7654, https://doi.org/10.1002/anie.201201084.
[168] A. Sun, Y. Zhan, Q. Feng, W. Yang, H. Dong, Y. Liu, X. Chen, Y. Chen, Assembly of MXene/ZnO heterojunction onto electrospun poly(arylene ether nitrile) fibrous membrane for favorable oil/water separation with high permeability and synergetic antifouling performance, J. Membr. Sci. 663 (2022) 120933, https://doi.org/10.1016/j.memsci.2022.120933.
[169] M. Wang, N. Zhang, Y. Feng, Z. Hu, Q. Shao, X. Huang, Partially pyrolyzed binary metal-organic framework nanosheets for efficient electrochemical hydrogen peroxide synthesis, Angew. Chem. Int. Ed. (2020) 14373–14377, https://doi.org/10.1002/anie.202006422.
[170] M. Wang, N. Zhang, Y. Feng, Z. Hu, Q. Shao, X. Huang, Partially pyrolyzed binary metal–organic framework nanosheets for efficient electrochemical hydrogen peroxide synthesis, Angew. Chem. Int. Ed. 59 (34) (2020) 14373–14377.
[171] Y. Li, L. Liu, T. Meng, L. Wang, Z. Xie, Structural engineering of ionic MOF@COF heterointerface for exciton-boosting sunlight-driven photocatalytic filter, ACS Nano 17 (3) (2023) 2932–2942, https://doi.org/10.1021/acsnano.2c11339.
[172] C. Li, C. Chen, J. Zhao, M. Tan, S. Zhai, Y. Wei, L. Wang, T. Dai, Electrospun fibrous membrane containing a cyclodextrin covalent organic framework with antibacterial properties for accelerating wound healing, ACS Biomater. Sci. Eng. 7 (8) (2021) 3898–3907, https://doi.org/10.1021/acsbiomaterials.1c00648.
[173] X. Zhao, L.-Y. Wang, C.-Y. Tang, X.-J. Zha, Y. Liu, B.-H. Su, K. Ke, R.-Y. Bao, M.-B. Yang, W. Yang, Smart Ti3C2T x MXene fabric with fast humidity response and joule heating for healthcare and medical therapy applications, ACS Nano 14 (7) (2020) 8793–8805, https://doi.org/10.1021/acsnano.0c03391.
[174] S.M. George, B. Kandasubramanian, Advancements in MXene-Polymer composites for various biomedical applications, Ceram. Int. 46 (7) (2020) 8522–8535, https://doi.org/10.1016/j.ceramint.2019.12.257.
[175] H.E. Karahan, K. Goh, C. Zhang, E. Yang, C. Yıldırım, C.Y. Chuah, M.G. Ahunbay, J. Lee, Ş.B. Tantekin-Ersolmaz, Y. Chen, MXene materials for designing advanced separation membranes, Adv. Mater. 32 (29) (2020) 1906697, https://doi.org/10.1002/adma.201906697.
[176] S. Sharma, A. Chhetry, M. Sharifuzzaman, H. Yoon, J.Y. Park, Wearable capacitive pressure sensor based on MXene composite nanofibrous scaffolds for reliable human physiological signal acquisition, ACS Appl. Mater. Interfaces 12 (19) (2020) 22212–22224, https://doi.org/10.1021/acsami.0c05819.
[177] A. Levitt, S. Seyedin, J. Zhang, X. Wang, J.M. Razal, G. Dion, Y. Gogotsi, Bath electrospinning of continuous and scalable multifunctional MXene-infiltrated nanoyarns, Small 16 (26) (2020) 2002158, https://doi.org/10.1002/smll.202002158.
[178] X. Gao, Z.-K. Li, J. Xue, Y. Qian, L.-Z. Zhang, J. Caro, H. Wang, Titanium carbide Ti_3C_2Tx (MXene) enhanced PAN nanofiber membrane for air purification, J. Membr. Sci. 586 (2019) 162–169, https://doi.org/10.1016/j.memsci.2019.05.058.
[179] X. Zhou, Z. Wang, Y.K. Chan, Y. Yang, Z. Jiao, L. Li, J. Li, K. Liang, Y. Deng, Infection micromilieu-activated nanocatalytic membrane for orchestrating rapid sterilization and stalled chronic wound regeneration, Adv. Funct. Mater. 32 (7) (2021) 2109469, https://doi.org/10.1002/adfm.202109469.
[180] Y. Wang, P. Li, P. Xiang, J. Lu, J. Yuan, J. Shen, Electrospun polyurethane/keratin/AgNP biocomposite mats for biocompatible and antibacterial wound dressings, J. Mater. Chem. B 4 (4) (2016) 635–648, https://doi.org/10.1039/C5TB02358K.
[181] X. She, H. Xu, Y. Xu, J. Yan, J. Xia, L. Xu, Y. Song, Y. Jiang, Q. Zhang, H. Li, Exfoliated graphene-like carbon nitride in organic solvents: enhanced photocatalytic activity and highly selective and sensitive sensor for the detection of trace amounts of Cu2+, J. Mater. Chem. A 2 (8) (2014) 2563–2570, https://doi.org/10.1039/c3ta13768f.
[182] A. Ahmadi, M. Hajilou, S. Zavari, S. Yaghmaei, A comparative review on adsorption and photocatalytic degradation of classified dyes with metal/non-metal-based modification of graphitic carbon nitride nanocomposites: synthesis, mechanism, and affecting parameters, J. Clean. Prod. 382 (2023) 134967, https://doi.org/10.1016/j.jclepro.2022.134967.
[183] P. Suyana, P. Ganguly, B.N. Nair, S.C. Pillai, U.S. Hareesh, Structural and compositional tuning in g-C3N4 based systems for photocatalytic antibiotic degradation, Chem. Eng. J. Adv. 8 (2021) 100148, https://doi.org/10.1016/j.ceja.2021.100148.
[184] W. Wang, C. Zhou, Y. Yang, G. Zeng, C. Zhang, Y. Zhou, J. Yang, D. Huang, H. Wang, W. Xiong, Carbon nitride based photocatalysts for solar photocatalytic disinfection, can we go further? Chem. Eng. J. 404 (2021) 126540 https://doi.org/10.1016/j.cej.2020.126540.
[185] Y. Zou, P. Wang, A. Zhang, Z. Qin, Y. Li, Y. Xianyu, H. Zhang, Covalent organic framework-incorporated nanofibrous membrane as an intelligent platform for wound dressing, ACS Appl. Mater. Interfaces 14 (7) (2022) 8680–8692, https://doi.org/10.1021/acsami.1c19754.
[186] Y. Zhao, C. Tian, Y. Liu, Z. Liu, J. Li, Z. Wang, X. Han, All-in-one bioactive properties of photothermal nanofibers for accelerating diabetic wound healing, Biomaterials 295 (2023) 122029, https://doi.org/10.1016/j.biomaterials.2023.122029.
[187] W. Xiao, Q. Li, H. He, W. Li, X. Cao, H. Dong, Patterning multi-nanostructured poly(l-lactic acid) fibrous matrices to manipulate biomolecule distribution and functions, ACS Appl. Mater. Interfaces 10 (10) (2018) 8465–8473, https://doi.org/10.1021/acsami.7b18423.
[188] A.A. Shitole, P.W. Raut, N. Sharma, P. Giram, A.P. Khandwekar, B. Garnaik, Electrospun polycaprolactone/hydroxyapatite/ZnO nanofibers as potential biomaterials for bone tissue regeneration, J. Mater. Sci. Mater. Med. 30 (5) (2019) 51, https://doi.org/10.1007/s10856-019-6255-5.
[189] K.N. Chen, F.N.I. Sari, J.M. Ting, Multifunctional TiO_2/polyacrylonitrile nanofibers for high efficiency PM2.5 capture, UV filter, and anti-bacteria activity, Appl. Surf. Sci. 493 (2019) 157–164, https://doi.org/10.1016/j.apsusc.2019.07.020.
[190] M. Hu, K. Korschelt, M. Viel, N. Wiesmann, M. Kappl, J. Brieger, K. Landfester, H. Therien-Aubin, W. Tremel, Nanozymes in nanofibrous mats with haloperoxidase-like activity to combat biofouling, ACS Appl. Mater. Interfaces 10 (51) (2018) 44722–44730, https://doi.org/10.1021/acsami.8b16307.
[191] L. Xie, Y. Shu, Y. Hu, J. Cheng, Y. Chen, SWNTs-PAN/TPU/PANI composite electrospun nanofiber membrane for point-of-use efficient electrochemical disinfection: new strategy of CNT disinfection, Chemosphere 251 (2020) 126286, https://doi.org/10.1016/j.chemosphere.2020.126286.
[192] M. Heidari, S.H. Bahrami, M. Ranjbar-Mohammadi, P.J.M.s. Milan, e. C, Smart electrospun nanofibers containing PCL/gelatin/graphene oxide for application in nerve tissue engineering, Mater. Sci. Eng. C 103 (2019) 109768, https://doi.org/10.1016/j.msec.2019.109768.
[193] D. Dogan, F.R. Karaduman, N. Horzum, A.U. Metin, Boron nitride decorated poly (vinyl alcohol)/poly(acrylic acid) composite nanofibers: a promising material for biomedical applications, J. Mech. Behav. Biomed. Mater. 141 (2023) 105773, https://doi.org/10.1016/j.jmbbm.2023.105773.
[194] X. Zhang, Q. Li, L. Li, J. Ouyang, T. Wang, J. Chen, X. Hu, Y. Ao, D. Qin, L. Zhang, J. Xue, J. Cheng, W. Tao, Bioinspired mild photothermal effect-reinforced multifunctional fiber scaffolds promote bone regeneration, ACS Nano 17 (7) (2023) 6466–6479, https://doi.org/10.1021/acsnano.2c11486.
[195] X. You, M. Wang, G. Jiang, X. Zhao, Z. Wang, F. Liu, C. Zhao, Z. Qiu, R. Zhao, Multifunctional porous nanofibrous membranes with superior antifouling properties for oil-water separation and photocatalytic degradation, J. Membr. Sci. 668 (2023) 121245, https://doi.org/10.1016/j.memsci.2022.121245.
[196] E.A. Mayerberger, R.M. Street, R.M. McDaniel, M.W. Barsoum, C.L. Schauer, Antibacterial properties of electrospun Ti_3C_2Tz (MXene)/chitosan nanofibers, RSC Adv. 8 (62) (2018) 35386–35394, https://doi.org/10.1039/C8RA06274A.
[197] Y. Wang, S. Li, W. Shi, S. Li, Preparation and characterization of electrospinning gelatin nanofiber membranes containing carvacrol nanoparticles, ChemistrySelect 9 (4) (2024) e202302050, https://doi.org/10.1002/slct.202302050.
[198] R. Jiang, T. Yan, Y.Q. Wang, Z.J. Pan, The preparation of PA6/CS-NPs nanofiber filaments with excellent antibacterial activity via a one-step multineedle electrospinning method with liquid bath circling system, J. Appl. Polym. Sci. 137 (36) (2020) e49053, https://doi.org/10.1002/app.49053.
[199] M.K. Haider, D. Kharaghani, L. Sun, S. Ullah, M.N. Sarwar, A. Ullah, M. Khatri, Y. Yoshiko, M. Gopiraman, I.S. Kim, Synthesized bioactive lignin nanoparticles/polycaprolactone nanofibers: a novel nanobiocomposite for bone tissue engineering, Biomater. Adv. 144 (2023) 213203, https://doi.org/10.1016/j.bioadv.2022.213203.
[200] M. Amantay, Y. Ma, L. Chen, H. osman, L. Mengping, T. Jiang, T. Zhou, T. Ye, Y. Wang, Electrospinning fibers modified with near infrared light-excited copper nanoparticles for antibacterial and bone regeneration, Adv. Mater. Interfac. 10 (31) (2023) 2300113, https://doi.org/10.1002/admi.202300113.
[201] M.M. Aljohani, A. Abu-Rayyan, N.H. Elsayed, F.A. Alatawi, M. Al-Anazi, S. K. Mustafa, R.K. Albalawi, R. Abdelmonem, One-pot microwave synthesis of chitosan-stabilized silver nanoparticles entrapped polyethylene oxide nanofibers, with their intrinsic antibacterial and antioxidant potency for wound healing, Int.

J. Biol. Macromol. 235 (2023) 123704, https://doi.org/10.1016/j.ijbiomac.2023.123704.
[202] A. Ghaee, M. Karimi, M. Lotfi-Sarvestani, B. Sadatnia, V.J.M.s. Hoseinpour, engineering, Preparation of hydrophilic polycaprolactone/modified ZIF-8 nanofibers as a wound dressing using hydrophilic surface modifying macromolecules, Mater. Sci. Eng. C 103 (2019) 109767, https://doi.org/10.1016/j.msec.2019.109767.
[203] X. Zhang, L. Li, J. Ouyang, L. Zhang, J. Xue, H. Zhang, W. Tao, Electroactive electrospun nanofibers for tissue engineering, Nano Today 39 (2021) 101196, https://doi.org/10.1016/j.nantod.2021.101196.
[204] G. Ramanathan, L.S. Seleenmary Sobhanadhas, G.F. Sekar Jeyakumar, V. Devi, U. T. Sivagnanam, P. Fardim, Fabrication of biohybrid cellulose acetate-collagen bilayer matrices as nanofibrous spongy dressing material for wound-healing application, Biomacromolecules 21 (6) (2020) 2512–2524, https://doi.org/10.1021/acs.biomac.0c00516.
[205] S. Yang, X. Li, P. Liu, M. Zhang, C. Wang, B. Zhang, Multifunctional chitosan/polycaprolactone nanofiber scaffolds with varied dual-drug release for wound-healing applications, ACS Biomater. Sci. Eng. 6 (8) (2020) 4666–4676, https://doi.org/10.1021/acsbiomaterials.0c00674.
[206] H. Yu, X. Chen, J. Cai, D. Ye, Y. Wu, L. Fan, P. Liu, Novel porous three-dimensional nanofibrous scaffolds for accelerating wound healing, Chem. Eng. J. 369 (2019) 253–262, https://doi.org/10.1016/j.cej.2019.03.091.
[207] L.M. Delgado, K. Fuller, D.I. Zeugolis, Influence of cross-linking method and disinfection/sterilization treatment on the structural, biophysical, biochemical, and biological properties of collagen-based devices, ACS Biomater. Sci. Eng. 4 (8) (2018) 2739–2747, https://doi.org/10.1021/acsbiomaterials.8b00052.
[208] Y. Ding, Y. Hao, Z. Yuan, B. Tao, M. Chen, C. Lin, P. Liu, K. Cai, A dual-functional implant with an enzyme-responsive effect for bacterial infection therapy and tissue regeneration, Biomater. Sci. 8 (7) (2020) 1840–1854, https://doi.org/10.1039/C9BM01924C.
[209] Y. Xi, J. Ge, Y. Guo, B. Lei, P.X. Ma, Biomimetic elastomeric polypeptide-based nanofibrous matrix for overcoming multidrug-resistant bacteria and enhancing full-thickness wound healing/skin regeneration, ACS Nano 12 (11) (2018) 10772–10784, https://doi.org/10.1021/acsnano.8b01152.
[210] C. Liu, J. Shen, K.W.K. Yeung, S.C. Tjong, Development and antibacterial performance of novel polylactic acid-graphene oxide-silver nanoparticle hybrid nanocomposite mats prepared by electrospinning, ACS Biomater. Sci. Eng. 3 (3) (2017) 471–486, https://doi.org/10.1021/acsbiomaterials.6b00766.
[211] Y. Xie, Q. Zhang, W. Zheng, X. Jiang, Small molecule-capped gold nanoclusters for curing skin infections, ACS Appl. Mater. Interfaces 13 (30) (2021) 35306–35314, https://doi.org/10.1021/acsami.1c04944.
[212] S. Homaeigohar, M.A. Assad, A.H. Azari, F. Ghorbani, C. Rodgers, M.J. Dalby, K. Zheng, R. Xu, M. Elbahri, A.R. Boccaccini, Biosynthesis of zinc oxide nanoparticles on l-carnosine biofunctionalized polyacrylonitrile nanofibers; a biomimetic wound healing material, ACS Appl. Bio Mater. 6 (10) (2023) 4290–4303, https://doi.org/10.1021/acsabm.3c00499.
[213] L. Cai, X. Zhu, H. Ruan, J. Yang, W. Wei, Y. Wu, L. Zhou, H. Jiang, M. Ji, J. Chen, Curcumin-stabilized silver nanoparticles encapsulated in biocompatible electrospun nanofibrous scaffold for sustained eradication of drug-resistant bacteria, J. Hazard Mater. 452 (2023) 131290, https://doi.org/10.1016/j.jhazmat.2023.131290.
[214] X. Zhao, L.Y. Wang, C.Y. Tang, K. Li, Y.H. Huang, Y.R. Duan, S.T. Zhang, K. Ke, B. H. Su, W. Yang, Electro-microenvironment modulated inhibition of endogenous biofilms by piezo implants for ultrasound-localized intestinal perforation disinfection, Biomaterials 295 (2023) 122055, https://doi.org/10.1016/j.biomaterials.2023.122055.
[215] T.V. Patil, S. Deb Dutta, D.K. Patel, K. Ganguly, K.-T. Lim, Electrospinning near infra-red light-responsive unzipped CNT/PDA nanofibrous membrane for enhanced antibacterial effect and rapid drug release, Appl. Surf. Sci. 612 (2023), https://doi.org/10.1016/j.apsusc.2022.155949.
[216] Y. Shi, M. Zhou, S. Zhao, H. Li, W. Wang, J. Cheng, L. Jin, Y. Wang, Janus amphiphilic nanofiber membranes synergistically drive antibacterial and anti-inflammatory strategies for skin wound healing, Mater. Des. 227 (2023) 111778, https://doi.org/10.1016/j.matdes.2023.111778.
[217] J. Hou, L. Chen, Z. Liu, J. Li, J. Yang, A. Zhong, M. Zhou, Y. Sun, L. Guo, Y. Yang, J. Sun, Z. Wang, Sustained release of N-acetylcysteine by sandwich structured polycaprolactone/collagen scaffolds for wound healing, J. Biomed. Mater. Res. 107 (7) (2019) 1414–1424, https://doi.org/10.1002/jbm.a.36656.
[218] F. Jonidi Shariatzadeh, S. Currie, S. Logsetty, R. Spiwak, S. Liu, Enhancing wound healing and minimizing scarring: a comprehensive review of nanofiber technology in wound dressings, Prog. Mater. Sci. 147 (2024), https://doi.org/10.1016/j.pmatsci.2024.101350.
[219] R. Huang, B. Lin, Z. Lei, L. Xu, H. Zhang, W. Wang, Y. Zhang, S. Xiao, Y. Long, J. Li, X. Li, On-site construction of a full-thickness skin equivalent with endothelial tube networks via multilayer electrospinning for wound coverage, ACS Biomater. Sci. Eng. 9 (11) (2023) 6241–6255, https://doi.org/10.1021/acsbiomaterials.3c00913.
[220] Q. Zhang, J. Zhu, X. Fei, M. Zhu, A Janus nanofibrous scaffold integrated with exercise-driven electrical stimulation and nanotopological effect enabling the promotion of tendon-to-bone healing, Nano Today 55 (2024), https://doi.org/10.1016/j.nantod.2024.102208.
[221] H. Min, K. Li, Q. Wang, X. Gao, L. Xie, W. Tian, A novel filler of biocomposites for long-term self-regulated delivery of immunomodulatory and antibacterial components to accelerate bone regeneration, Compos. B Eng. 238 (2022) 109942, https://doi.org/10.1016/j.compositesb.2022.109942.
[222] Z. Qu, Y. Wang, Y. Dong, X. Li, L. Hao, L. Sun, L. Zhou, R. Jiang, W. Liu, Intelligent electrospinning nanofibrous membranes for monitoring and promotion of the wound healing, Mater. Today Bio 26 (2024) 101093, https://doi.org/10.1016/j.mtbio.2024.101093.
[223] J. Qu, X. Zhao, Y. Liang, Y. Xu, P.X. Ma, B. Guo, Degradable conductive injectable hydrogels as novel antibacterial, anti-oxidant wound dressings for wound healing, Chem. Eng. J. 362 (2019) 548–560, https://doi.org/10.1016/j.cej.2019.01.028.
[224] G.G. de Lima, D.W. de Lima, M.J. de Oliveira, A.B. Lugão, M.T. Alcântara, D. M. Devine, M.J. de Sá, Synthesis and in vivo behavior of PVP/CMC/agar hydrogel membranes impregnated with silver nanoparticles for wound healing applications, ACS Appl. Bio Mater. 1 (6) (2018) 1842–1852, https://doi.org/10.1021/acsabm.8b00369.
[225] Y. Liang, X. Zhao, T. Hu, B. Chen, Z. Yin, P.X. Ma, B. Guo, Adhesive hemostatic conducting injectable composite hydrogels with sustained drug release and photothermal antibacterial activity to promote full-thickness skin regeneration during wound healing, Small 15 (12) (2019) 1900046, https://doi.org/10.1002/smll.201900046.
[226] W. Li, Q. Yu, H. Yao, Y. Zhu, P.D. Topham, K. Yue, L. Ren, L. Wang, Superhydrophobic hierarchical fiber/bead composite membranes for efficient treatment of burns, Acta Biomater. 92 (2019) 60–70, https://doi.org/10.1016/j.actbio.2019.05.025.
[227] L. Sukhodub, M. Kumeda, L. Sukhodub, V. Bielai, M. Lyndin, Metal ions doping effect on the physicochemical, antimicrobial, and wound healing profiles of alginate-based composite, Carbohydr. Polym. 304 (2023) 120486, https://doi.org/10.1016/j.carbpol.2022.120486.
[228] Y. Xie, S. Chen, X. Peng, X. Wang, Z. Wei, J.J. Richardson, K. Liang, H. Ejima, J. Guo, C. Zhao, Alloyed nanostructures integrated metal-phenolic nanoplatform for synergistic wound disinfection and revascularization, Bioact. Mater. 16 (2022) 95–106, https://doi.org/10.1016/j.bioactmat.2022.03.004.
[229] S.S. Nanda, T. Wang, M.I. Hossain, H.Y. Yoon, S.T. Selvan, K. Kim, D.K. Yi, Gold-nanorod-based scaffolds for wound-healing applications, ACS Appl. Nano Mater. 5 (6) (2022) 8640–8648, https://doi.org/10.1021/acsanm.2c02230.
[230] R. Yang, Y. Zheng, Y. Zhang, G. Li, Y. Xu, Y. Zhang, Y. Xu, C. Zhuang, P. Yu, L. Deng, W. Cui, Y. Chen, L. Wang, Bipolar metal flexible electrospun fibrous membrane based on metal–organic framework for gradient healing of tendon-to-bone interface regeneration, Adv. Healthcare Mater. 11 (12) (2022) 2200072, https://doi.org/10.1002/adhm.202200072.
[231] L. Yin, Q. Tang, Q. Ke, X. Zhang, J. Su, H. Zhong, L. Fang, Sequential anti-infection and proangiogenesis of DMOG@ZIF-8/Gelatin-PCL electrospinning dressing for chronic wound healing, ACS Appl. Mater. Interfaces 15 (42) (2023) 48903–48912, https://doi.org/10.1021/acsami.3c09584.
[232] J. Chen, F. Xue, W. Du, X. Deng, Y. Wu, H. Chen, Endogenous Fe2+-activated nanomedicine to amplify ROS generation and in-situ response NIR-II photothermal therapy of tumor, Chem. Eng. J. 471 (2023) 144358, https://doi.org/10.1016/j.cej.2023.144358.
[233] W. Song, H. Yang, Y. Sun, Y. Yang, Q. Dong, P. He, G. Liu, Z. Zhao, L. Qin, S. Gao, J. Liu, H. Zhou, H. Wang, Multifunctional zeolitic imidazolate framework nanocomposites as Fenton catalysts for synergistic chemodynamic-photothermal-chemo therapy, ACS Appl. Nano Mater. 6 (21) (2023) 19926–19938, https://doi.org/10.1021/acsanm.3c03729.
[234] N. Guo, Y. Xia, Y. Duan, Q. Wu, L. Xiao, Y. Shi, B. Yang, Y. Liu, Self-enhanced photothermal-chemodynamic antibacterial agents for synergistic anti-infective therapy, Chin. Chem. Lett. 34 (2) (2023) 107542, https://doi.org/10.1016/j.cclet.2022.05.056.
[235] Y. Huang, L. Qi, Z. Liu, Y. Jiang, J. Wang, L. Liu, Y. Li, L. Zhang, G. Feng, Radially electrospun fibrous membrane incorporated with copper peroxide nanodots capable of self-catalyzed chemodynamic therapy for angiogenesis and healing acceleration of diabetic wounds, ACS Appl. Mater. Interfaces 15 (30) (2023) 35986–35998, https://doi.org/10.1021/acsami.3c06703.
[236] L. Qi, Y. Huang, D. Sun, Z. Liu, Y. Jiang, J. Liu, J. Wang, L. Liu, G. Feng, Y. Li, L. Zhang, Guiding the path to healing: CuO2-laden nanocomposite membrane for diabetic wound treatment, Small 20 (3) (2023) 2305100, https://doi.org/10.1002/smll.202305100.
[237] B. Xu, G. Cai, Y. Gao, M. Chen, C. Xu, C. Wang, D. Yu, D. Qi, R. Li, J. Wu, Nanofibrous dressing with nanocomposite monoporous microspheres for chemodynamic antibacterial therapy and wound healing, ACS Omega 8 (41) (2023) 38481–38493, https://doi.org/10.1021/acsomega.3c05271.
[238] L. He, D. Di, X. Chu, X. Liu, Z. Wang, J. Lu, S. Wang, Q. Zhao, Photothermal antibacterial materials to promote wound healing, J. Contr. Release 363 (2023) 180–200, https://doi.org/10.1016/j.jconrel.2023.09.035.
[239] O. Demirel, S. Kolgesiz, S. Yuce, S. Hayat Soytaş, D.Y. Koseoglu-Imer, H. Unal, Photothermal electrospun nanofibers containing polydopamine-coated halloysite nanotubes as antibacterial air filters, ACS Appl. Nano Mater. 5 (12) (2022) 18127–18137, https://doi.org/10.1021/acsanm.2c04026.
[240] J. Huo, Q. Jia, H. Huang, J. Zhang, P. Li, X. Dong, W. Huang, Emerging photothermal-derived multimodal synergistic therapy in combating bacterial infections, Chem. Soc. Rev. 50 (15) (2021) 8762–8789, https://doi.org/10.1039/d1cs00074h.
[241] Y. Ding, L. Xu, S. Chen, Y. Zhu, Y. Sun, L. Ding, B. Yan, S. Ramakrishna, J. Zhang, Y.-Z. Long, Mxene composite fibers with advanced thermal management for inhibiting tumor recurrence and accelerating wound healing, Chem. Eng. J. 459 (2023) 141529, https://doi.org/10.1016/j.cej.2023.141529.
[242] C. Xue, L. Sutrisno, M. Li, W. Zhu, Y. Fei, C. Liu, X. Wang, K. Cai, Y. Hu, Z. Luo, Implantable multifunctional black phosphorus nanoformulation-deposited biodegradable scaffold for combinational photothermal/chemotherapy and

wound healing, Biomaterials 269 (2021) 120623, https://doi.org/10.1016/j.biomaterials.2020.120623.
[243] X. Zhang, N. Yu, Q. Ren, S. Niu, L. Zhu, L. Hong, K. Cui, X. Wang, W. Jiang, M. Wen, Z. Chen, Janus nanofiber membranes with photothermal-enhanced biofluid drainage and sterilization for diabetic wounds, Adv. Funct. Mater. (2024) 2315020, https://doi.org/10.1002/adfm.202315020.
[244] X. Xu, X. Liu, L. Tan, Z. Cui, X. Yang, S. Zhu, Z. Li, X. Yuan, Y. Zheng, K.W. K. Yeung, P.K. Chu, S. Wu, Controlled-temperature photothermal and oxidative bacteria killing and acceleration of wound healing by polydopamine-assisted Au-hydroxyapatite nanorods, Acta Biomater. 77 (2018) 352–364, https://doi.org/10.1016/j.actbio.2018.07.030.
[245] X. Jin, Z. Ou, G. Zhang, R. Shi, J. Yang, W. Liu, G. Luo, J. Deng, W. Wang, A CO-mediated photothermal therapy to kill drug-resistant bacteria and minimize thermal injury for infected diabetic wound healing, Biomater. Sci. 11 (18) (2023) 6236–6251, https://doi.org/10.1039/d3bm00774j.
[246] F. Wang, Q. Wu, G. Jia, L. Kong, R. Zuo, K. Feng, M. Hou, Y. Chai, J. Xu, C. Zhang, Q. Kang, Black phosphorus/MnO2 nanocomposite disrupting bacterial thermotolerance for efficient mild-temperature photothermal therapy, Adv. Sci. 10 (30) (2023) 2303911, https://doi.org/10.1002/advs.202303911.
[247] X. Lin, Y. Fang, Z. Hao, H. Wu, M. Zhao, S. Wang, Y. Liu, Bacteria-triggered multifunctional hydrogel for localized chemodynamic and low-temperature photothermal sterilization, Small 17 (51) (2021) 2103303, https://doi.org/10.1002/smll.202103303.
[248] Z. Wang, Y. Peng, Y. Zhou, S. Zhang, J. Tan, H. Li, D. He, L. Deng, Pd-Cu nanoalloy for dual stimuli-responsive chemo-photothermal therapy against pathogenic biofilm bacteria, Acta Biomater. 137 (2022) 276–289, https://doi.org/10.1016/j.actbio.2021.10.028.
[249] T. Hu, Z. Wang, W. Shen, R. Liang, D. Yan, M. Wei, Recent advances in innovative strategies for enhanced cancer photodynamic therapy, Theranostics 11 (7) (2021) 3278–3300, https://doi.org/10.7150/thno.54227.
[250] S. Wu, C. Xu, Y. Zhu, L. Zheng, L. Zhang, Y. Hu, B. Yu, Y. Wang, F.J. Xu, Biofilm-sensitive photodynamic nanoparticles for enhanced penetration and antibacterial efficiency, Adv. Funct. Mater. (2021) 2103591, https://doi.org/10.1002/adfm.202103591.
[251] B.N. Im, H. Shin, B. Lim, J. Lee, K.S. Kim, J.M. Park, K. Na, Helicobacter pylori-targeting multiligand photosensitizer for effective antibacterial endoscopic photodynamic therapy, Biomaterials 271 (2021), https://doi.org/10.1016/j.biomaterials.2021.120745.
[252] B. Zhou, X. Sun, B. Dong, S. Yu, L. Cheng, S. Hu, W. Liu, L. Xu, X. Bai, L. Wang, H. Song, Antibacterial PDT nanoplatform capable of releasing therapeutic gas for synergistic and enhanced treatment against deep infections, Theranostics 12 (6) (2022) 2580–2597, https://doi.org/10.7150/thno.70277.
[253] T. Ma, X. Zhai, M. Jin, Y. Huang, M. Zhang, H. Pan, X. Zhao, Y. Du, Multifunctional wound dressing for highly efficient treatment of chronic diabetic wounds, View 3 (6) (2022) 20220045, https://doi.org/10.1002/viw.20220045.
[254] M. Godoy-Gallardo, U. Eckhard, L.M. Delgado, Y.J.D. de Roo Puente, M. Hoyos-Nogués, F.J. Gil, R.A. Perez, Antibacterial approaches in tissue engineering using metal ions and nanoparticles: from mechanisms to applications, Bioact. Mater. 6 (12) (2021) 4470–4490, https://doi.org/10.1016/j.bioactmat.2021.04.033.
[255] J. Zhang, H. Guo, M. Liu, K. Tang, S. Li, Q. Fang, H. Du, X. Zhou, X. Lin, Y. Yang, B. Huang, D. Yang, Recent design strategies for boosting chemodynamic therapy of bacterial infections, Explorations (2023) 20230087, https://doi.org/10.1002/exp.20230087.
[256] L. Liu, X. Pan, S. Liu, Y. Hu, D. Ma, Near-infrared light-triggered nitric oxide release combined with low-temperature photothermal therapy for synergetic antibacterial and antifungal, Smart Materials in Medicine 2 (2021) 302–313, https://doi.org/10.1016/j.smaim.2021.08.003.
[257] L. Ma, Y. Zhou, Z. Zhang, Y. Liu, D. Zhai, H. Zhuang, Q. Li, J. Yuye, C. Wu, J. Chang, Multifunctional bioactive Nd-Ca-Si glasses for fluorescence thermometry, photothermal therapy, and burn tissue repair, Sci. Adv. 6 (2020) eabb1311, https://doi.org/10.1126/sciadv.abb1311.
[258] Q. Deng, P. Sun, L. Zhang, Z. Liu, H. Wang, J. Ren, X. Qu, Porphyrin MOF dots–based, function-adaptive nanoplatform for enhanced penetration and photodynamic eradication of bacterial biofilms, Adv. Funct. Mater. 29 (30) (2019) 1903018, https://doi.org/10.1002/adfm.201903018.
[259] Y. Zhao, Y. Liu, C. Tian, Z. Liu, K. Wu, C. Zhang, X. Han, Construction of antibacterial photothermal PCL/AgNPs/BP nanofibers for infected wound healing, Mater. Des. 226 (2023), https://doi.org/10.1016/j.matdes.2023.111670.
[260] Y. Huang, S. He, S. Yu, H.M. Johnson, Y.K. Chan, Z. Jiao, S. Wang, Z. Wu, Y. Deng, MXene-decorated nanofibrous membrane with programmed antibacterial and anti-inflammatory effects via steering NF-κB pathway for infectious cutaneous regeneration, Small 20 (4) (2023) 2304119, https://doi.org/10.1002/smll.202304119.
[261] Y. Yang, X. Zhou, Y.K. Chan, Z. Wang, L. Li, J. Li, K. Liang, Y. Deng, Photo-activated nanofibrous membrane with self-rechargeable antibacterial function for stubborn infected cutaneous regeneration, Small 18 (12) (2022) e2105988, https://doi.org/10.1002/smll.202105988.
[262] Z. Wang, B. Du, X. Gao, Y. Huang, M. Li, Z. Yu, J. Li, X. Shi, Y. Deng, K. Liang, Endogenous oxygen-evolving bio-catalytic fabrics with fortified photonic disinfection for invasive bacteria-caused refractory cutaneous regeneration, Nano Today 46 (2022) 101595, https://doi.org/10.1016/j.nantod.2022.101595.
[263] Z. Wang, J. Li, Y. Qiao, X. Liu, Y. Zheng, Z. Li, J. Shen, Y. Zhang, S. Zhu, H. Jiang, Y. Liang, Z. Cui, P.K. Chu, S. Wu, Rapid ferroelectric-photoexcited bacteria-killing of Bi4Ti3O12/Ti3C2Tx nanofiber membranes, Adv. Fiber Mater. 5 (2) (2022) 484–496, https://doi.org/10.1007/s42765-022-00234-8.
[264] S. Wang, Y. Qiao, X. Liu, S. Zhu, Y. Zheng, H. Jiang, Y. Zhang, J. Shen, Z. Li, Y. Liang, Z. Cui, P.K. Chu, S. Wu, Reduced graphene oxides modified Bi2Te3 nanosheets for rapid photo-thermoelectric catalytic therapy of bacteria-infected wounds, Adv. Funct. Mater. 33 (3) (2022) 2210098, https://doi.org/10.1002/adfm.202210098.
[265] W.-H. Dong, J.-X. Liu, X.-J. Mou, G.-S. Liu, X.-W. Huang, X. Yan, X. Ning, S. J. Russell, Y.-Z. Long, Performance of polyvinyl pyrrolidone-isatis root antibacterial wound dressings produced in situ by handheld electrospinner, Colloids Surf. B Biointerfaces 188 (2020), https://doi.org/10.1016/j.colsurfb.2019.110766.
[266] R. Dong, Y. Li, M. Chen, P. Xiao, Y. Wu, K. Zhou, Z. Zhao, B.Z. Tang, In situ electrospinning of aggregation-induced emission nanofibrous dressing for wound healing, Small Methods 6 (5) (2022) 2101247, https://doi.org/10.1002/smtd.202101247.
[267] Z. Wen, Y. Chen, P. Liao, F. Wang, W. Zeng, S. Liu, H. Wu, N. Wang, L. Moroni, M. Zhang, Y. Duan, H. Chen, In situ precision cell electrospinning as an efficient stem cell delivery approach for cutaneous wound healing, Adv. Healthcare Mater. 12 (26) (2023) 2300970, https://doi.org/10.1002/adhm.202300970.
[268] Y. Yue, X. Gong, W. Jiao, Y. Li, X. Yin, Y. Si, J. Yu, B. Ding, In-situ electrospinning of thymol-loaded polyurethane fibrous membranes for waterproof, breathable, and antibacterial wound dressing application, J. Colloid Interface Sci. 592 (2021) 310–318, https://doi.org/10.1016/j.jcis.2021.02.048.
[269] J. Zhang, Y.-T. Zhao, P.-Y. Hu, J.-J. Liu, X.-F. Liu, M. Hu, Z. Cui, N. Wang, Z. Niu, H.-F. Xiang, Y.-Z. Long, Laparoscopic electrospinning for in situ hemostasis in minimally invasive operation, Chem. Eng. J. 395 (2020) 125089, https://doi.org/10.1016/j.cej.2020.125089.
[270] J.-X. Liu, W.-H. Dong, X.-J. Mou, G.-S. Liu, X.-W. Huang, X. Yan, C.-F. Zhou, S. Jiang, Y.-Z. Long, In situ electrospun zein/thyme essential oil-based membranes as an effective antibacterial wound dressing, ACS Appl. Bio Mater. 3 (1) (2019) 302–307, https://doi.org/10.1021/acsabm.9b00823.
[271] J. Zhang, C.-L. Liu, J.-J. Liu, X.-H. Bai, Z.-K. Cao, J. Yang, M. Yu, S. Ramakrishna, Y.-Z. Long, Eluting mode of photodynamic nanofibers without photosensitizer leakage for one-stop treatment of outdoor hemostasis and sterilizing superbacteria, Nanoscale 13 (12) (2021) 6105–6116, https://doi.org/10.1039/d1nr00179e.
[272] X.-F. Liu, J. Zhang, J.-J. Liu, Q.-H. Zhou, Z. Liu, P.-Y. Hu, Z. Yuan, S. Ramakrishna, D.-P. Yang, Y.-Z. Long, Bifunctional CuS composite nanofibers via in situ electrospinning for outdoor rapid hemostasis and simultaneous ablating superbug, Chem. Eng. J. 401 (2020) 126096, https://doi.org/10.1016/j.cej.2020.126096.
[273] R.-H. Dong, Y.-X. Jia, C.-C. Qin, L. Zhan, X. Yan, L. Cui, Y. Zhou, X. Jiang, Y.-Z. Long, In situ deposition of a personalized nanofibrous dressing via a handy electrospinning device for skin wound care, Nanoscale 8 (6) (2016) 3482–3488, https://doi.org/10.1039/C5NR08367B.
[274] S. Zhang, L. Wang, T. Xu, X. Zhang, Luminescent MOF-based nanofibers with visual monitoring and antibacterial properties for diabetic wound healing, ACS Appl. Mater. Interfaces 15 (7) (2023) 9110–9119, https://doi.org/10.1021/acsami.2c21786.
[275] F. Mottaghitalab, H. Hosseinkhani, M.A. Shokrgozar, C. Mao, M. Yang, M. Farokhi, Silk as a potential candidate for bone tissue engineering, J. Contr. Release 215 (2015) 112–128, https://doi.org/10.1016/j.jconrel.2015.07.031.
[276] A. Ho-Shui-Ling, J. Bolander, L.E. Rustom, A.W. Johnson, F.P. Luyten, C. Picart, Bone regeneration strategies: engineered scaffolds, bioactive molecules and stem cells current stage and future perspectives, Biomaterials 180 (2018) 143–162, https://doi.org/10.1016/j.biomaterials.2018.07.017.
[277] M.A. Al-Baadani, K. Hii Ru Yie, A.M. Al-Bishari, B.A. Alshobi, Z. Zhou, K. Fang, B. Dai, Y. Shen, J. Ma, J. Liu, X. Shen, Co-electrospinning polycaprolactone/gelatin membrane as a tunable drug delivery system for bone tissue regeneration, Mater. Des. 209 (2021) 109962, https://doi.org/10.1016/j.matdes.2021.109962.
[278] C. Wang, M. Wang, Electrospun multicomponent and multifunctional nanofibrous bone tissue engineering scaffolds, J. Mater. Chem. B 5 (7) (2017) 1388–1399, https://doi.org/10.1039/c6tb02907h.
[279] X. Shen, Y. Zhang, P. Ma, L. Sutrisno, Z. Luo, Y. Hu, Y. Yu, B. Tao, C. Li, K. Cai, Fabrication of magnesium/zinc-metal organic framework on titanium implants to inhibit bacterial infection and promote bone regeneration, Biomaterials 212 (2019) 1–16, https://doi.org/10.1016/j.biomaterials.2019.05.008.
[280] R. Whitaker, B. Hernaez-Estrada, R.M. Hernandez, E. Santos-Vizcaino, K. L. Spiller, Immunomodulatory biomaterials for tissue repair, Chem. Rev. 121 (18) (2021) 11305–11335, https://doi.org/10.1021/acs.chemrev.0c00895.
[281] J. Dong, W. Wang, W. Zhou, S. Zhang, M. Li, N. Li, G. Pan, X. Zhang, J. Bai, C. Zhu, Immunomodulatory biomaterials for implant-associated infections: from conventional to advanced therapeutic strategies, Biomater. Res. 26 (1) (2022) 72, https://doi.org/10.1186/s40824-022-00326-x.

[282] C.R. Arciola, D. Campoccia, L. Montanaro, Implant infections: adhesion, biofilm formation and immune evasion, Nat. Rev. Microbiol. 16 (7) (2018) 397–409, https://doi.org/10.1038/s41579-018-0019-y.
[283] K. Hayashi, M. Shimabukuro, K. Ishikawa, Antibacterial honeycomb scaffolds for achieving infection prevention and bone regeneration, ACS Appl. Mater. Interfaces 14 (3) (2022) 3762–3772, https://doi.org/10.1021/acsami.1c20204.
[284] D.M. Ibrahim, E.S. Sani, A.M. Soliman, N. Zandi, E. Mostafavi, A.M. Youssef, N. K. Allam, N. Annabi, Bioactive and elastic nanocomposites with antimicrobial properties for bone tissue regeneration, ACS Appl. Bio Mater. 3 (5) (2020) 3313–3325, https://doi.org/10.1021/acsabm.0c00250.
[285] N. Goonoo, A. Fahmi, U. Jonas, F. Gimie, I.A. Arsa, S. Benard, H. Schönherr, A. Bhaw-Luximon, Improved multicellular response, biomimetic mineralization, angiogenesis, and reduced foreign body response of modified polydioxanone scaffolds for skeletal tissue regeneration, ACS Appl. Mater. Interfaces 11 (6) (2019) 5834–5850, https://doi.org/10.1021/acsami.8b19929.
[286] D.E. Place, R.K.S. Malireddi, J. Kim, P. Vogel, M. Yamamoto, T.-D. Kanneganti, Osteoclast fusion and bone loss are restricted by interferon inducible guanylate binding proteins, Nat. Commun. 12 (1) (2021) 496, https://doi.org/10.1038/s41467-020-20807-8.
[287] W. Liu, K. Zhang, J. Nan, P. Lei, Y. Sun, Y. Hu, Nano artificial periosteum PCL/Ta/ZnO accelerates repair of periosteum via antibacterial, promoting vascularization and osteogenesis, Biomater. Adv. 154 (2023) 213624, https://doi.org/10.1016/j.bioadv.2023.213624.
[288] X. Wang, P. Shen, N. Gu, Y. Shao, M. Lu, C. Tang, C. Wang, C. Chu, F. Xue, J. Bai, Dual Mg-reinforced PCL membrane with a Janus structure for vascularized bone regeneration and bacterial elimination, ACS Biomater. Sci. Eng. 10 (1) (2023) 537–549, https://doi.org/10.1021/acsbiomaterials.3c01360.
[289] G. Guo, Q. Xu, C. Zhu, J. Yu, Q. Wang, J. Tang, Z. Huan, H. Shen, J. Chang, X. Zhang, Dual-temporal bidirectional immunomodulation of Cu-Zn Bi-layer nanofibrous membranes for sequentially enhancing antibacterial activity and osteogenesis, Appl. Mater. Today 22 (2021) 100888, https://doi.org/10.1016/j.apmt.2020.100888.
[290] B. Wang, J. Wang, J. Shao, P.H. Kouwer, E.M. Bronkhorst, J.A. Jansen, X. F. Walboomers, F.J.A.h.m. Yang, A tunable and injectable local drug delivery system for personalized periodontal application, J. Contr. Release 324 (2020) 134–145, https://doi.org/10.1016/j.jconrel.2020.05.004.
[291] Y. Li, Y.-Q. Chi, C.-H. Yu, Y. Xie, M.-Y. Xia, C.-L. Zhang, X. Han, Q. Peng, Drug-free and non-crosslinked chitosan scaffolds with efficient antibacterial activity against both Gram-negative and Gram-positive bacteria, Carbohydr. Polym. 241 (2020) 116386, https://doi.org/10.1016/j.carbpol.2020.116386.
[292] C. Vaquette, S.P. Pilipchuk, P.M. Bartold, D.W. Hutmacher, W.V. Giannobile, S. Ivanovski, Tissue engineered constructs for periodontal regeneration: current status and future perspectives, Adv. Healthcare Mater. 7 (21) (2018) 1800457, https://doi.org/10.1002/adhm.201800457.
[293] P. Aprile, D. Letourneur, T. Simon-Yarza, Membranes for guided bone regeneration: a road from bench to bedside, Adv. Healthcare Mater. 9 (19) (2020) 2000707, https://doi.org/10.1002/adhm.202000707.
[294] K. Kim, Y. Su, A.J. Kucine, K. Cheng, D. Zhu, Guided bone regeneration using barrier membrane in dental applications, ACS Biomater. Sci. Eng. 9 (10) (2023) 5457–5478, https://doi.org/10.1021/acsbiomaterials.3c00690.
[295] H. Tang, C. Qi, Y. Bai, X. Niu, X. Gu, Y. Fan, Incorporation of magnesium and zinc metallic particles in PLGA Bi-layered membranes with sequential ion release for guided bone regeneration, ACS Biomater. Sci. Eng. 9 (6) (2023) 3239–3252, https://doi.org/10.1021/acsbiomaterials.3c00179.
[296] H. Wang, D. Wang, H. Huangfu, H. Lv, Q. Qin, S. Ren, Y. Zhang, L. Wang, Y. Zhou, Branched AuAg nanoparticles coated by metal–phenolic networks for treating bacteria-induced periodontitis via photothermal antibacterial and immunotherapy, Mater. Des. 224 (2022) 111401, https://doi.org/10.1016/j.matdes.2022.111401.
[297] X. Liu, X. He, D. Jin, S. Wu, H. Wang, M. Yin, A. Aldalbahi, M. El-Newehy, X. Mo, J. Wu, A biodegradable multifunctional nanofibrous membrane for periodontal tissue regeneration, Acta Biomater. 108 (2020) 207–222, https://doi.org/10.1016/j.actbio.2020.03.044.
[298] D.M. dos Santos, L.M. Dias, A.K. Surur, D.A. de Moraes, A.C. Pavarina, C. R. Fontana, D.S. Correa, Electrospun composite bead-on-string nanofibers containing CaO2 nanoparticles and MnO2 nanosheets as oxygen-release systems for biomedical applications, ACS Appl. Nano Mater. 5 (10) (2022) 14425–14436, https://doi.org/10.1021/acsanm.2c02774.
[299] X. Wang, H. Fan, F. Zhang, S. Zhao, Y. Liu, Y. Xu, R. Wu, D. Li, Y. Yang, L.J.A.B. S. Liao, Antibacterial properties of bilayer biomimetic nano-ZnO for dental implants, ACS Biomater. Sci. Eng. 6 (4) (2020) 1880–1886, https://doi.org/10.1021/acsbiomaterials.9b01695.
[300] D. Lee, S.J. Lee, J.-H. Moon, J.H. Kim, D.N. Heo, J.B. Bang, H.-N. Lim, I.K. Kwon, Preparation of antibacterial chitosan membranes containing silver nanoparticles for dental barrier membrane applications, J. Ind. Eng. Chem. 66 (2018) 196–202, https://doi.org/10.1016/j.jiec.2018.05.030.
[301] J. Xiang, Y. Li, M. Ren, P. He, F. Liu, Z. Jing, Y. Li, H. Zhang, P. Ji, S. Yang, Sandwich-like nanocomposite electrospun silk fibroin membrane to promote osteogenesis and antibacterial activities, Appl. Mater. Today 26 (2022) 101273 (Sandwich-likenanocompositeelectrospunsilkfibroinmembranetopromoteosteogenesisandantibacterialactivities).
[302] A. Nasajpour, S. Ansari, C. Rinoldi, A.S. Rad, T. Aghaloo, S.R. Shin, Y.K. Mishra, R. Adelung, W. Swieszkowski, N. Annabi, A multifunctional polymeric periodontal membrane with osteogenic and antibacterial characteristics, Adv. Funct. Mater. 28 (3) (2018) 1703437, https://doi.org/10.1002/adfm.201703437.
[303] M. Lian, Y. Han, B. Sun, L. Xu, X. Wang, B. Ni, W. Jiang, Z. Qiao, K. Dai, X. Zhang, A multifunctional electrowritten bi-layered scaffold for guided bone regeneration, Acta Biomater. 118 (2020) 83–99, https://doi.org/10.1016/j.actbio.2020.08.017.
[304] K. Chachlioutaki, C. Karavasili, E. Adamoudi, A. Tsitsos, V. Economou, C. Beltes, N. Bouropoulos, O.L. Katsamenis, R. Doherty, A. Bakopoulou, Electrospun nanofiber films suppress inflammation in vitro and eradicate endodontic bacterial infection in an E. Faecalis-infected ex vivo human tooth culture model, ACS Biomater. Sci. Eng. 8 (5) (2022) 2096–2110, https://doi.org/10.1021/acsbiomaterials.2c00150.
[305] M. Alimohammadi, Y. Aghli, O. Fakhraei, A. Moradi, M. Passandideh-Fard, M. H. Ebrahimzadeh, A. Khademhosseini, A. Tamayol, S.A. Mousavi Shaegh, Electrospun nanofibrous membranes for preventing tendon adhesion, ACS Biomater. Sci. Eng. 6 (8) (2020) 4356–4376, https://doi.org/10.1021/acsbiomaterials.0c00201.
[306] R.M. Domingues, S. Chiera, P. Gershovich, A. Motta, R.L. Reis, M.E. Gomes, Enhancing the biomechanical performance of anisotropic nanofibrous scaffolds in tendon tissue engineering: reinforcement with cellulose nanocrystals, Adv. Healthcare Mater. 5 (11) (2016) 1364–1375, https://doi.org/10.1002/adhm.201501048.
[307] C. Rinoldi, E. Kijeńska, A. Chlanda, E. Choinska, N. Khenoussi, A. Tamayol, A. Khademhosseini, W. Swieszkowski, Nanobead-on-string composites for tendon tissue engineering, J. Mater. Chem. B 6 (19) (2018) 3116–3127, https://doi.org/10.1039/C8TB00246K.
[308] J. Zhang, C. Xiao, X. Zhang, Y. Lin, H. Yang, Y.S. Zhang, J. Ding, An oxidative stress-responsive electrospun polyester membrane capable of releasing anti-bacterial and anti-inflammatory agents for postoperative anti-adhesion, J. Contr. Release 335 (2021) 359–368, https://doi.org/10.1016/j.jconrel.2021.04.017.
[309] S. Liu, S. Liu, X. Liu, J. Zhao, W. Cui, C. Fan, Antibacterial antiadhesion membranes from silver-nanoparticle-doped electrospun poly(L-lactide) nanofibers, J. Appl. Polym. Sci. 129 (6) (2013) 3459–3465, https://doi.org/10.1002/app.39099.
[310] C.-H. Chen, S.-H. Chen, K.T. Shalumon, J.-P. Chen, Dual functional core–sheath electrospun hyaluronic acid/polycaprolactone nanofibrous membranes embedded with silver nanoparticles for prevention of peritendinous adhesion, Acta Biomater. 26 (2015) 225–235, https://doi.org/10.1016/j.actbio.2015.07.041.
[311] Q. Zhang, Y. Yang, D. Suo, S. Zhao, J.C.-W. Cheung, P.H.-M. Leung, X. Zhao, A biomimetic adhesive and robust Janus patch with anti-oxidative, anti-inflammatory, and anti-bacterial activities for tendon repair, ACS Nano 17 (17) (2023) 16798–16816, https://doi.org/10.1021/acsnano.3c03556.
[312] M. Georgiou, S.C.J. Bunting, H.A. Davies, A.J. Loughlin, J.P. Golding, J. B. Phillips, Engineered neural tissue for peripheral nerve repair, Biomaterials 34 (30) (2013) 7335–7343, https://doi.org/10.1016/j.biomaterials.2013.06.025.
[313] X. Gu, F. Ding, D.F. Williams, Neural tissue engineering options for peripheral nerve regeneration, Biomaterials 35 (24) (2014) 6143–6156, https://doi.org/10.1016/j.biomaterials.2014.04.064.
[314] H. Zhang, D. Lan, B. Wu, X. Chen, X. Li, Z. Li, F. Dai, Electrospun piezoelectric scaffold with external mechanical stimulation for promoting regeneration of peripheral nerve injury, Biomacromolecules 24 (7) (2023) 3268–3282, https://doi.org/10.1021/acs.biomac.3c00311.
[315] W. Kong, Y. Zhao, Y. Xiaoyu, J. Chen, Y. Chen, Z. Zhao, X. Chen, F. Wang, C. Fu, Combined treatment using novel multifunctional MAu-GelMA hydrogel loaded with neural stem cells and electrical stimulation promotes functional recovery from spinal cord injury, Ceram. Int. 49 (12) (2023) 20623–20636, https://doi.org/10.1016/j.ceramint.2023.03.193.

Shengqiu Chen is currently a postdoctoral fellow at Innovation Research Center for Diabetic Foot in West China Hospital of Sichuan University, collaborating with Prof. Xiaobing Fu. She received her Ph. D degree in Biomedical Engineering at Sichuan University in 2021, under the supervision of Prof. Changsheng Zhao. Her current research interests include electrospinning membranes, antibacterial and antioxidant nanomaterials, small extracellular vesicles, and diabetic wound therapies.

Xingwu Ran is currently a full professor and the head of Department of Endocrinology and Metabolism, Diabetic Foot Care Center, and Innovation Research Center for Diabetic Foot at West China Hospital in Sichuan University. He received his B. D. degree in Clinical Medicine from West China Hospital at Sichuan University in 1990. His current scientific research interests include drug molecules, exosomes, functional biomaterials and explore their potential applications in diagnoses and therapies of diabetic foot ulcers.

Cuiping Zhang is currently a full Professor at the Medical Innovation Research Division of Chinese PLA General Hospital (Beijing, China). She obtained her Ph. D degree in Pathology and Pathophysiology from the Academy of Military Medical Sciences in 2006. Her current research focuses on the design and fabrication of various biomaterials including advanced engineered small extracellular vesicles, hydrogel dressings, microneedle patches, and electrospinning membranes for skin tissue repair and regeneration.

Xiaobing Fu is currently a full professor at Chinese PLA General Hospital. He received Ph. D degree in 1993 at University of Madrid, Spain. He was appointed as a full Professor in 1995 at PLA 304th Hospital. He was elected as an academician of the Chinese Academy of Engineering in 2009. His scientific interests focus on the tissue repair and functional skin regeneration in war trauma and post-trauma, especially on the regeneration of skin appendages, including sweat glands, sebaceous glands as well as hair follicles.

Changsheng Zhao is currently a full professor at College of Polymer Science and Engineering in Sichuan University. He received Ph. D degree in Biomedical Engineering from Sichuan University in 1998. He was awarded funding from the National Science Fund for Distinguished Young Scholars Program in 2012. His current scientific interests are the development of functional nanomaterials, polymer-nanomaterial composites, blood compatible, biological active polymers and the regarding functional membranes.